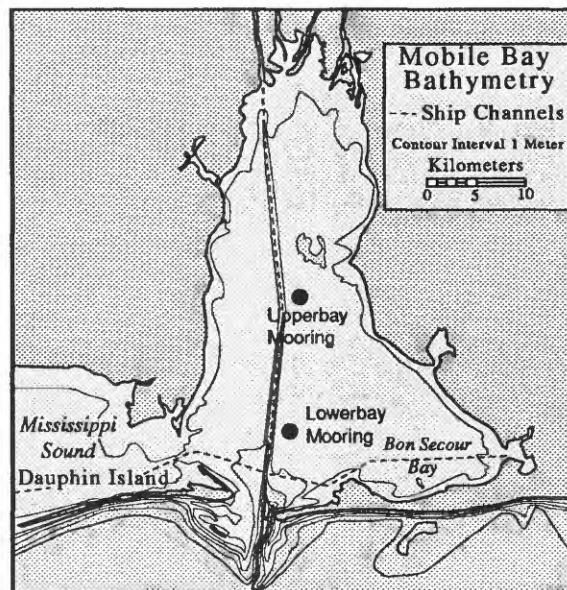


U.S. DEPARTMENT OF THE INTERIOR
U. S. GEOLOGICAL SURVEY

**Wave Data in Mobile Bay, Alabama
from March 1991 to May 1992**

by

Scott L. Pendygraft¹ and Guy Gelfenbaum¹



Open File Report 94-17

This report is preliminary and has not been reviewed for conformity with U. S. Geological Survey editorial standards. Any use of trade, product, or firm names is for descriptive purposes only and does not imply endorsement by the U. S. Government.

¹ USGS, Center for Coastal Geology, 600 4th Street South, St. Petersburg, Florida 33701

Wave Data in Mobile Bay, Alabama
from March 1991 to May 1992

- I. Project Description
 - A. Overview
 - B. Station Information
 - C. Report Overview
- II. Preparation of Data
 - A. Reading of Raw Data Files
 - B. Conversion of Raw Data into Pressure Values
 - C. Processing of Pressure Values
- III. Analysis of Data
 - A. Methods of Analysis
 - B. Generation of Wave Statistics
 - C. Comparison of Water Depth Time Series
- IV. Results
 - A. Wave Conditions
 - B. Wave Statistics
 - C. Polar Plots
- VI. Acknowledgments
- V. References
- VII. Appendix
 - A. Julian Date Calendars
 - B. Calibration Coefficients and Equations
 - C. Time Series Graphs: Mooring 3771
 - D. Time Series Graphs: Mooring 3871
 - E. Time Series Graphs: Mooring 3951

PROJECT DESCRIPTION

Overview

The coasts of Alabama and Mississippi have diverse usage. The region supports a multi-million dollar commercial fishery, is a major resource for recreation, is the terminus of the Tenn-Tom Waterway, and is home to a rapidly growing natural gas exploration program. These coastal areas are being stressed by a variety of problems of societal importance:

- Mobile Bay sediments contain elevated concentration of metals and have sustained occurrences of low-oxygen water causing stress on commercially important fisheries.
- The region is frequently swept by devastating hurricanes and has severe problems with barrier island movement and erosion.

In 1989 the United States Geological Survey initiated a four year study of the Alabama and Mississippi coastlines. The overall objectives were: (1) to determine coastal erosion rates and causes, recent sedimentologic history, and geologic framework, and (2) to determine the transport and deposition of pollutants and the extent of sediment-related pollution in the area.

These project objectives were accomplished by investigating specific marine and coastal processes using the following techniques:

- High resolution seismic surveys and coring.
- Mapping current and historical shoreline change.
- Measurement of contaminants in bottom sediments.
- Long term monitoring of circulation and sediment transport through moored instrumentation, hydrographic surveys, and satellite imagery.

This open file report focuses on the acquisition, processing, and analysis of time series wave data as part of a larger project to monitor circulation and sediment transport in Mobile Bay, Alabama (Figure 1).

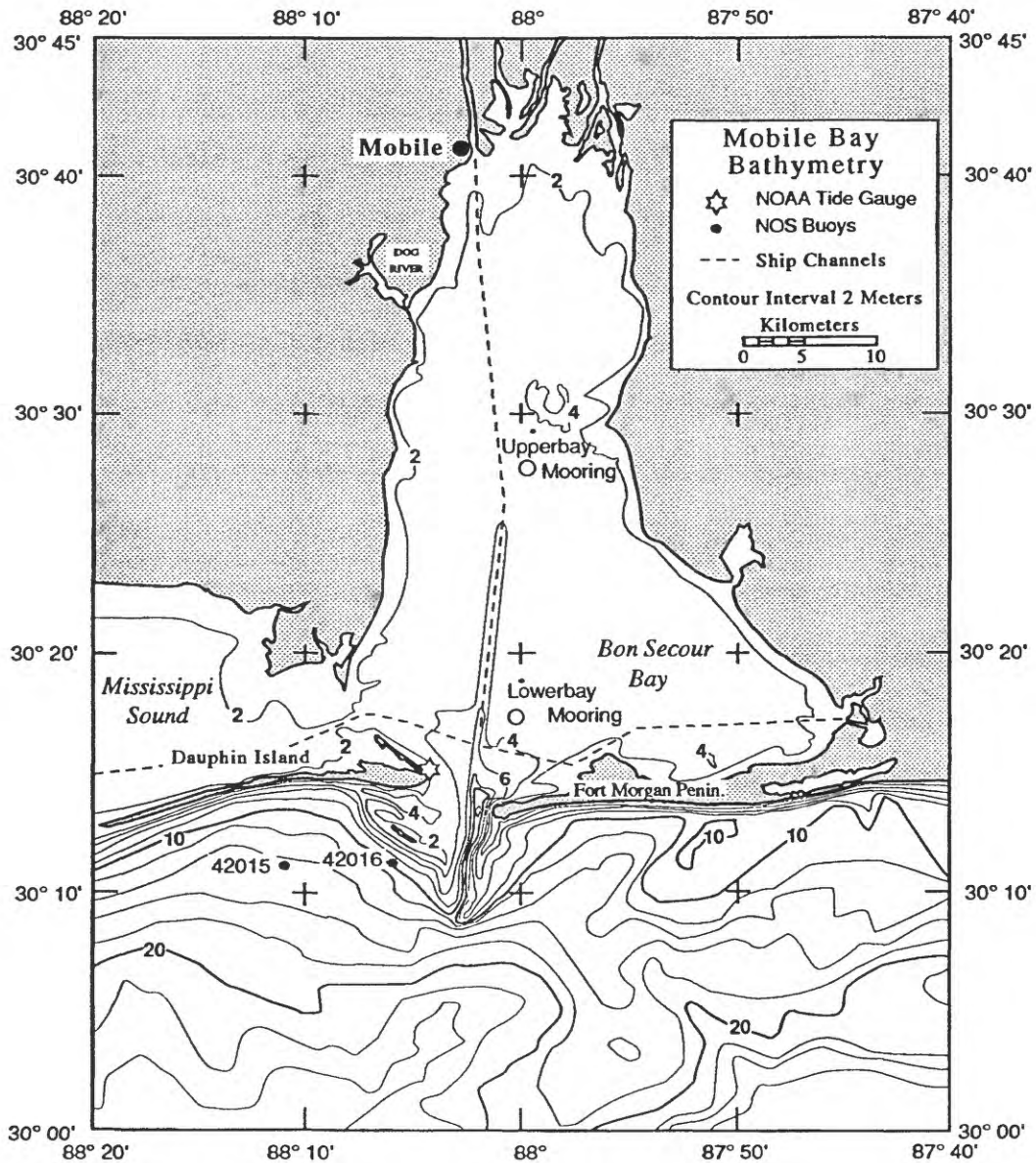


Figure 1. Mobile Bay, Alabama is a shallow water estuary in the northern Gulf of Mexico. The Bay is approximately 60 km long, has a surface area of 1050 km² and is 3-4 m deep except for a 12 m deep dredged shipping channel. The bottom is composed predominately of mud in clay and silty clay size ranges.

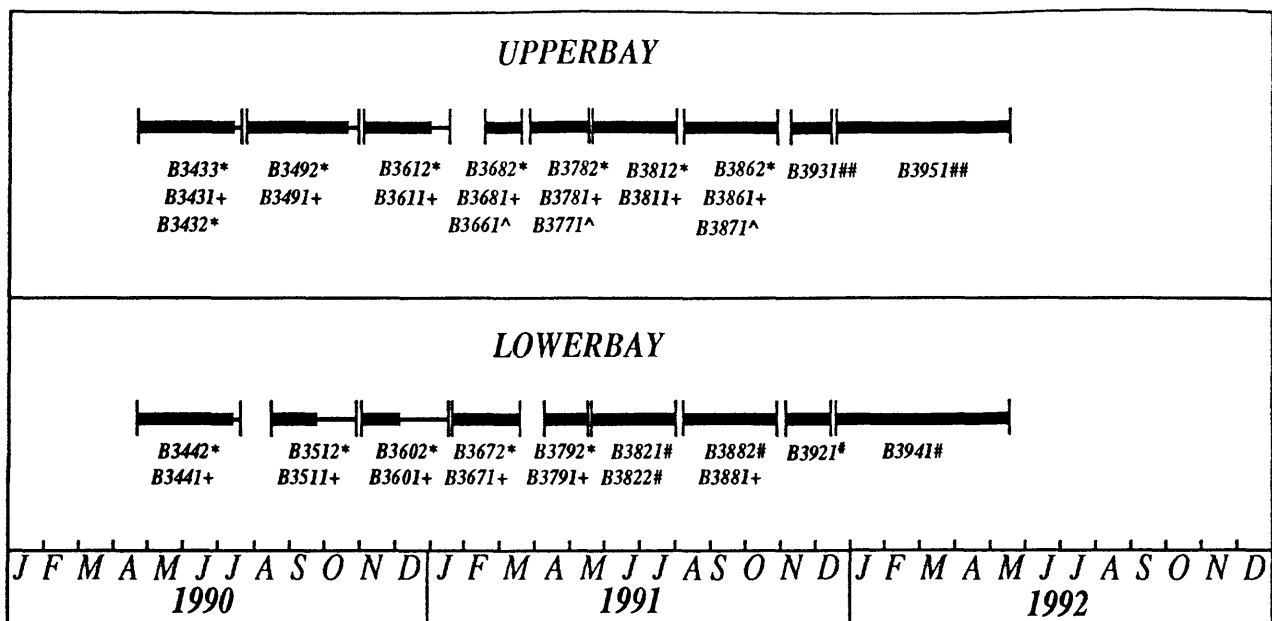
Station Information

Mobile Bay is located on the northern coast of the Gulf of Mexico east of the Mississippi River Delta. It is connected to both the Gulf of Mexico and east Mississippi Sound. Geomorphologically it is a combination of the drowned river valley and bar-built estuarine types. It drains a watershed of 11.3×10^4 km² and is the terminus of the Mobile River System, which has the sixth largest discharge on the North American Continent (Shroeder and Wiseman, 1988).

Important features of Mobile Bay are (1) triangular shape with the long axis running north and south; (2) relatively shallow overall but with significant exceptions (i.e. East Main Pass and the eastern side of the middle and upper Bay); (3) major openings to the Gulf of Mexico and East Mississippi sound in the southwest corner; (4) a major river delta at the northern end; (5) a large, relatively isolated area in the southeast corner, Bon Secour Bay; and (6) numerous man-made channels, the principle one being the Main Shipping Channel (120 m x 12 m) running from Main Pass to the Port of Mobile (Shroeder and Lysinger, 1979).

Waves were sampled by pressure sensors placed at two independent stations located on the bottom of Mobile Bay. The stations were referenced as UPPERBAY and LOWERBAY with latitude and longitude coordinates of 30° 27.97 N, 88° 00.11 W and 30° 17.7 N, 87° 59.8 W, respectively.

Data from both stations was recorded onto data loggers placed on moorings from April 1990 through May 1992. Several different instruments were used to collect and record data during individual moorings. Figure 2 is a summary of the data files recorded throughout the project with detailed information about the individual instruments. This report focuses on data acquired from the UPPERBAY station from March 1991 through May 1992.



- * Seacat Instrument Array - Temperature, Conductivity, Trasmisivity
- + TDR Pressure Sensor - Temperature, Pressure
- ^ BURP - Pressure
- # Bass Instrument Array - Temperature, Conductivity, Trasmisivity, Pressure, Current
- ## Bassless Bass Instrument Array - Temperature, Conductivity, Trasmisivity, Pressure

Figure 2. Summary of data file records collected throughout Mobile Bay project. Included are data loggers with instru- ment array information.

Report Overview

The goals of this report are to outline the procedures for the processing and analysis of pressure data and to report the wave conditions from the UPPER- BAY moorings 3771, 3871, and 3951. The processing of the data includes: unar- chiving of data files, extraction of raw binary data, translation of binary data into ASCII format, and conversion of ASCII pressure data into water depth val- ues. Raw pressure data or processed wave data are available from the authors on request.

For the analysis of the pressure data, several time series graphs were used in conjunction with wind time series data from the C-Man (Coastal-Marine Automated Network) station on Dauphin Island in order to establish causal rela- tionships between wind and wave properties.

PREPARATION OF DATA

Reading of Raw Data Files

The pressure data from Mobile Bay consists of continuous data sets which were broken into individual binary data files upon reading to facilitate processing. Each file consisted of time series records sampled at 2 Hz with a duration of approximately 2.5 days. Figure 3 contains the structural diagrams of the 3771, 3871, and 3951 moorings.

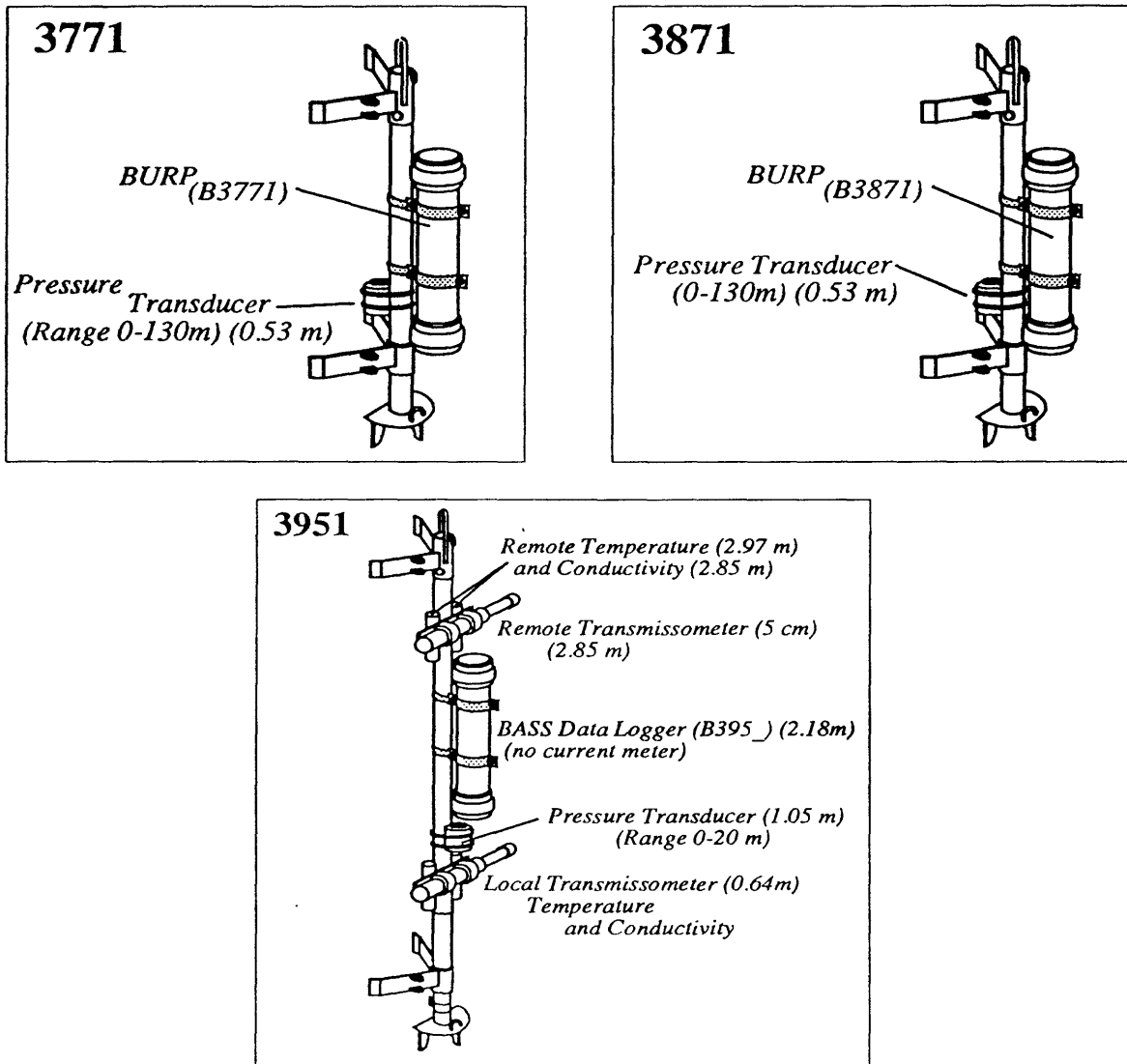


Figure 3. Structural diagrams 3771, 3871, and 3951. Shown are moorings with data loggers and associated instruments.

The 3771 and 3871 data sets were recorded onto BURst Pressure (BURP) data loggers in identical formats so that processing procedures were similar for data extraction and calibration. The 3951 data set was recorded onto a Benthic Acoustic Stress Sensor (BASS) data logger with a different format which required a separate procedure to extract the raw binary data. The calibration procedure, however, was similar to the 3771 and 3871 data sets.

The files for each of the data sets were indexed by the mooring number and a numerical suffix. For example, the 3951 data set contained 41 five megabyte raw data files, the first was named 3951.001 and the last 3951.206. The 3871 data set contained 32 three megabyte raw data files and the 3771 contained 30 three megabyte files.

As the data files were unarchived for analysis, a different nomenclature was established. The numerical suffix was replaced with sequential letters of the alphabet and a '.dat' suffix. Thus, 3951.001 became 3951a.dat and 3951.206 became 3951pp.dat. This allowed greater flexibility with the filenames that was necessary due to the great number of individual data sets created from each raw data file.

Conversion of Raw Data into Pressure Values

Conversion of the raw binary data into ASCII values was accomplished using C language programs generated to read and process the raw binary data into uncalibrated ASCII values. The first 17.06 minutes (2048 data points) of pressure data from the top of every hour was taken from each raw data file. This interval was chosen to obtain a data record long enough to get a valid sample of wave data but not so long that wave conditions changed. The goal was to generate a data record that accurately reflects rapid changes in wave conditions over time. In addition, the number of data points was made to equal a power of two in order to increase execution speed of the Fourier Transform calculations.

The 17.06 minutes of data was recorded in a separate ASCII file which was indexed by a unique filename consisting of the Julian date of the sample, the original raw data file reference letter, a single digit year number (i.e. 1 or 2 for 1991 or 1992), the hour, minute, and second of the starting point of the time series interval, and a '.out' suffix. For example, the filename for the file 3871aa.dat from October 4, 1991 at 16:00 is '277aa11600.out' and the filename for a sample from the 3951v.dat data file taken on February 24, 1992 at 21:00 is '055v22100.out'. Julian Date calendars are contained in Appendix A.

This nomenclature was chosen for several reasons: First, it was an easy way to separate the first 17.06 minutes of data out of every hour. Second, it broke the large raw data file into smaller ASCII data sets which were easier to work with. Third, the smaller ASCII data sets with unique filenames allowed quick, easy and reliable access to any specific hour of data that was of interest.

After the translation of binary data into ASCII format, the raw data was calibrated into pressure values using the calibration equations provided by the instrument manufacturer. Appendix B contains the calibration coefficients and equations for the pressure sensors used on the 3771, 3871, and 3951 moorings. The equations calculate pressure (in psi) given the temperature and pressure period (in usec). The pressure values were converted into millibars then related to water depth with the following equation:

$$\text{WaterDepth}(m) = (\text{Pressure}(m\text{bars}) - 1000)/100$$

These water depth values were written to another ASCII file in matrix format for use in generating wave statistics such as significant wave height and wave period.

Processing of Pressure Values

Before any analysis was performed, some simple adjustments were made to the pressure values. First, bad data points were corrected. This was accomplished by taking the mean and standard deviation of the 17.06 minute data set. The data was then de-meanned and individual data points compared against the mean of the entire data set. A copy of the original 17.06 minute data set was made and all data greater than 10 standard deviations were removed. The mean of this new data set was taken and used to replace any data point greater than 10 standard deviations in the original 17.06 minute data set.

There were very few bad data points in the 3771, 3871, and 3951 data sets: Approximately 100 out of 3,360,000 for the 3771, 220 out of 3,590,4000 for 3871 and 11,000 out of 6,691,200 for 3951. The bad data points could be due to a number of factors. Instrument malfunction and instrument bio-fouling are possible sources of errors. However, the data transfer and archiving processes can also be a source of errors, as was suspect in the 3951 data set.

Once the data sets were corrected of bad data points the water level was adjusted for the height of the instrument from the bottom of the Bay floor. For the 3771, 3871, and 3951 instruments, the bottom plate of the mooring was .10 meters from the Bay floor. The pressure sensor for the 3771 and 3871 moorings were .53 meters from the bottom plate of the mooring for a total of .63 meters from the Bay floor. The 3951 mooring pressure sensor was located 1.05 meters from the bottom plate of the mooring for a total height of 1.15 meters (Figure 4). These heights were added to the water depth values (in meters) for a total water depth used in the wave analysis.

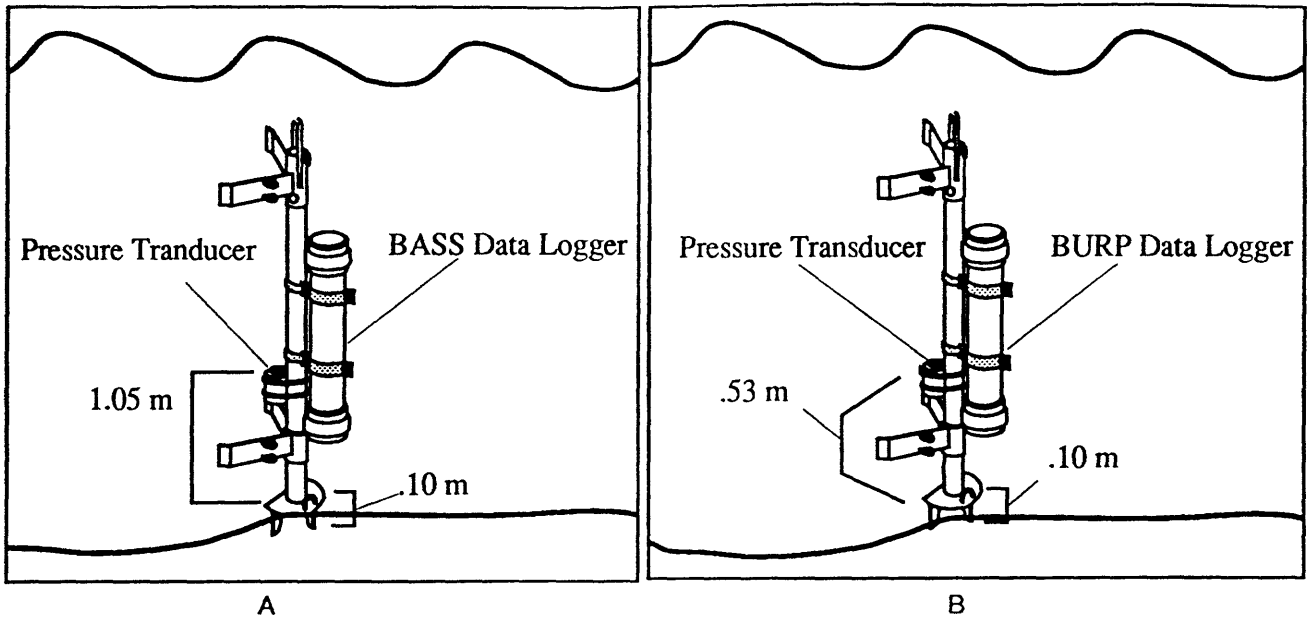


Figure 4. Diagrammatic representation of instrument heights from the ocean bottom. (A) The 3951 used a BASS data logger. (B) The 3771 and 3871 moorings used BURP data loggers .

ANALYSIS OF DATA

Methods of Analysis

A Fast Fourier transform (FFT) algorithm was used to estimate power spectra for the 17.06 minute data sets in order to calculate significant wave height, peak wave period, and mean wave period. Spectra were calculated using FFT algorithms found in Matlab's Signal Processing Toolbox. However, in order to obtain an accurate power spectrum of surface water level fluctuations, adjustments to the spectral data were made.

These adjustments were necessary to account for the difference in vertical water motion caused by the waves between the water surface and the Bay floor. Wave motions near the bottom are dampened compared to wave motions at the water surface. These differences in water motions are problematic since the data was collected by instruments placed close to the bottom and used to estimate wave dynamics at the water surface.

The problem is complicated because the attenuation of wave energy is frequency dependent. Higher frequency waves are attenuated more than lower frequency waves. An algorithm was developed following Guza and Thornton (1980) using linear wave theory which adjusts the pressure fluctuations with respect to water depth for each frequency. This gives an adjusted spectra for pressure fluctuations at the surface. Accounting for the attenuation in pressure fluctuations with depth results in an accurate measure of the wave dynamics at the water surface.

Significant wave height (H_s), peak period and mean period of the pressure data were computed using the following formulas:

$$\text{variance} = (\sum_{\text{imin}}^{\text{imax}} \text{PowerSpectrum})/N$$

$$H_{rms} = 2\sqrt{2} \cdot \sqrt{\text{variance}}$$

$$H_s = 1.42 H_{rms}$$

$$\text{Peak Period} = 1/\text{PeakFreq}$$

$$\text{Mean Period} = 1/\text{AveFreq}$$

Where $imin$ and $imax$ are minimum and maximum frequencies over which the average frequency is computed from the PowerSpectrum, N is the length of the PowerSpectrum, PeakFreq is the peak frequency of PowerSpectrum in Hz, and AveFreq is the weighted average frequency computed between the $imin$ and $imax$ values.

Once wave statistics were calculated, graphs for each of the hourly data sets were generated containing three plots, the name of the data file, the date on which the data were sampled, and the computed wave statistics (see Figure 5 for example).

The three plots include a time series plot of water depth and two spectral density plots. The bottom left plot is a standard power spectrum estimation for the detection of narrow-band signals buried in wide-band noise at the water depth of the instrument. The bottom right is a power spectrum of pressure fluctuations at the surface.

April 30 1991 17:00 UCT File: 120bb11700.mat Hsign = 0.6557 m Peak Period = 3.459 s

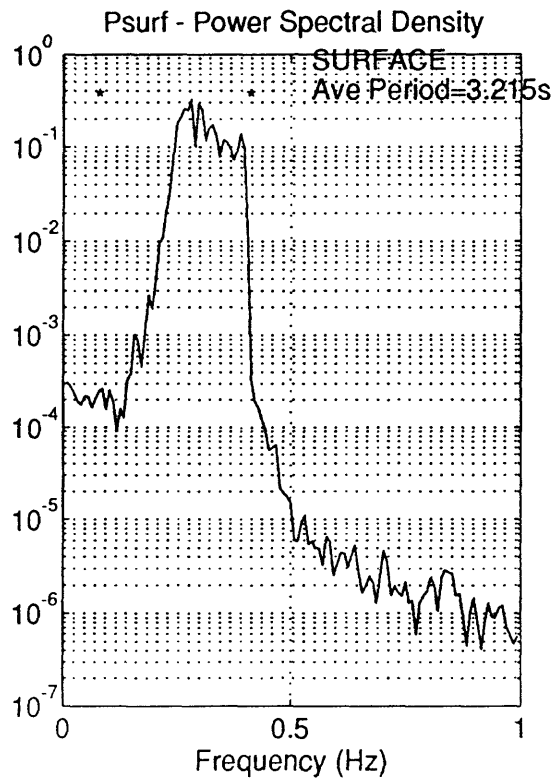
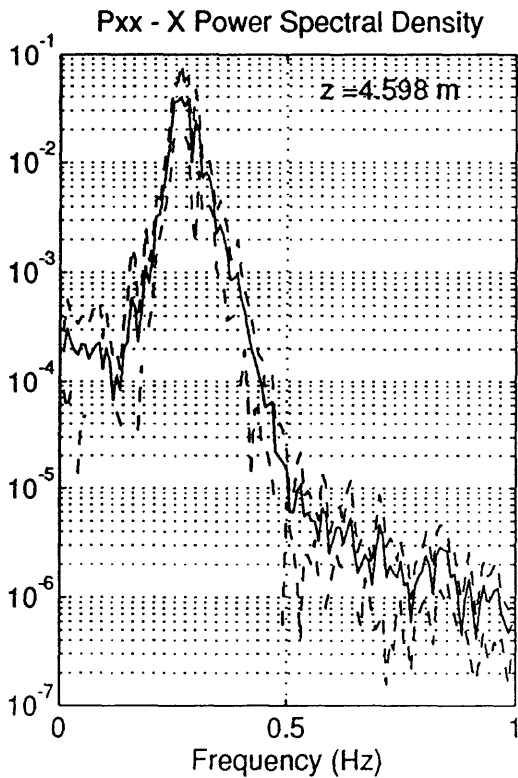
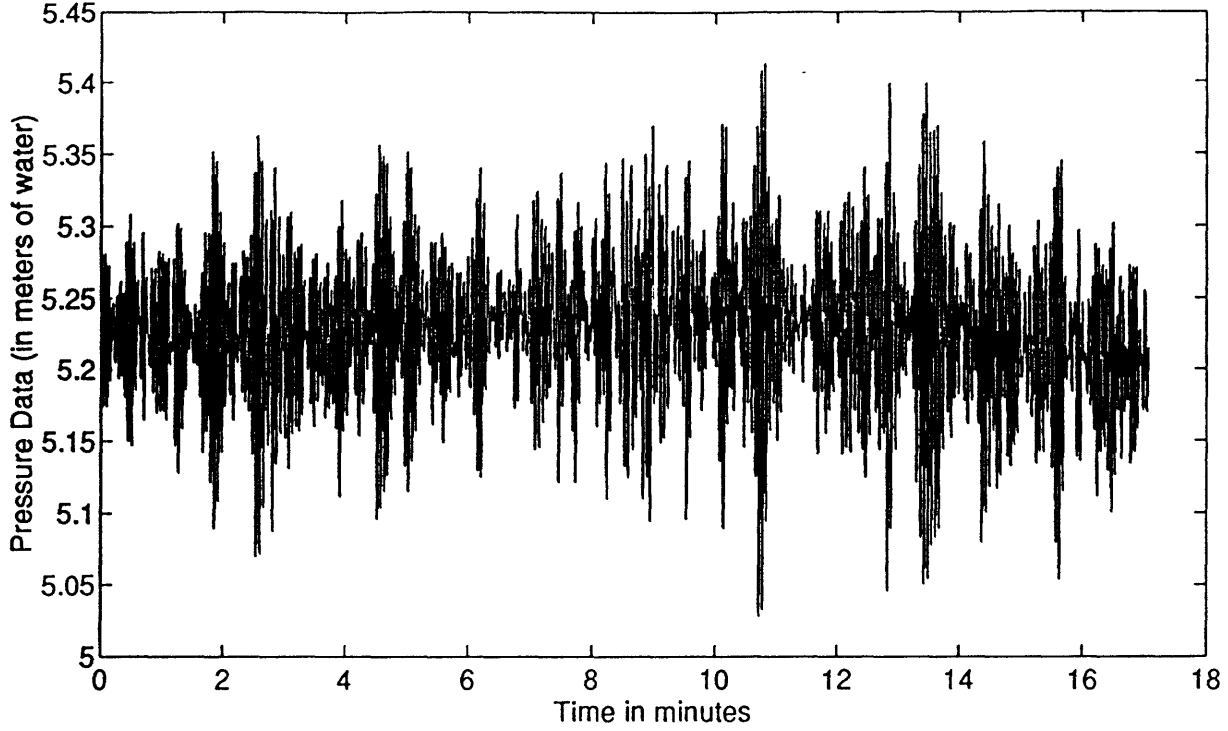


Figure 5. Wave statistic data sheet sample. Upper plot is time series of surface water elevation. Lower left plot is a standard power spectrum estimation at the depth of the instrument, including 95% confidence estimates. Lower right plot is a power spectrum of pressure fluctuation corrected for attenuation up to frequencies less than 0.5 Hz.

The surface spectrum implements the Welch method of power spectrum estimation. This method involves averaging across adjacent records to obtain more reliable spectral estimates. The two asterisks on the surface spectrum plot at .06 Hz (16.66 s) and .40 Hz (2.50 s) represent the minimum(*imin*) and maximum(*imax*) frequencies over which to calculate the wave parameters. The high frequency cutoff represents the maximum frequency at which wave motions were detected at the sensor.

Comparison of Water Depth Time Series

There were two primary concerns in processing the data: First, the data needed to be taken from its raw binary format, converted into ASCII values, and processed into the correct water depth. Second, the time series data needed to be accurately time stamped. With the great volume of data processed, an error of a few seconds could be compounded into a noticeable shift of events. It was necessary to develop ways to check the accuracy of the data processing.

Two checks were performed to validate the accuracy of the time series data. The first consisted of matching theoretical tide predictions against the measured water depths. The second check involved comparing pressure data taken from a TDR pressure sensor placed within several meters of the "UPPERBAY" station. The TDR sensor samples pressure over an hourly time period and stores the average. A comparison of de-measured values from the TDR and the wave pressure data gives an indication of processing accuracy. If there were no processing errors in the data then a high correlation between the water depth calculated from the wave measurements and the experimental data from the TDR pressure sensor would be expected. Any errors in processing would manifest themselves as shifts in water depths.

Two TDR mooring data files were used for comparison to calculated water depth: 3781 to compare to 3771 and 3861 to compare to 3871. The 3951 mooring does not have a corresponding TDR data set available. The TDR data were acquired in processed form as water depth in meters. The TDR and pressure data are de-measured and shown in Figure 6. There are slight differences in the amplitudes of many of the peaks and troughs, but both have high correlation coefficients (Table 1).

Table 1

Correlation Coefficients

Mooring	<u>3771</u>	<u>3871</u>	<u>3951</u>
Predicted Tidal Heights & Water Depth	.7450	.8020	.7366
TDR Mooring & Pressure Data	.9684	.9560	N/A

Theoretical tide predictions were obtained from a program called Tides1 for IBM compatible computers. The Tides1 program generates the theoretical tide heights for several areas around the country for prescribed time periods. The Fowl River area in Mobile Bay was chosen since it is the closest in latitude and longitude ($30^{\circ} 26' N$, $88^{\circ} 07' W$) to the moorings.

The predicted tide height is reported as how high the water has risen from mean lower low water. The mean was removed from both the predicted and measured data then compared. The correlation coefficients are given in Table 1 and Figure 7 shows the three moorings plotted against the theoretical tides predictions. The rise and fall of water levels follow the general tidal pattern in the three moorings and they all yield high correlation coefficients. This indicates the pressure data was processed and time stamped accurately.

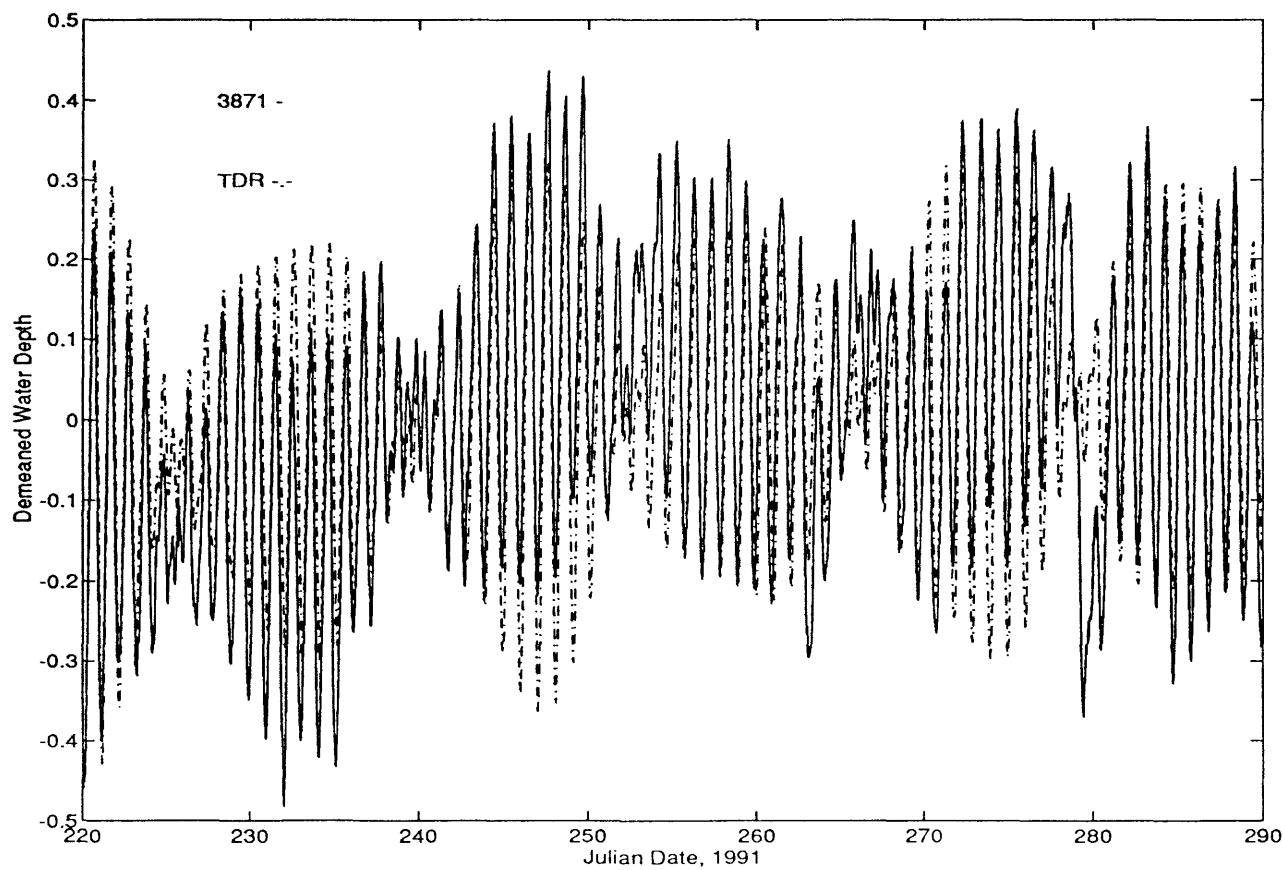
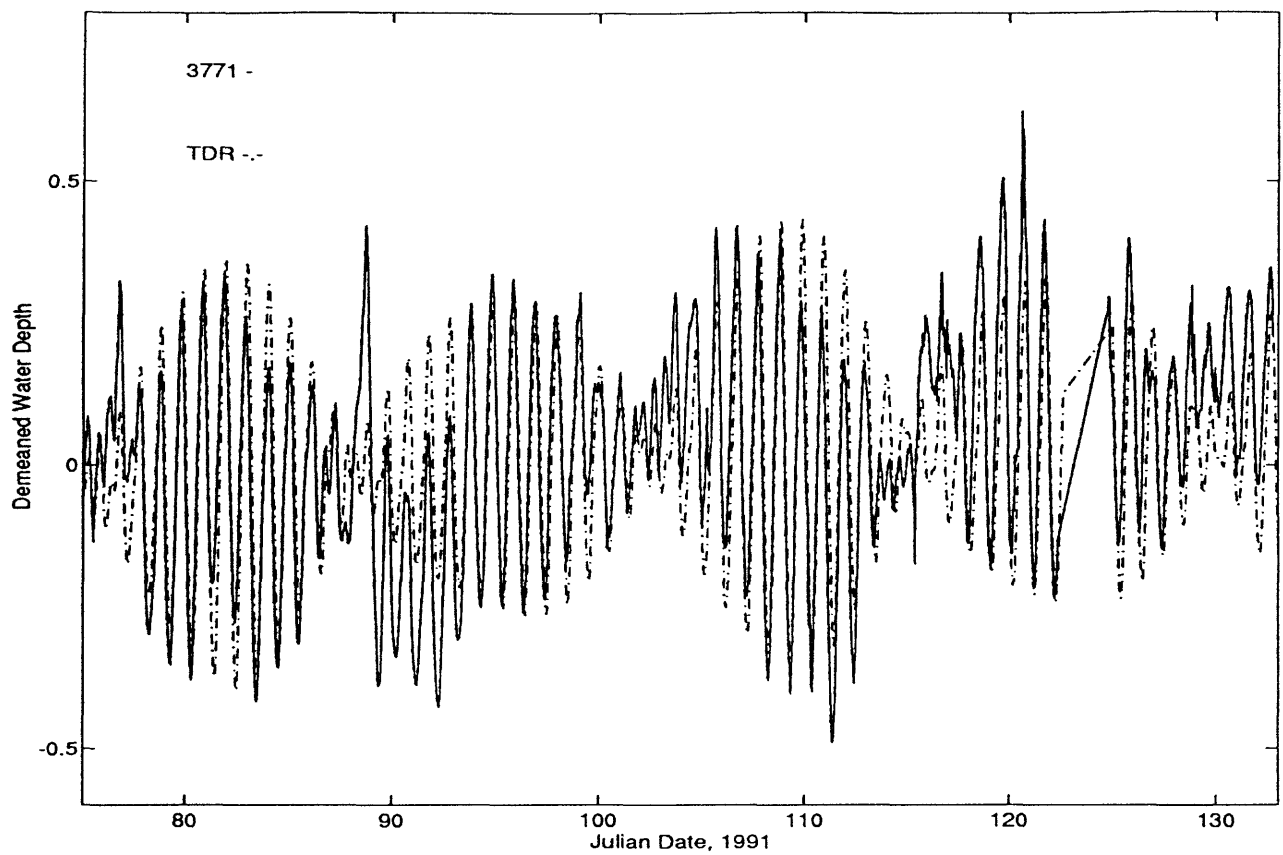


Figure 6. Comparison of TDR sensor data with pressure data collected during the 3771 and 3871 moorings.

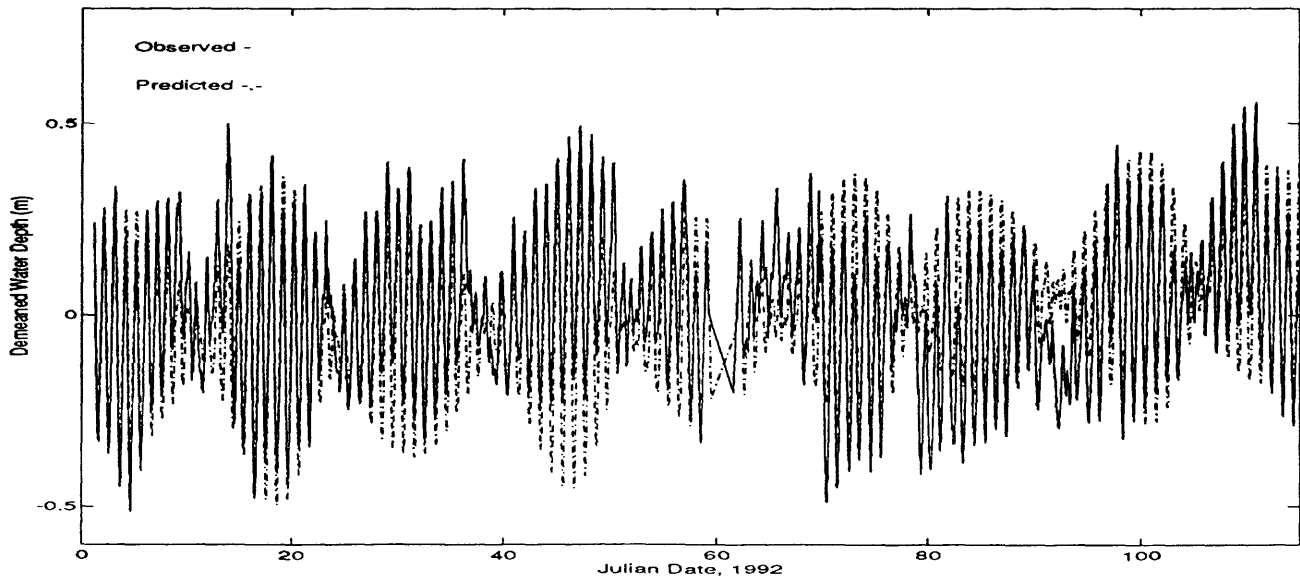
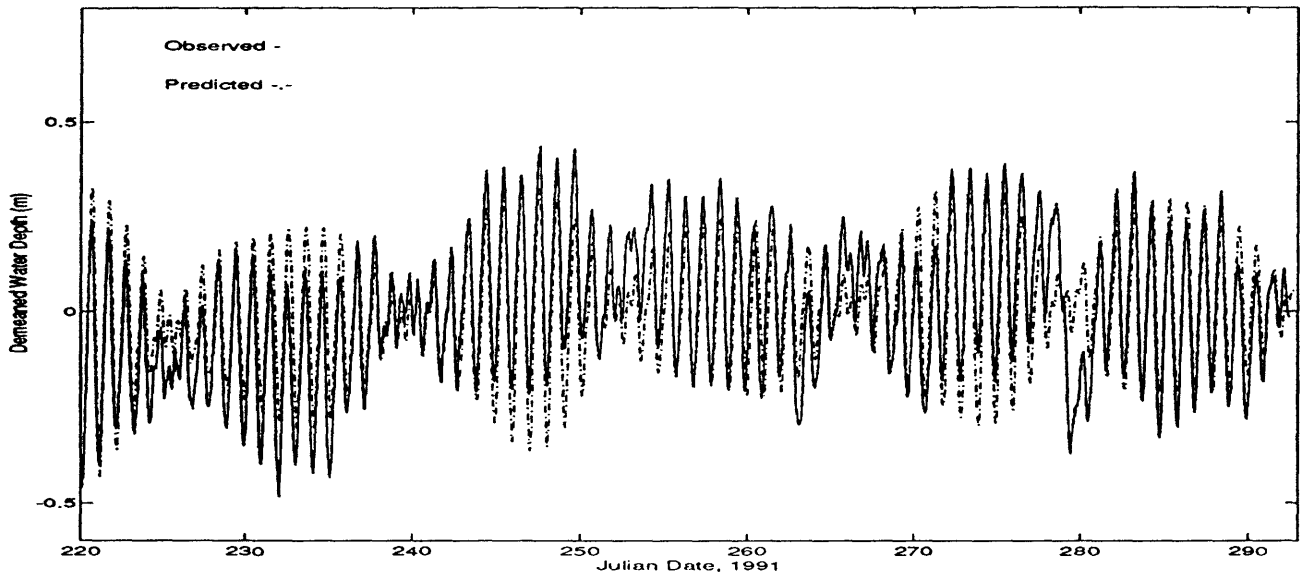
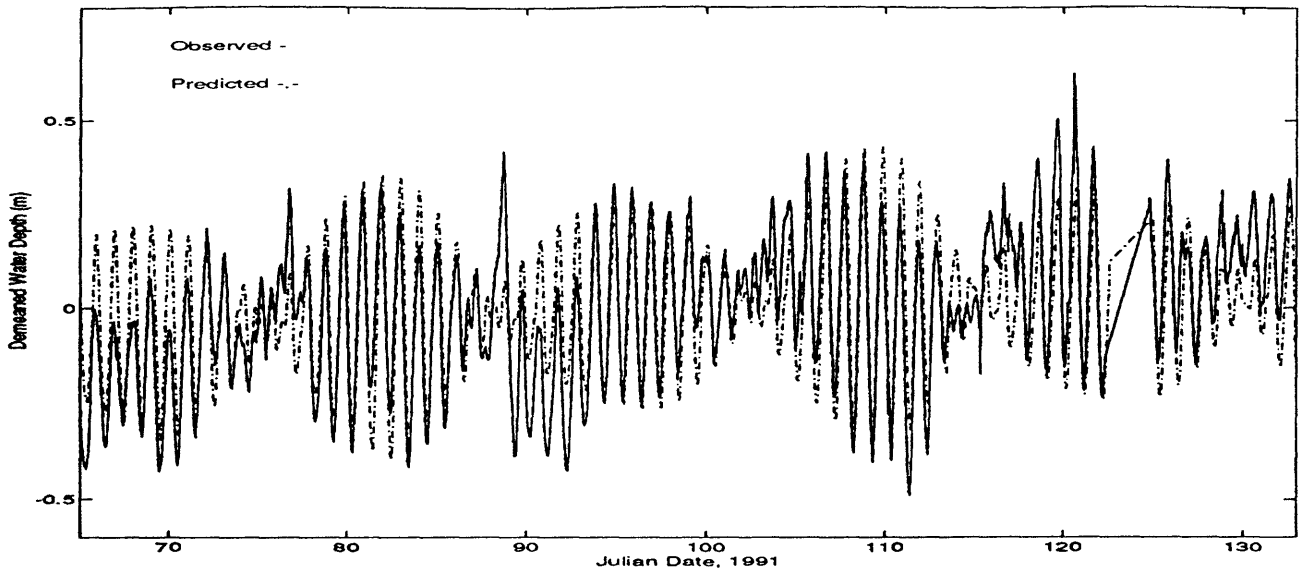


Figure 7. Comparison of predicted tidal values from Tides1 model and pressure data collected during 3771, 3871, and 3951 moorings.

RESULTS

Once the initial processing and analysis of the data was complete, a number of graphical approaches were utilized to further analyze wind and wave interactions in Mobile Bay. Wind time series data was acquired from the Dauphin Island C-Man station (Figure 1, at the NOAA Tide Gauge) for the corresponding time periods of the 3771, 3871, and 3951 data sets. Wind direction was recorded using the meteorological convention of reporting the direction wind is from (i.e. a north wind is a wind blowing from the north). Time series graphs and polar scatter plots best represented the data for our analysis.

Wave Conditions

The complete set of time series graphs for moorings 3771, 3871, and 3951 are shown in Appendices C, D, and E. The time series graphs consist of five separate subplots: wind speed, wind direction, significant wave height, average wave period, and water depth. The 'normfactor' on the average period subplot refers to the minimum significant wave height value allowed corresponding to meaningful average wave period values. When the significant wave height was less than the 'normfactor' of 0.3 m, the corresponding average period value was set to 2.5 s. This eliminated spurious wave period values when wave heights were small. The result was a graph showing only the major peaks in the average period data values.

Significant wave height and wave periods were more responsive to increases and decreases in wind speed than changes in wind direction. Several cases are given below and additional examples can be found throughout the time series graphs found in Appendices C, D, and E.

Julian dates 92-93 (April 2-3, 1991) in Appendix C6 show changes in wind direction with steady wind speed conditions. The wind direction shifts approxi-

mately 350° over a one day period but no significant changes are observed in the wave heights or wave periods.

Julian dates 116-117 (April 26-27, 1991) in Appendix C9 show an example of changes in wind speeds with unchanging wind directions. The significant wave height responds to the increase in wind speed, shows a corresponding decrease as wind speed decreases, then increases again with the increase in wind speed.

Julian dates 69-70 (March 9-10, 1992) in Appendix E11 show significant wave height increases as wind speed increases, decreases with the decrease of wind speed and a change of wind direction, then increases again with an increase in wind speed but no change in wind direction.

Wave Statistics

TABLE 2

Wave Statistics Summary

	<u>3771</u>	<u>3871</u>	<u>3951</u>
minimum Wind Speed(m/s)	0.0	0.0	0.0
maximum Wind Speed(m/s)	19.15	18.20	18.22
mean Wind Speed(m/s)	5.89	4.85	5.74
wind speed < 10 m/s	90.17%	95.35%	91.25%
wind speed > 10 m/s	9.83%	4.650%	8.75%
minimum Hs(m)	0.004	0.005	0.002
maximum Hs(m)	1.55	0.96	0.86
maximum Wave Period(s)	4.26	3.75	3.75
minimum Water Depth(m)	4.10	4.02	3.50
maximum Water Depth(m)	5.20	4.94	4.77

Table 2 contains the wind and wave statistics summaries for the 3771, 3871 and 3951 data sets. Wind speeds during the fall/winter months of the 3871 data

set vary between 0 and 18.20 m/s. 95% of the time, wind speeds were less than 10 m/s. Approximately 5% of the data corresponds to 'events' where the wind speed measures from 10 to 18.20 m/s.

Wind speeds during the spring months of the 3771 data set varied between 0 and 19.15 m/s. There were less calm winds and more 'events' in the 3771 and 3951 data sets: 90% and 91% calm winds and 10% and 9% stronger winds, respectively. The 3951 winter/spring wind speed data was comparable to the 3771 spring data showing a maximum wind speed within 1 m/s and a mean wind speed within 0.2 m/s.

Significant wave heights from the 3771, 3871 and 3951 data sets vary between 0 and 1 with the exception of one event of 1.6 m on April 3, 1991 (Julian date 120.6250) in the 3771 data set (APPENDIX C9). Significant wave height typically responded within one hour to changes in wind speed as evidenced in the cross-correlation data (Figure 8). The correlation coefficients of wind speed and significant wave height with zero lag are listed below.

Wind Speed and Significant Wave Height Correlation Coefficients

	<u>3771</u>	<u>3871</u>	<u>3951</u>
Correlation Coefficient	.7068	.6130	.7679

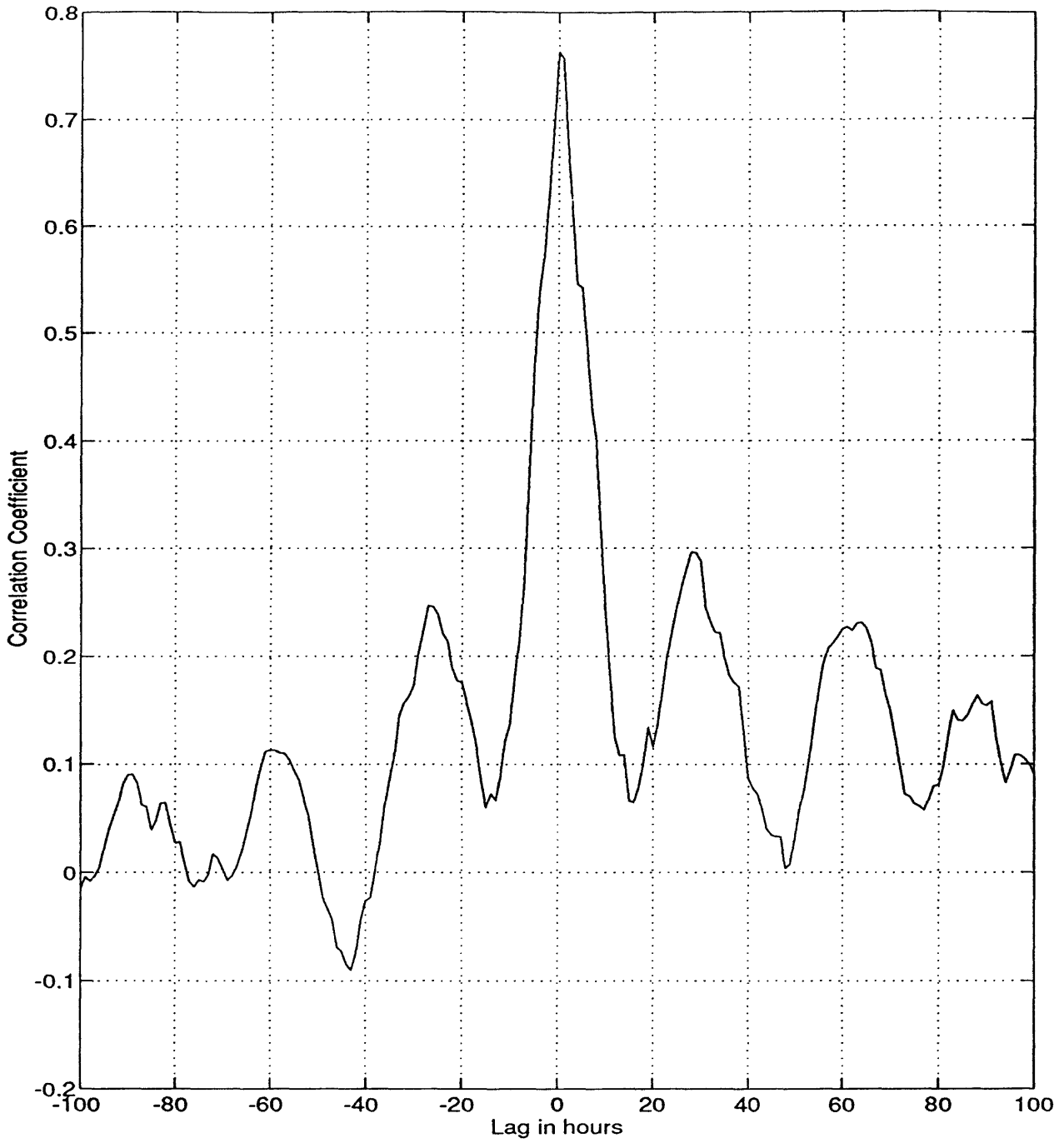


Figure 8. Cross correlation plot of wind speed and significant wave height from a 14 day period during the 3771 mooring. Correlation with zero lag indicates significant wave height responds within one hour to changes in wind speed.

Wind and Wave Interactions

For each mooring, the significant wave height and wind speed were sorted by the wind direction according to pre-determined boundaries in order to establish zones of near-similar fetch. Table 3 shows the degree boundaries used to sort the north, south, east, and west directions and Figure 9 is a plot of Mobile Bay showing the coordinate boundaries.

TABLE 3

<u>DIRECTION</u>	<u>INTERVAL</u>	<u>DEGREE MEASURE</u>
NORTH	330 - 30	60°
EAST	30 - 130	100°
SOUTH	130 - 230	100°
WEST	230 - 330	100°

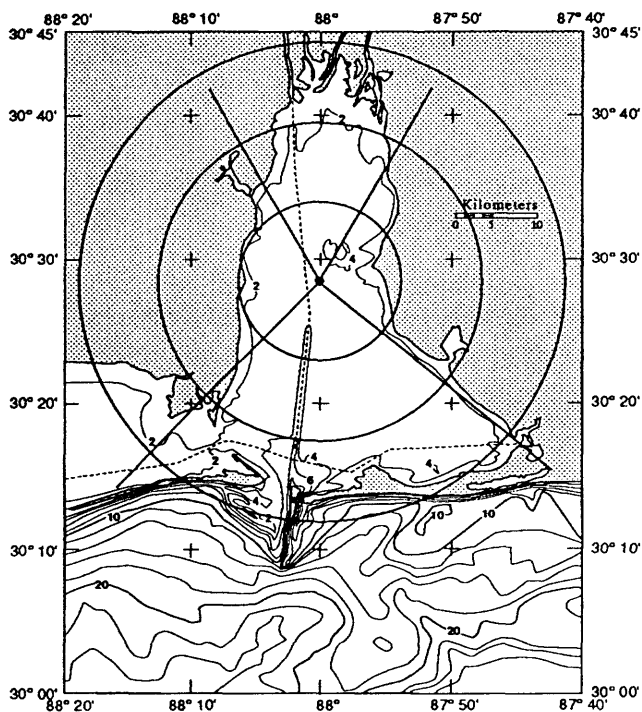


Figure 9. Plot of Mobile Bay coordinate boundaries used to sort wind directions.

Once the data was sorted into the appropriate direction, percentages of data points from each direction were generated for the three moorings. In addition, the three data sets were combined and winter, spring, and fall seasonal data isolated. These values are shown in Table 4 below.

TABLE 4
3771 Wind Statistics

<u>Direction</u>	<u>N</u>	<u>E</u>	<u>S</u>	<u>W</u>
# of data points	208	645	546	159
% of data points	13.3	39.5	34.8	10.21

3871 Wind Statistics

<u>Direction</u>	<u>N</u>	<u>E</u>	<u>S</u>	<u>W</u>
# of data points	373	647	399	280
% of data points	21.6	39.0	23.1	16.3

3951 Wind Statistics

<u>Direction</u>	<u>N</u>	<u>E</u>	<u>S</u>	<u>W</u>
# of data points	741	1061	623	775
% of data points	23.4	33.1	19.3	24.2

Winter Wind Statistics
December, January, February

<u>Direction</u>	<u>N</u>	<u>E</u>	<u>S</u>	<u>W</u>
# of data points	506	635	260	440
% of data points	27.5	34.5	14.1	23.9

Spring Wind Statistics
March, April, May

<u>Direction</u>	<u>N</u>	<u>E</u>	<u>S</u>	<u>W</u>
# of data points	443	1080	910	495
% of data points	15.1	36.9	31.1	16.9

Fall Wind Statistics
September, October

<u>Direction</u>	<u>N</u>	<u>E</u>	<u>S</u>	<u>W</u>
# of data points	307	468	192	165
% of data points	27.1	41.3	17.0	14.6

In all three data sets, winds were predominantly out of the east. Winds out of the north and south were comparable in the 3871 and 3951 data sets but south winds were more frequent than north winds in the 3771 data set. West winds were observed less frequently in the 3771 and 3871 data but were about equal to north wind percentages in the 3951 data.

The winter, spring, and fall wind statistics show winds were also predominantly out of the east. Fall and winter wind statistics show dominant north and east winds. The spring wind statistics also had dominant east winds but show a large increase in winds from the south.

Polar Plots

Two types of polar scatter plots were generated: plots of significant wave height verses wind direction, and plots of wind speed verses wind direction. Figures 10, 11, 12 show both polar plots for the 3771, 3871, and 3951 moorings.

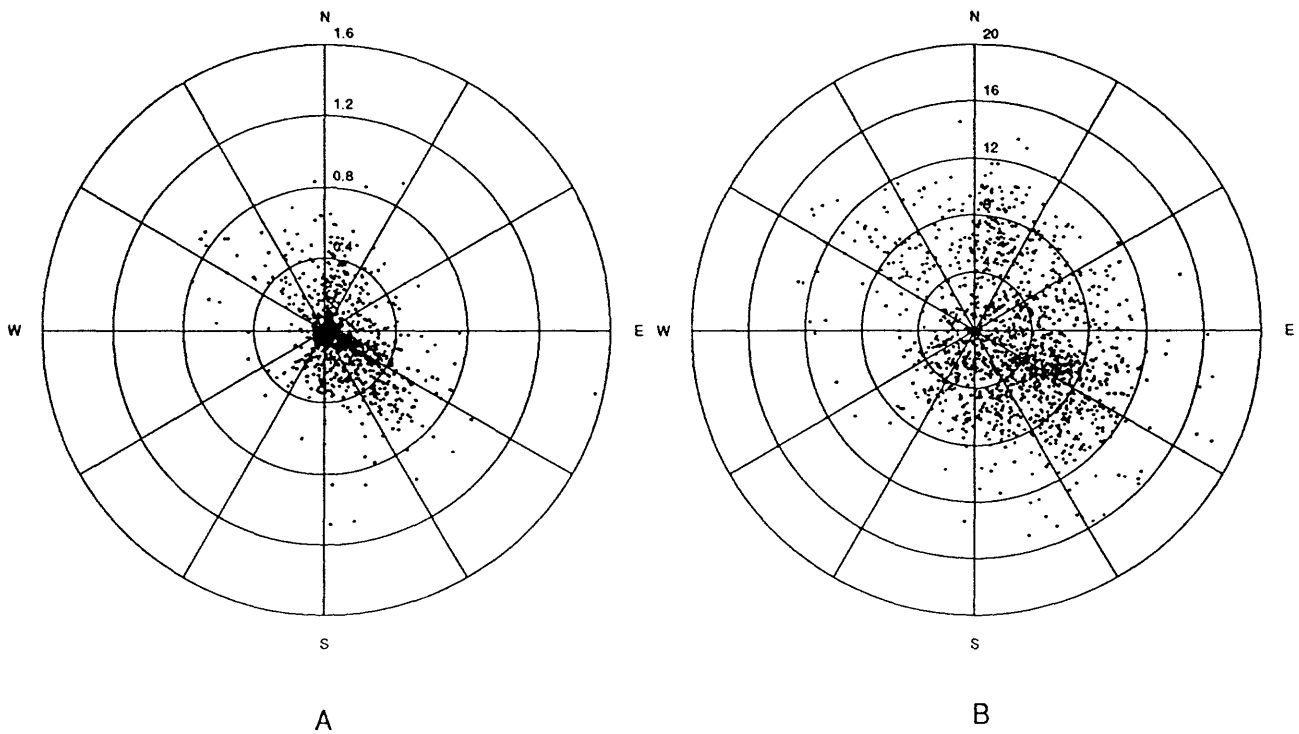


Figure 10. Directional scatter plots indicating (A) significant wave height verses wind direction and (B) wind speed verses wind direction for the 3771 mooring.

The polar scatter plots allowed observation of all data values on one 360 degree plot. This aided in observing patterns of wind and wave dynamics on a single polar graph as opposed to interpreting this information from time series plots.

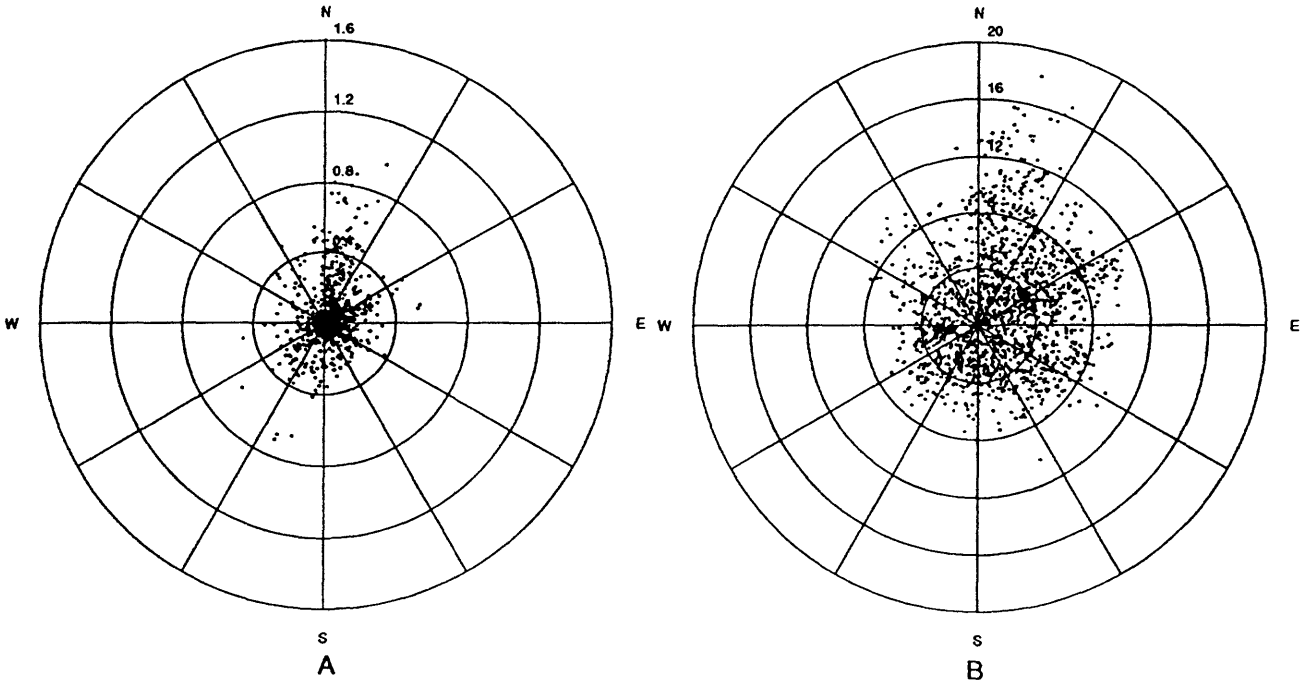


Figure 11. Directional scatter plots indicating (A) significant wave height verses wind direction and (B) wind speed verses wind direction for the 3871 mooring.

The 3871 data set (Figure 11) shows a clear trend toward higher wind speeds and significant wave heights when winds were from the north. Wind speeds from the north range from 0 to 18.12 m/s whereas wind speeds from all other directions were never greater than 11.22 m/s. Significant wave heights resulting from north winds range from 0 to 0.97 m where significant wave heights greater than 0.70 m were not observed during south, east, or west winds.

The 3771 (Figure 10) and 3951 (Figure 12) data sets did not show any clear trend toward higher wind speeds or significant wave heights out of any single direction. The 3771 data shows a slight trend toward larger wind speeds and significant wave heights due to winds out of the southeast where wind speeds range from 0 to 18.28 m/s and significant wave heights range from 0 to 1.55 m.

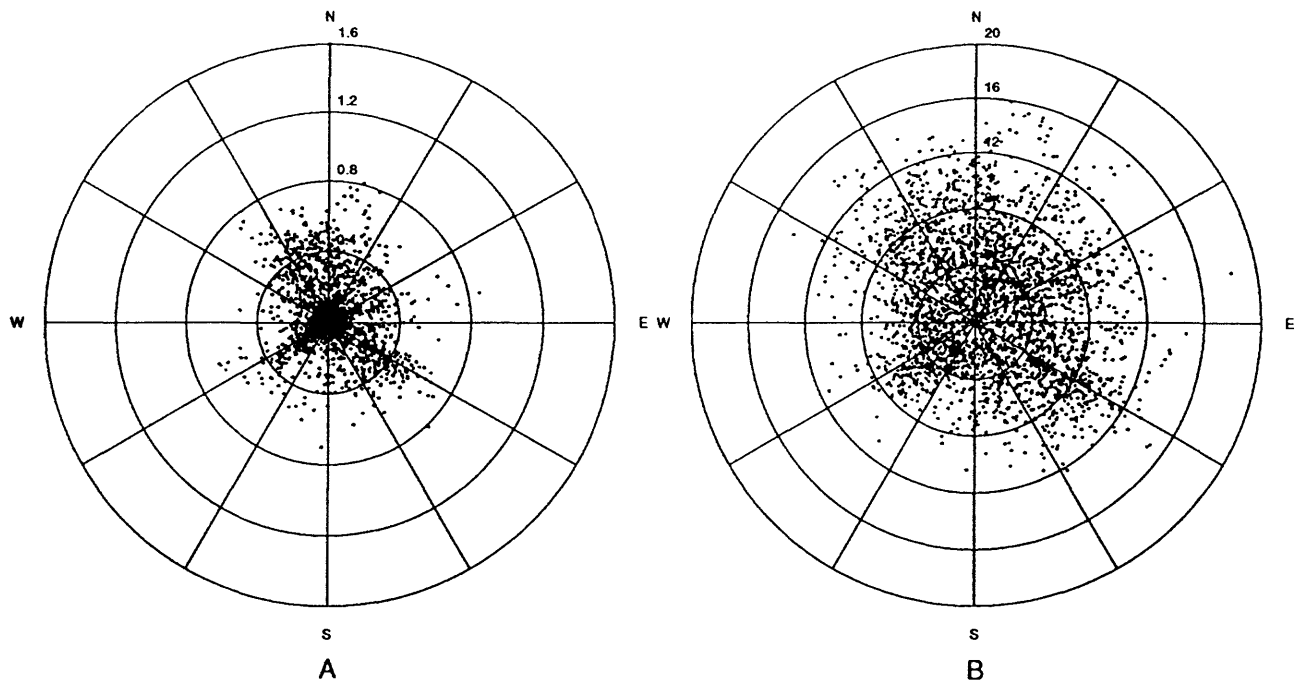


Figure 12. Directional scatter plots indicating (A) significant wave height verses wind direction and (B) wind speed verses wind direction for the 3951 mooring.

The spring data set (Figure 13) shows a trend of winds out of the south and east. The highest wind speeds were recorded out of the east (18.26 m/s) and the south (15.75 m/s). The largest significant wave heights were from winds out of the south (1.10 m) and east (1.00 m).

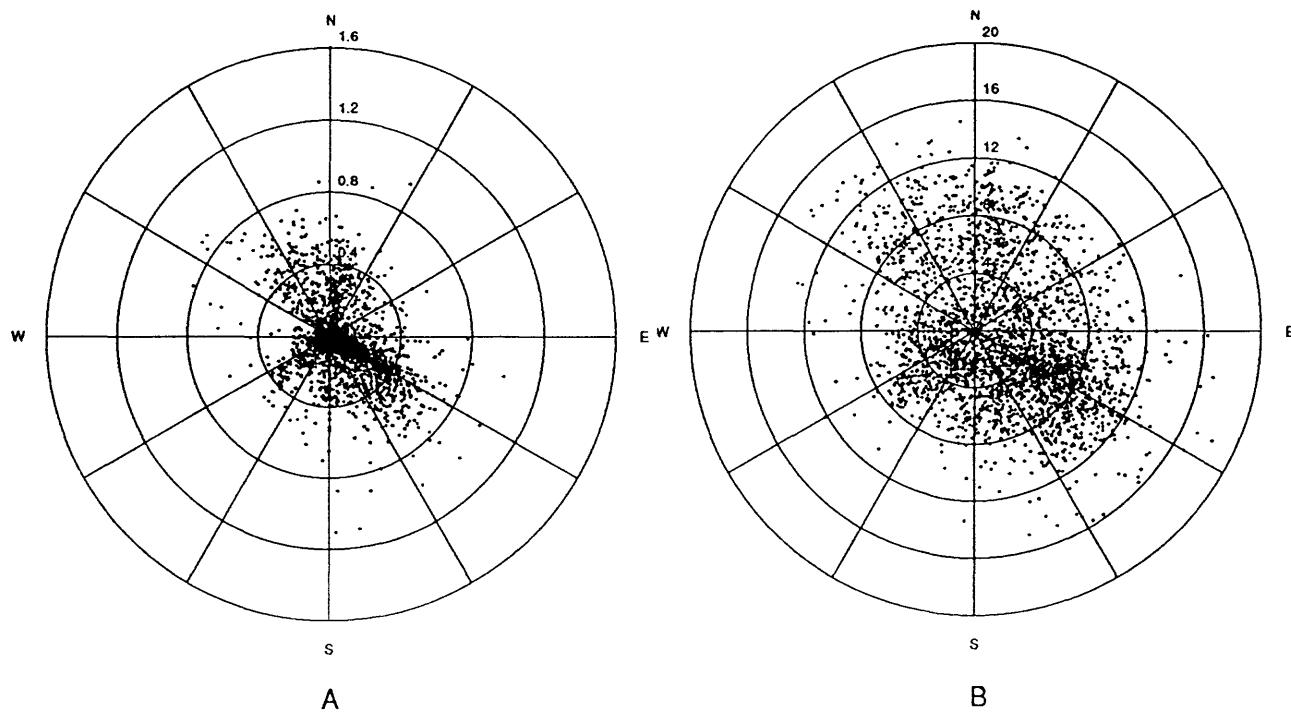


Figure 13. Directional scatter plots indicating (A) significant wave height verses wind direction and (B) wind speed verses wind direction for the spring wind statistics.

The winter data set (Figure 14) shows a slight trend of winds out the north and east. The highest wind speed were recorded out of the east (18.22 m/s) and the north (15.91 m/s) with the largest significant wave heights from winds out the the east (.86 m) and the north (.81 m).

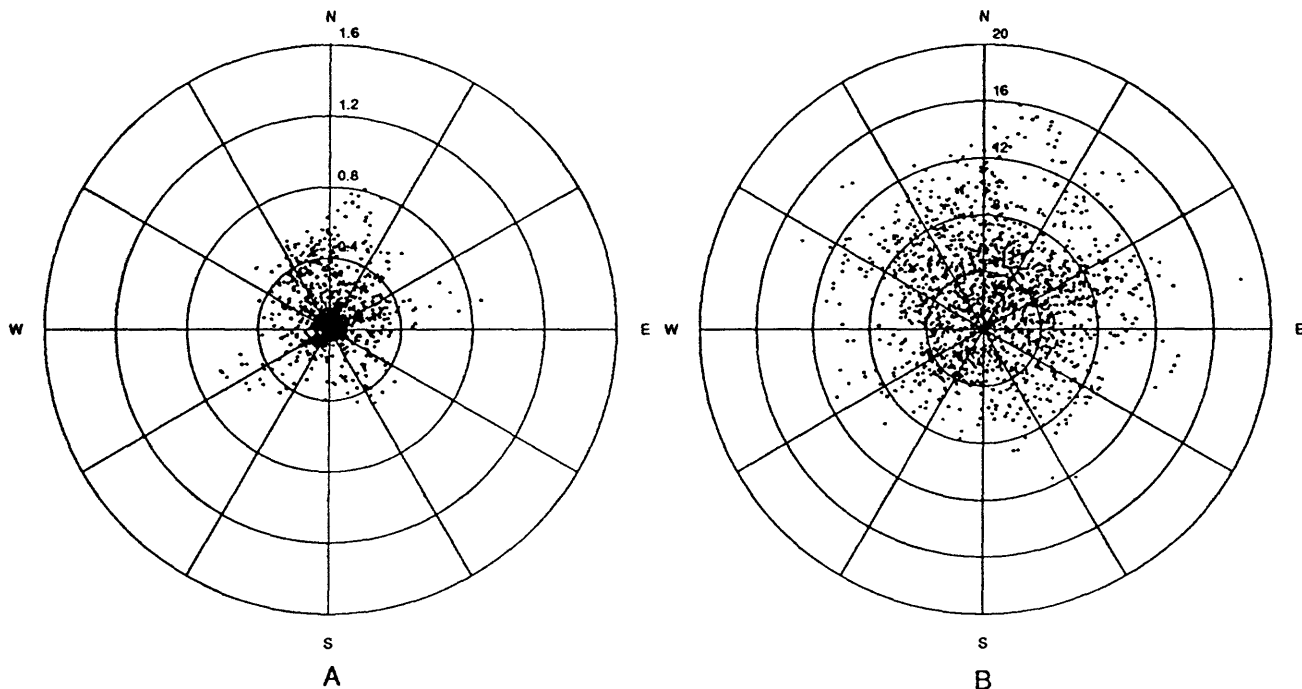


Figure 14. Directional scatter plots indicating (A) significant wave height verses wind direction and (B) wind speed verses wind direction for the winter wind statistics.

The fall data set (Figure 15) was composed of data sampled during September and October of the 3871 mooring. No other processed mooring data were available. There was a clear trend toward higher wind speeds and significant wave heights when winds were from the north as is shown above in the 3871 directional scatter plot. Wind speeds from the north range from 0 to 18.12 m/s where wind speeds from all other directions were never greater than 11 m/s. Significant wave heights during north winds range from 0 to .97 and significant wave heights greater than 0.70 were not observed during south, east, or west winds.

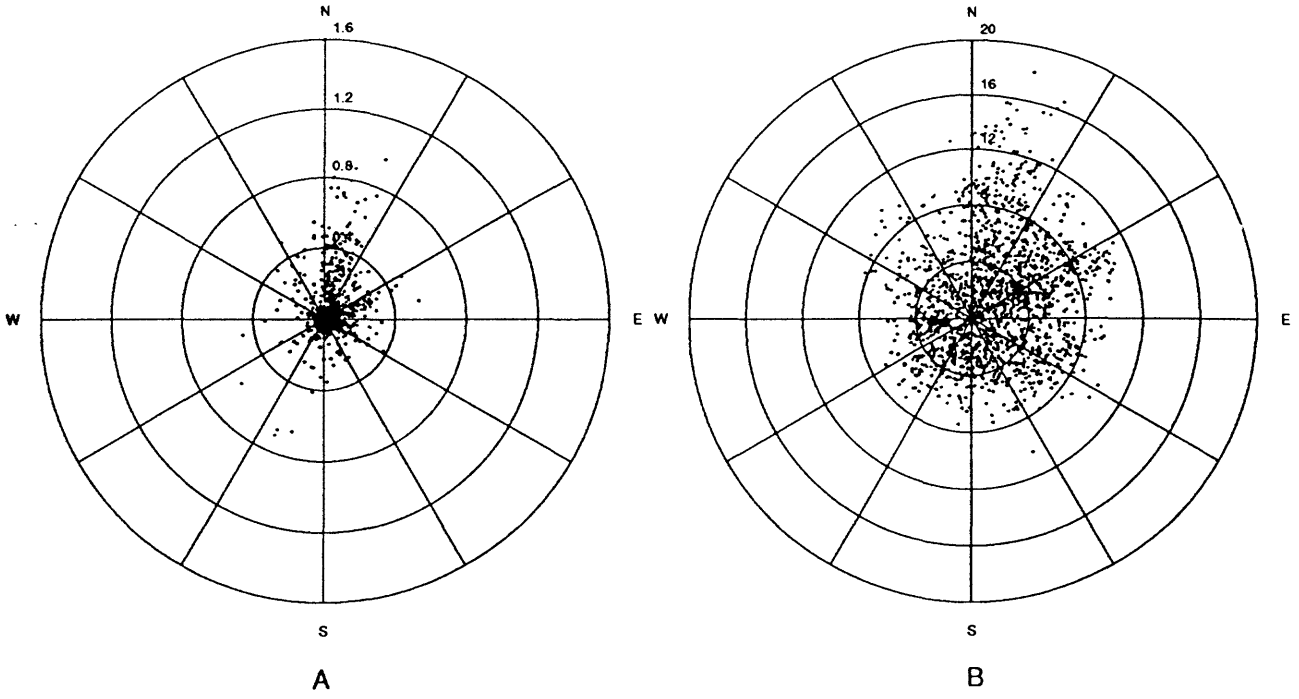


Figure 15. Directional scatter plots indicating (A) significant wave height verse wind direction and (B) wind speed verses wind direction for the fall wind statistics.

Acknowledgments

This work was funded by the United States Geological Survey's National Coastal Geology Program as part of the Alabama/Mississippi Coastal Erosion and Pollution Study. We would like to thank Drs. W.W. Schroeder and M. Noble for assisting in mooring design, B. Strahle and M. Martini for mooring deployment and data recovery, and M. Dardeay and A. Gunter for mooring maintenance.

REFERENCES

Guza, R. T. and Thornton, E. B., 1980, Local and Shoaled Comparisons of Sea Surface Elevations, Pressure, and Velocities: *Journal of Geophysical Research*, Vol. 85, No. C3, pp 1524-1530.

Schroeder, W. W. and Lysinger, R. W., 1979, Hydrography and Circulation of Mobile Bay, in *Symposium on the Natural Resources of Mobile Bay Estuary, Alabama*, in Loyacano, H. A. and Smith, J. P., eds., U.S. Army Corps of Engineers, Mobile District, Mobile Alabama, pp 75-94.

Schroeder, W. W. and Wiseman, W. J., 1988, The Mobile Bay Estuary Stratification, Oxygen depletion and Jubilees, *Hydrodynamics of Estuaries: Vol II Estuarine Case Studies*, pp 41-52.

APPENDIX A

Julian Date Calendars

Julian Date Calendar for Standard Years

Day	Jan	Feb	Mar	Apr	May	Jun	Jul	Aug	Sep	Oct	Nov	Dec	Day
1	1	32	60	91	121	152	182	213	244	274	305	335	1
2	2	33	61	92	122	153	183	214	245	275	306	336	2
3	3	34	62	93	123	154	184	215	246	276	307	337	3
4	4	35	63	94	124	155	185	216	247	277	308	338	4
5	5	36	64	95	125	156	186	217	248	278	309	339	5
6	6	37	65	96	126	157	187	218	249	279	310	340	6
7	7	38	66	97	127	158	188	219	250	280	311	341	7
8	8	39	67	98	128	159	189	220	251	281	312	342	8
9	9	40	68	99	129	160	190	221	252	282	313	343	9
10	10	41	69	100	130	161	191	222	253	283	314	344	10
11	11	42	70	101	131	162	192	223	254	284	315	345	11
12	12	43	71	102	132	163	193	224	255	285	316	346	12
13	13	44	72	103	133	164	194	225	256	286	317	347	13
14	14	45	73	104	134	165	195	226	257	287	318	348	14
15	15	46	74	105	135	166	196	227	258	288	319	349	15
16	16	47	75	106	136	167	197	228	259	289	320	350	16
17	17	48	76	107	137	168	198	229	260	290	321	351	17
18	18	49	77	108	138	169	199	230	261	291	322	352	18
19	19	50	78	109	139	170	200	231	262	292	323	353	19
20	20	51	79	110	140	171	201	232	263	293	324	354	20
21	21	52	80	111	141	172	202	233	264	294	325	355	21
22	22	53	81	112	142	173	203	234	265	295	326	356	22
23	23	54	82	113	143	174	204	235	266	296	327	357	23
24	24	55	83	114	144	175	205	236	267	297	328	358	24
25	25	56	84	115	145	176	206	237	268	298	329	359	25
26	26	57	85	116	146	177	207	238	269	299	330	360	26
27	27	58	86	117	147	178	208	239	270	300	331	361	27
28	28	59	87	118	148	179	209	240	271	301	332	362	28
29	29		88	119	149	180	210	241	272	302	333	363	29
30	30		89	120	150	181	211	242	273	303	334	364	30
31	31		90		151		212	243		304		365	31

Julian Date Calendar for Leap Years

Day	Jan	Feb	Mar	Apr	May	Jun	Jul	Aug	Sep	Oct	Nov	Dec	Day
1	1	32	61	92	122	153	183	214	245	275	306	336	1
2	2	33	62	93	123	154	184	215	246	276	307	337	2
3	3	34	63	94	124	155	185	216	247	277	308	338	3
4	4	35	64	95	125	156	186	217	248	278	309	339	4
5	5	36	65	96	126	157	187	218	249	279	310	340	5
6	6	37	66	97	127	158	188	219	250	280	311	341	6
7	7	38	67	98	128	159	189	220	251	281	312	342	7
8	8	39	68	99	129	160	190	221	252	282	313	343	8
9	9	40	69	100	130	161	191	222	253	283	314	344	9
10	10	41	70	101	131	162	192	223	254	284	315	345	10
11	11	42	71	102	132	163	193	224	255	285	316	346	11
12	12	43	72	103	133	164	194	225	256	286	317	347	12
13	13	44	73	104	134	165	195	226	257	287	318	348	13
14	14	45	74	105	135	166	196	227	258	288	319	349	14
15	15	46	75	106	136	167	197	228	259	289	320	350	15
16	16	47	76	107	137	168	198	229	260	290	321	351	16
17	17	48	77	108	138	169	199	230	261	291	322	352	17
18	18	49	78	109	139	170	200	231	262	292	323	353	18
19	19	50	79	110	140	171	201	232	263	293	324	354	19
20	20	51	80	111	141	172	202	233	264	294	325	355	20
21	21	52	81	112	142	173	203	234	265	295	326	356	21
22	22	53	82	113	143	174	204	235	266	296	327	357	22
23	23	54	83	114	144	175	205	236	267	297	328	358	23
24	24	55	84	115	145	176	206	237	268	298	329	359	24
25	25	56	85	116	146	177	207	238	269	299	330	360	25
26	26	57	86	117	147	178	208	239	270	300	331	361	26
27	27	58	87	118	148	179	209	240	271	301	332	362	27
28	28	59	88	119	149	180	210	241	272	302	333	363	28
29	29	60	89	120	150	181	211	242	273	303	334	364	29
30	30		90	121	151	182	212	243	274	304	335	365	30
31	31		91		152		213	244		305		366	31

APPENDIX B

Calibration Coefficients and Equations

Pressure Coefficients and Calibration Equations

MOORING # 3771,3871

SENSOR # 688

Calibration Equations

$$AD = ((AH - AC) / TR) * T$$

$$BD = ((BH - BC) / TR) * T$$

$$TOD = ((TOH - TOC) / TR) * T$$

$$A = AC + AD$$

$$B = BC + BD$$

$$TO = TOC + TOD$$

$$FO = (1.0 / TO) / *10^6$$

Calculate Pressure in psi

$$C = 1.0 - F / FO$$

$$APRESS = A * C - B * (C^2)$$

Convert psi to Millibars

$$PRESS = APRESS * G$$

Pressure Sensor Coefficients

T = Temperature (deg C)

F = Pressure Frequency

$$AH = 2316.34$$

$$AC = 2318.71$$

$$BH = 1359.52$$

$$BC = 1363.01$$

$$TOH = 24.50147$$

$$TOC = 24.50364$$

$$T1H = 26.96107$$

$$T1C = 26.96077$$

$$TR = 23.89$$

$$G = 68.946498$$

Instrument Manufacturer:

PAROSCIENTIFIC, INC

4500 148th AVENUE N.E

REDMOND, WA. 98052

Pressure Calibration Coefficients and Equations

MOORING # 3951

SENSOR # 47037

Calibration Equations

$$C = C_1 + C_2 * U + C_3 * U^2$$

$$D = D_1 + D_2 * U$$

$$T_0 = T_1 + T_2 * U + T_3 * U^2 + T_4 * U^3 + T_5 * U^4$$

Calculate Pressure in psi

$$Q = (1/F) * 10^6$$

$$APRESS = C(1 - T_0^2/T_2) * (1 - D(1 - T_0^2/T^2))$$

Convert psi to Millibars

$$PRESS = APRESS * G$$

Pressure Sensor Coefficients

$$C1 = 175.1086$$

$$C2 = -5.7076E-03$$

$$C3 = -1.8789E-05$$

$$D1 = 0.0456$$

$$D2 = 0.0$$

$$T1 = 24.3778$$

$$T2 = -1.3589$$

$$T3 = 1.1977E-04$$

$$T4 = 1.2322E-09$$

$$T5 = 0.0$$

Instrument Manufacturer:

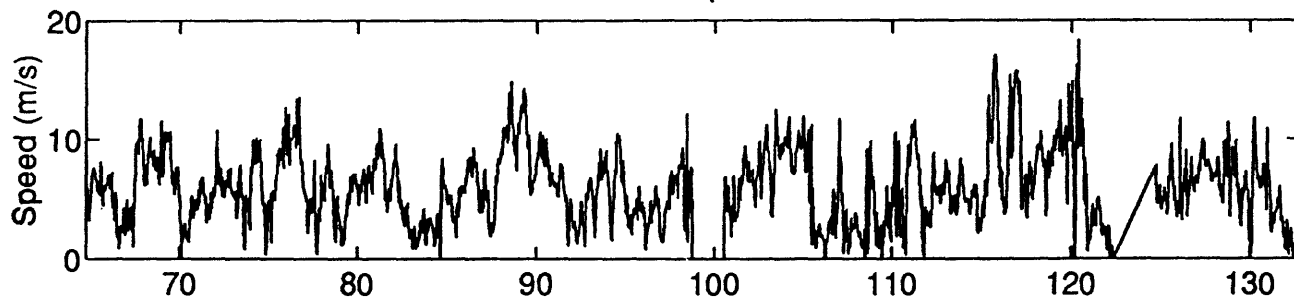
PAROSCIENTIFIC, INC
4500 148th AVENUE N.E
REDMOND, WA. 98052

APPENDIX C

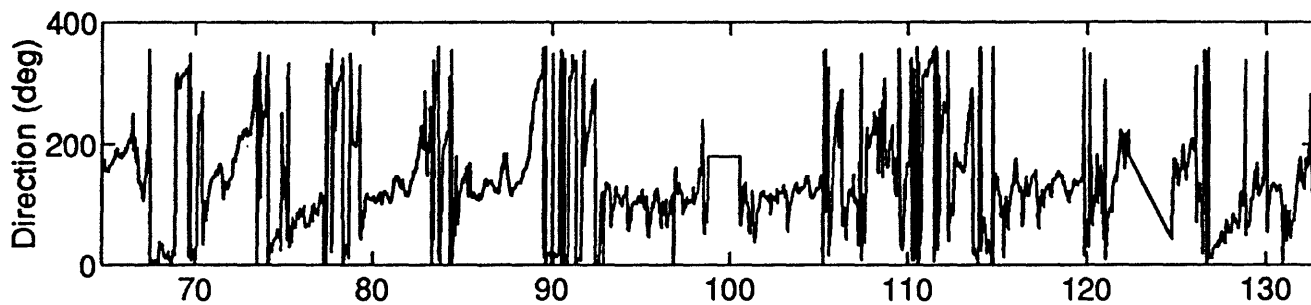
Time Series Graphs

Mooring 3771

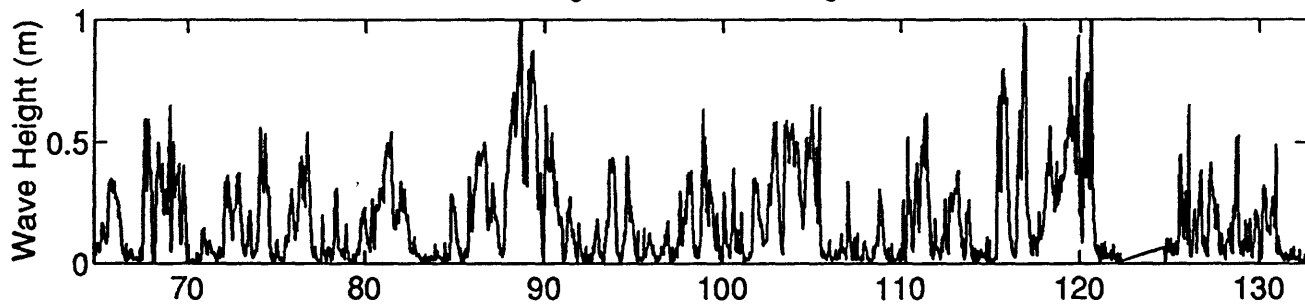
Wind Speed



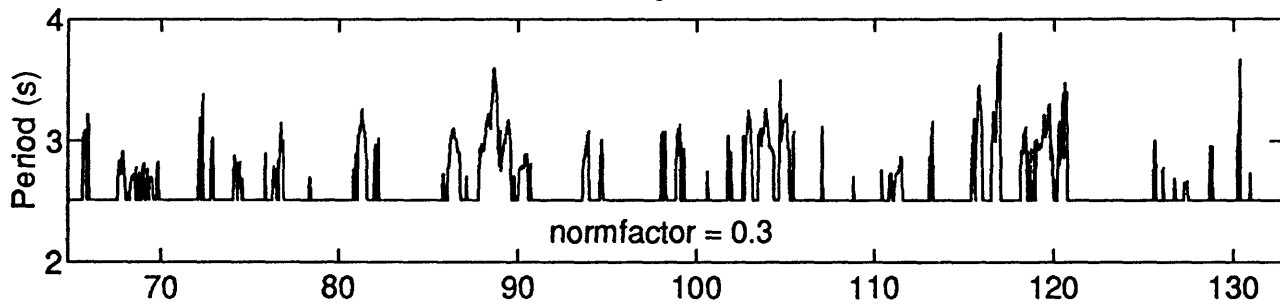
Wind Direction



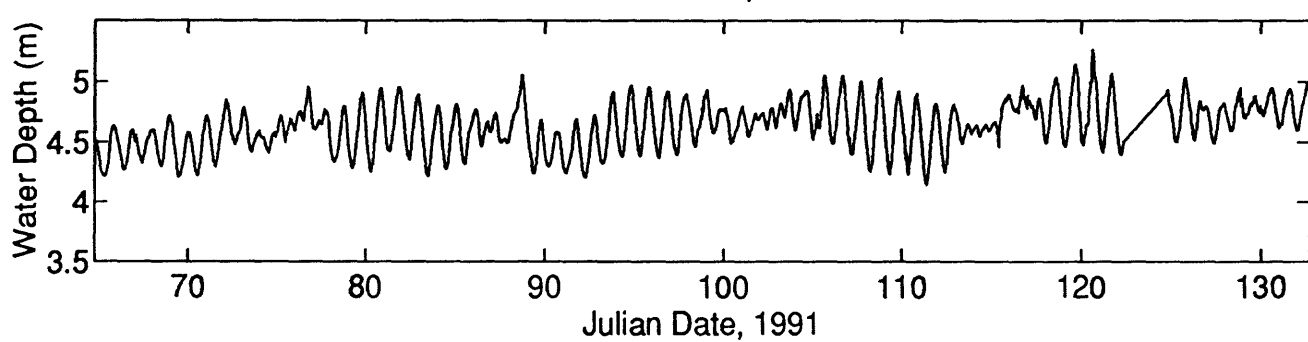
Significant Wave Height

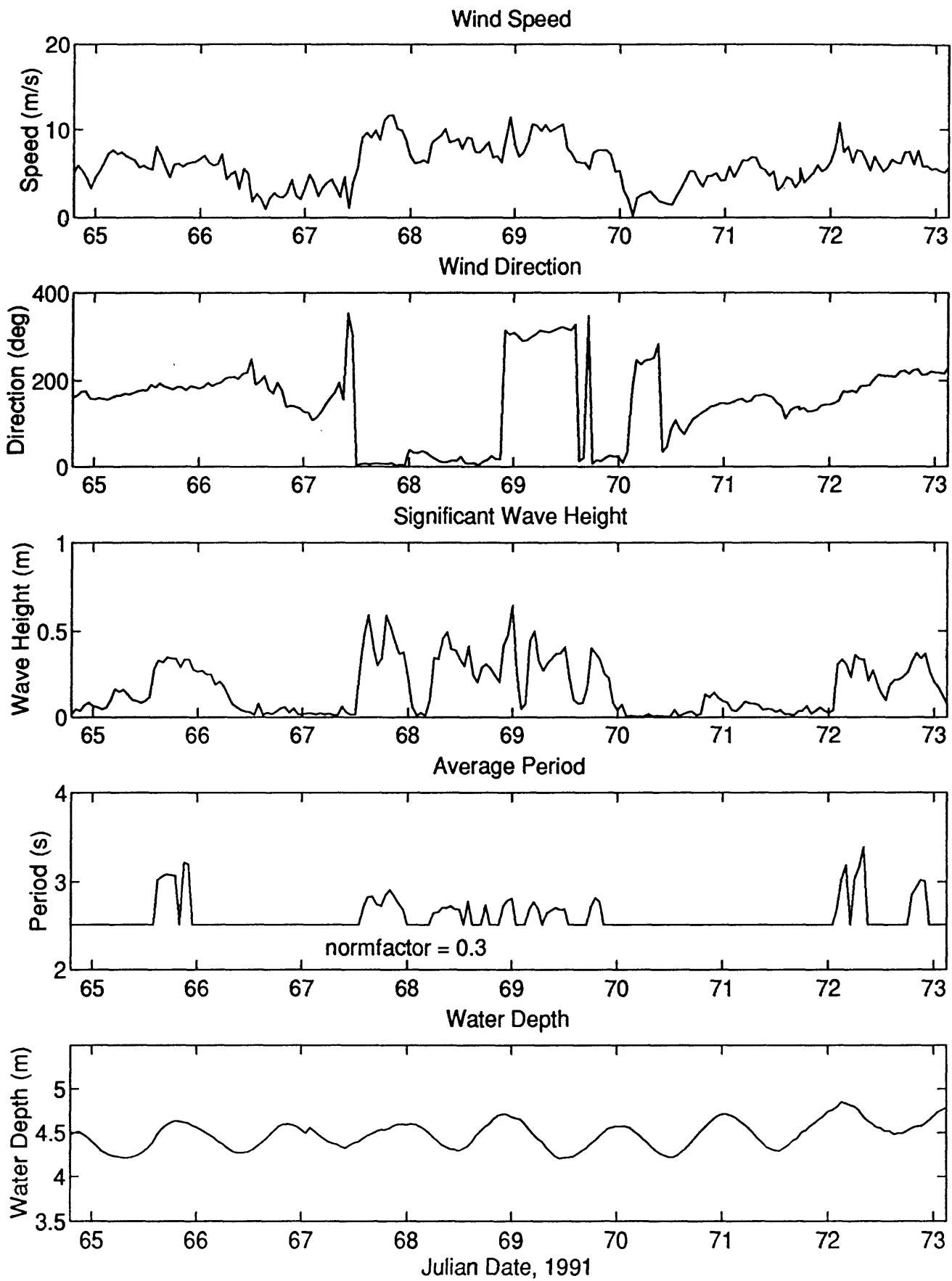


Average Period

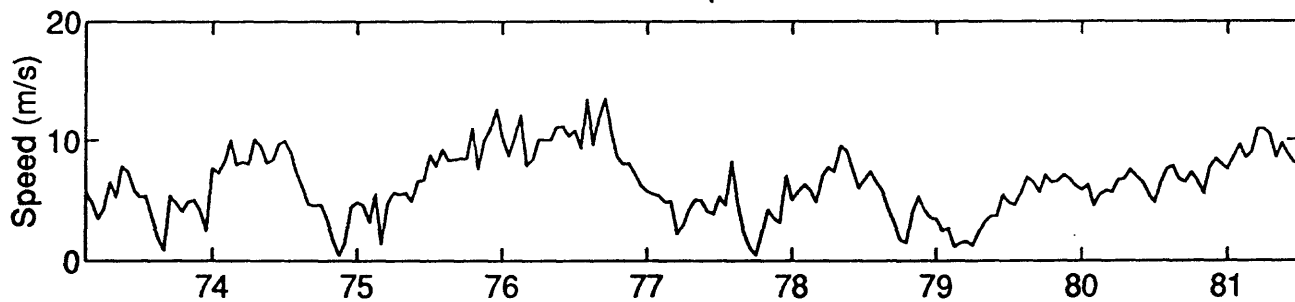


Water Depth

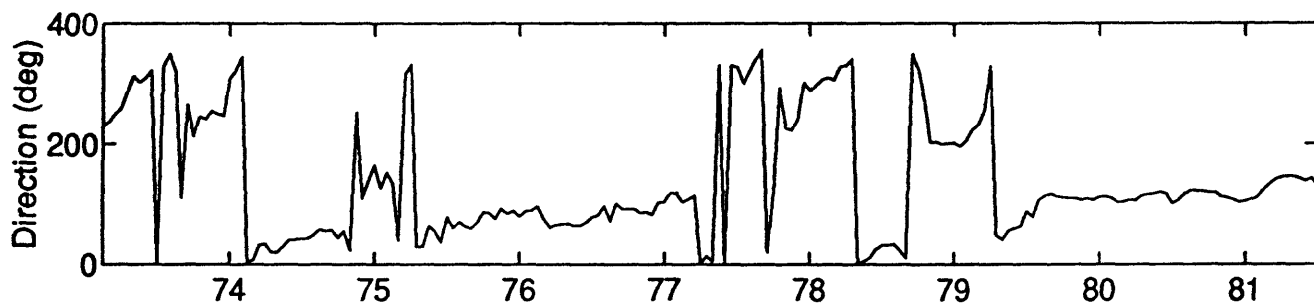




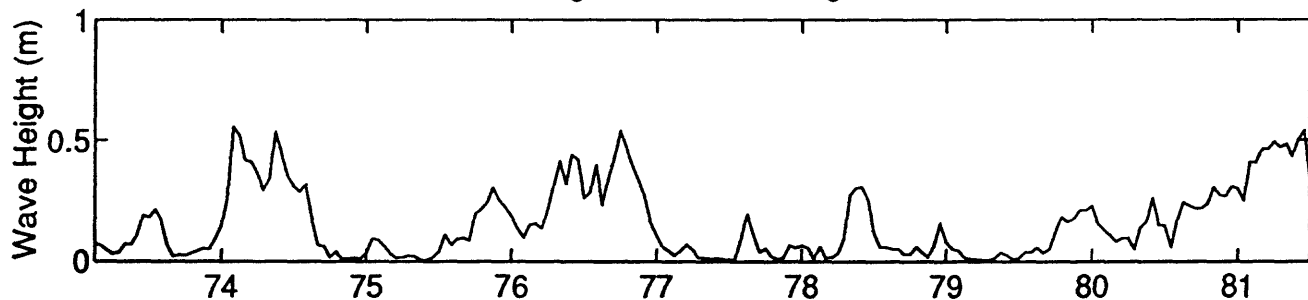
Wind Speed



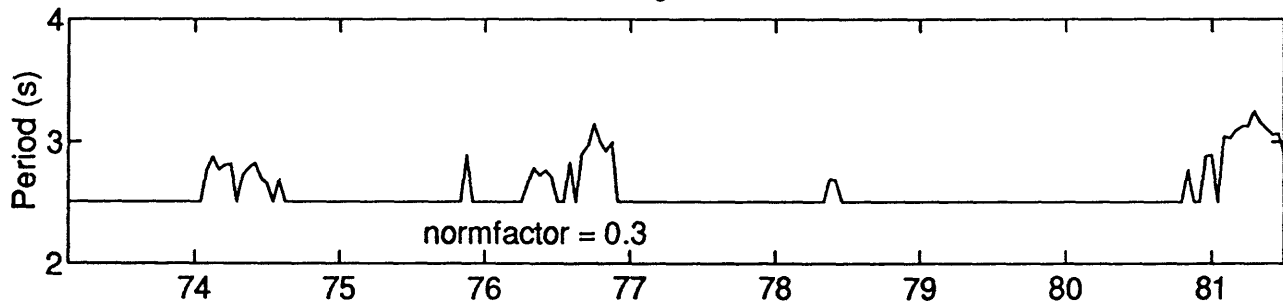
Wind Direction



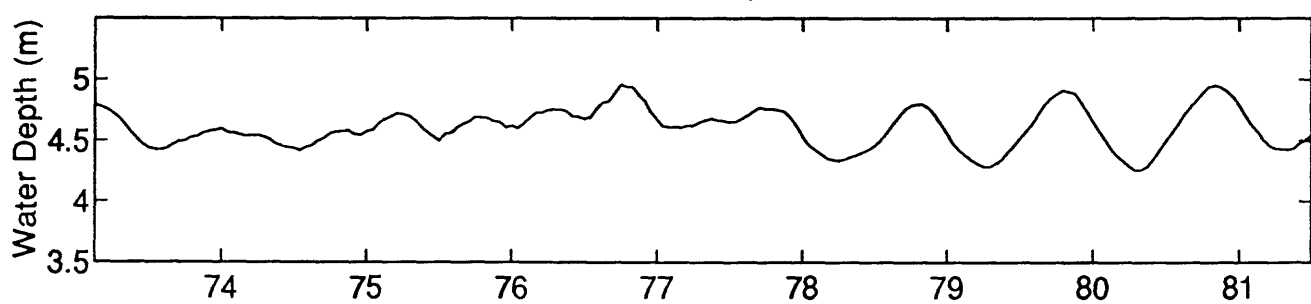
Significant Wave Height



Average Period

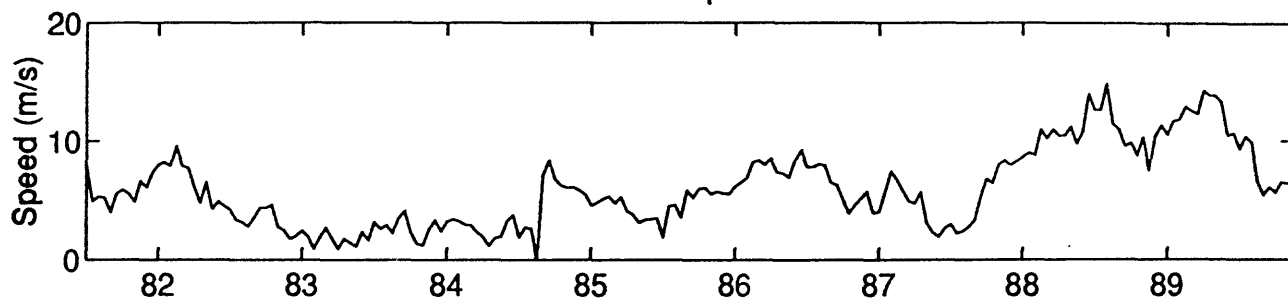


Water Depth

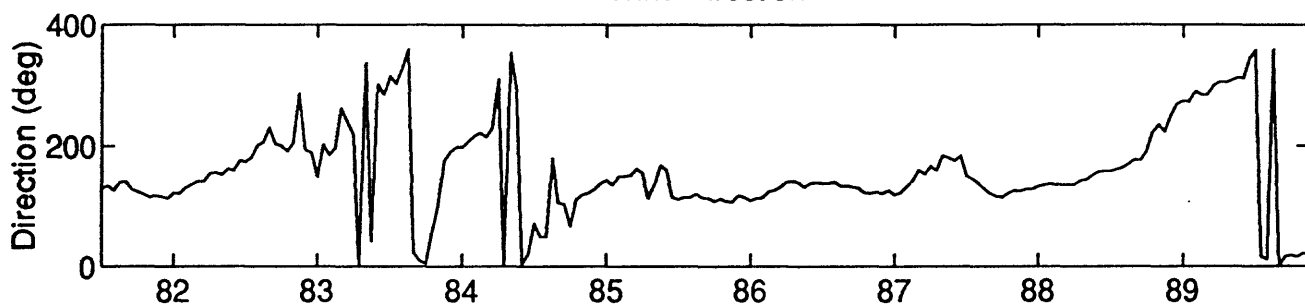


Julian Date, 1991

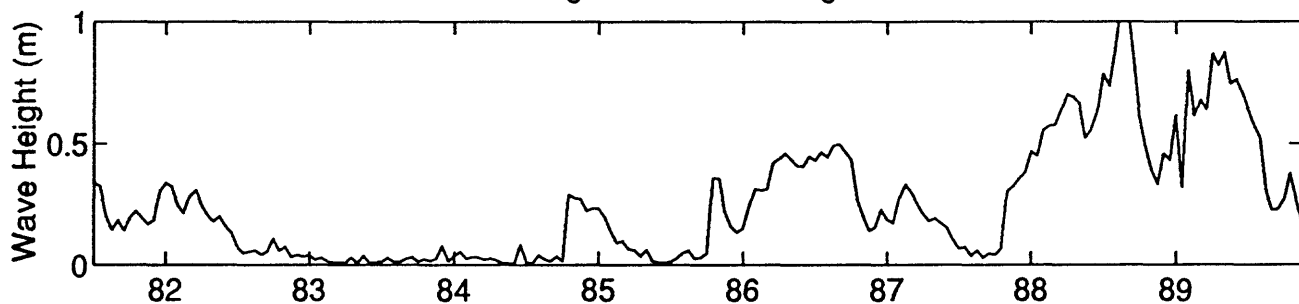
Wind Speed



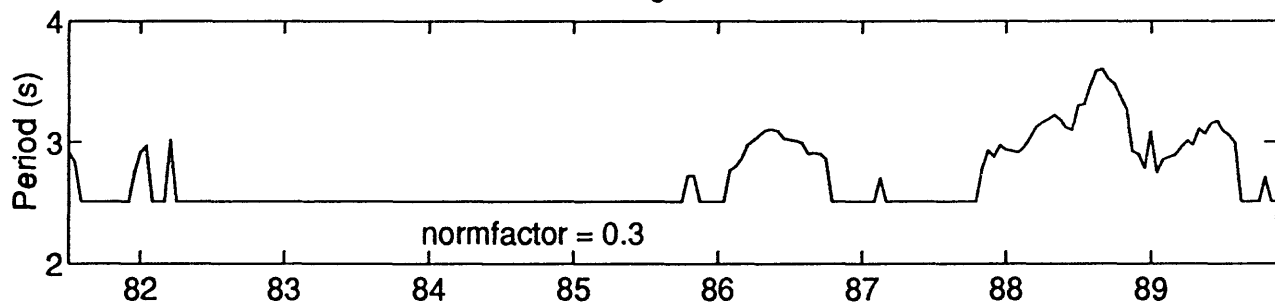
Wind Direction



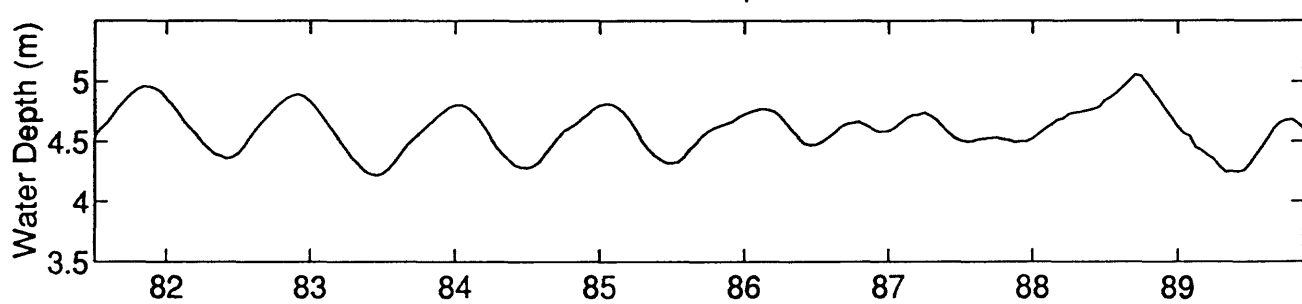
Significant Wave Height



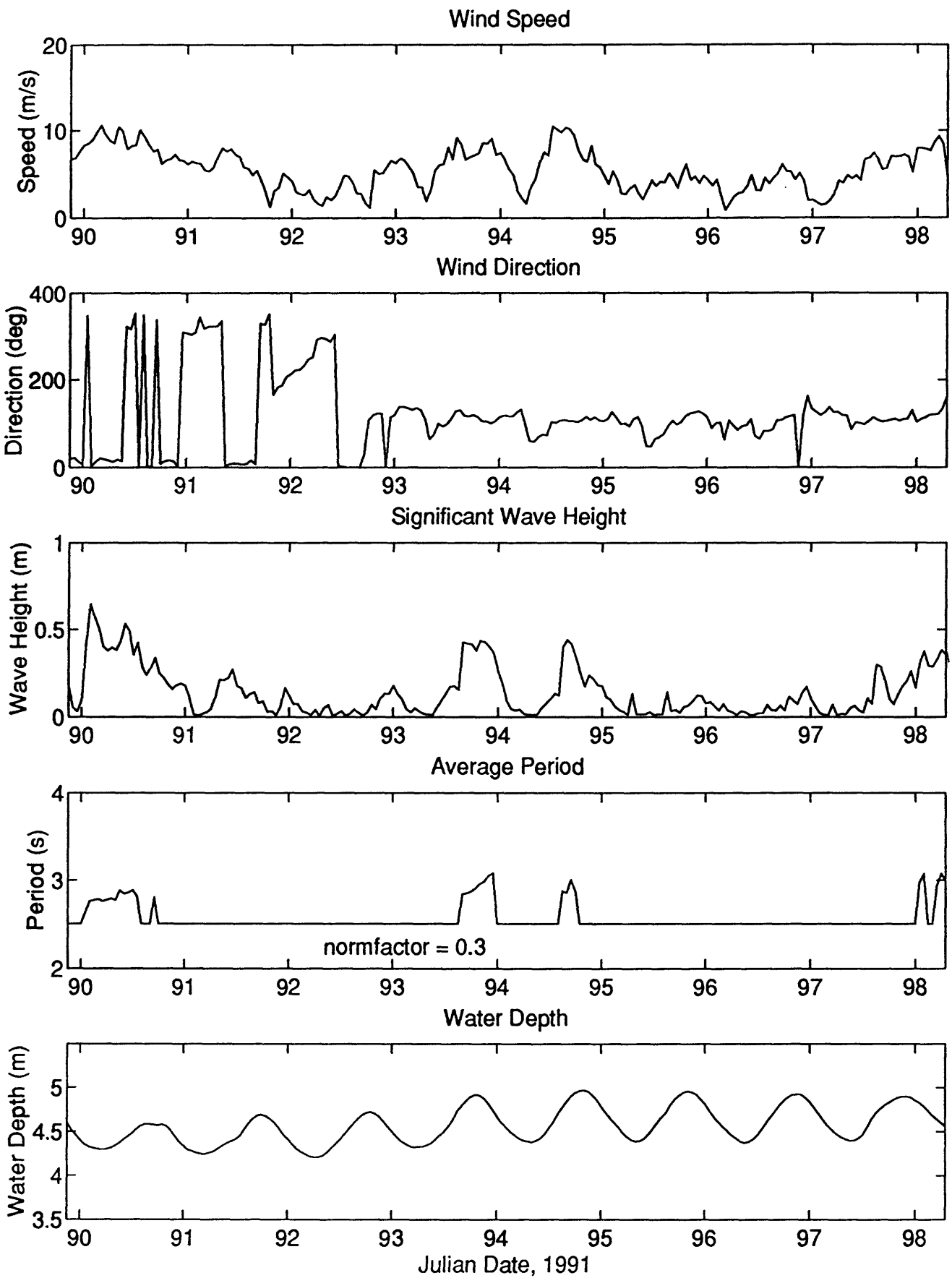
Average Period



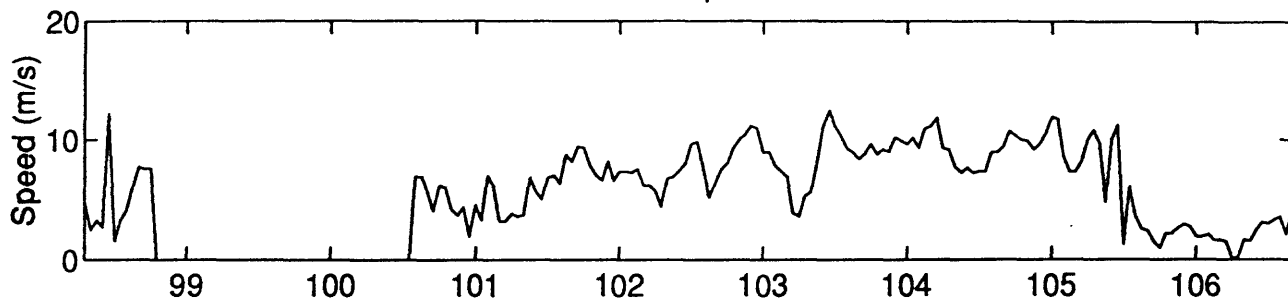
Water Depth



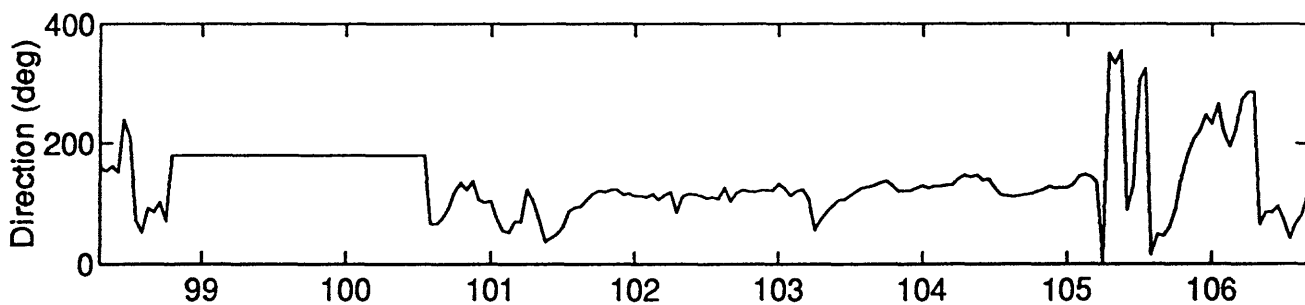
Julian Date, 1991



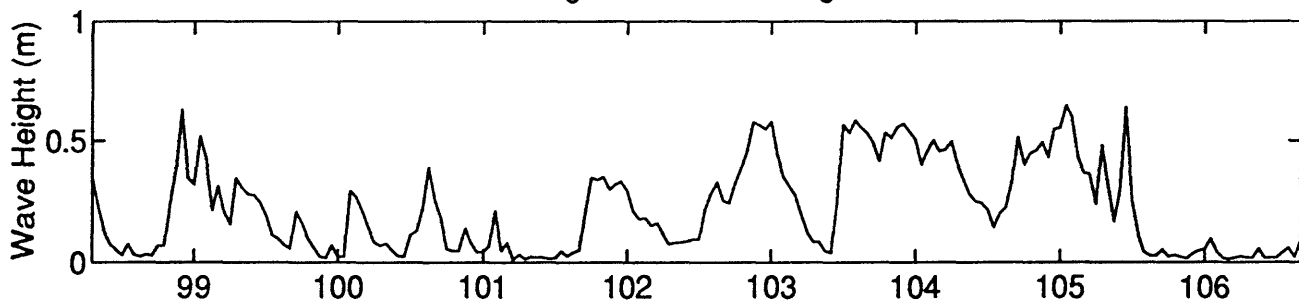
Wind Speed



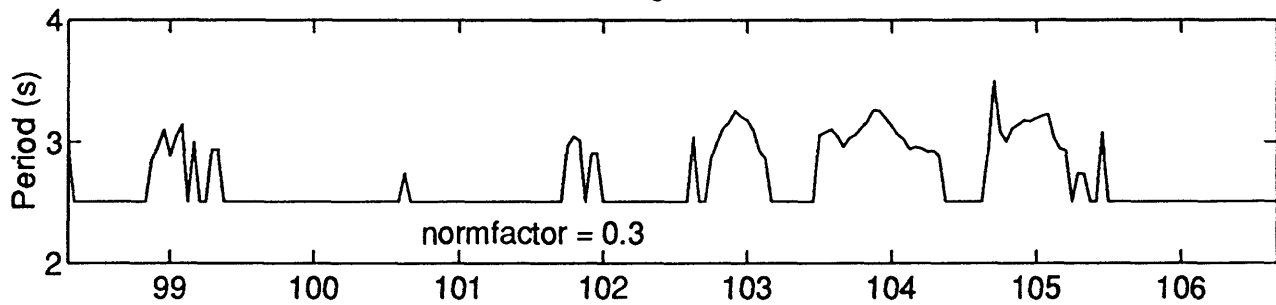
Wind Direction



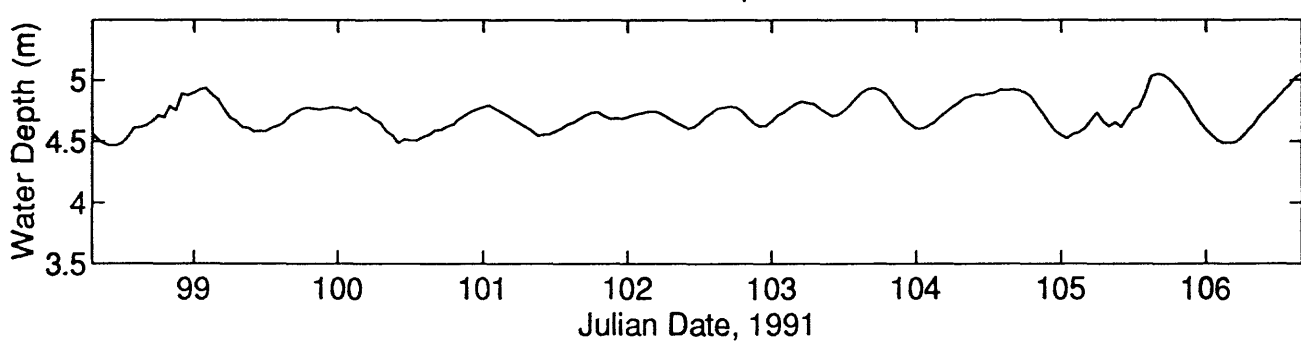
Significant Wave Height



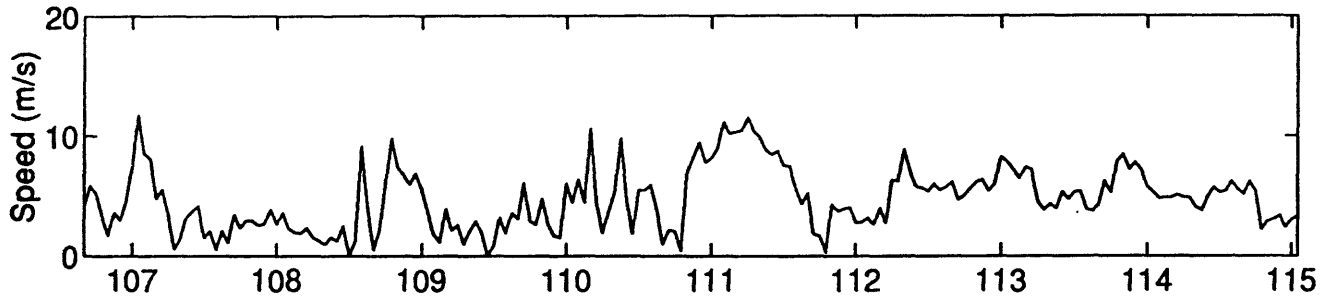
Average Period



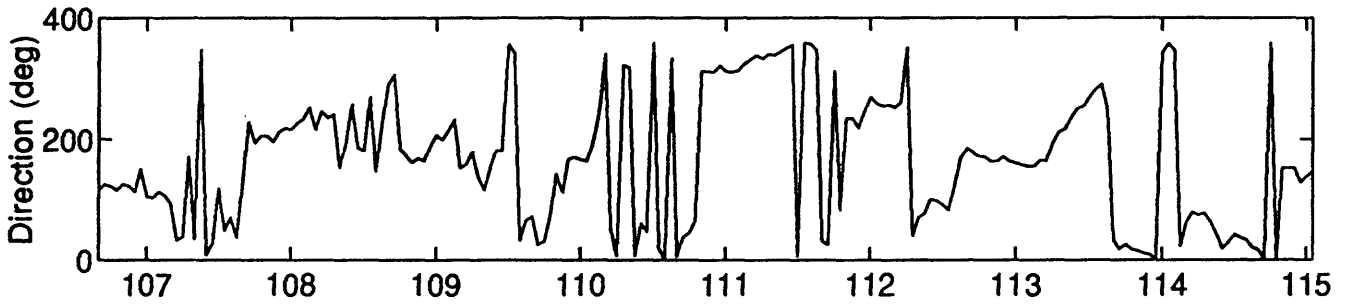
Water Depth



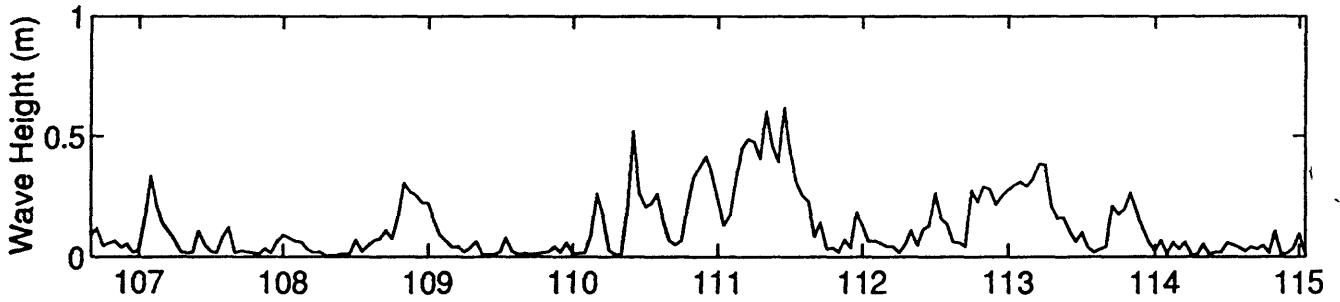
Wind Speed



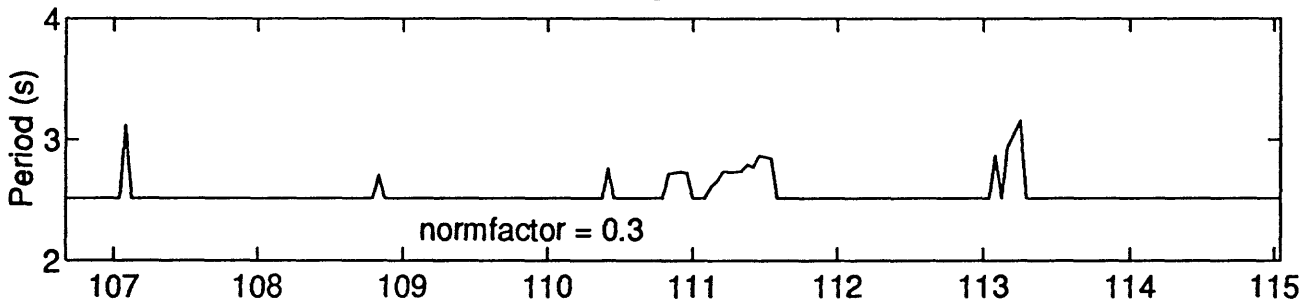
Wind Direction



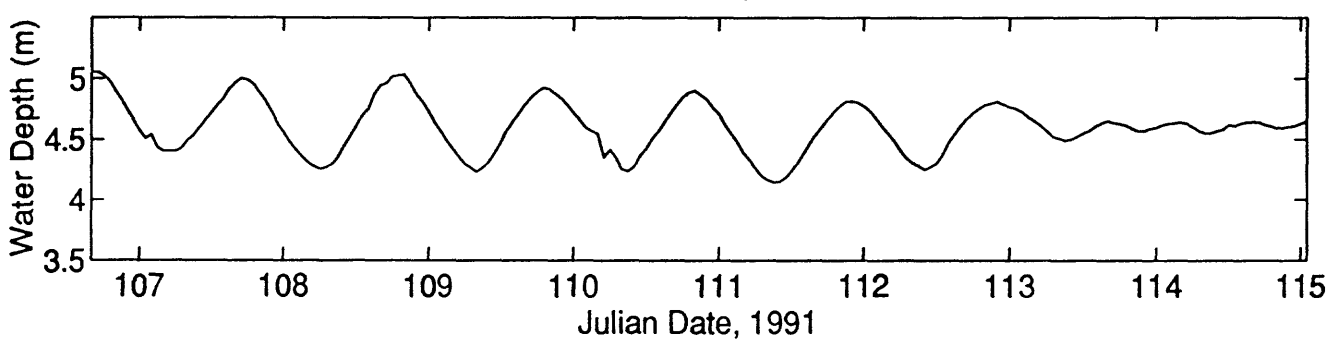
Significant Wave Height



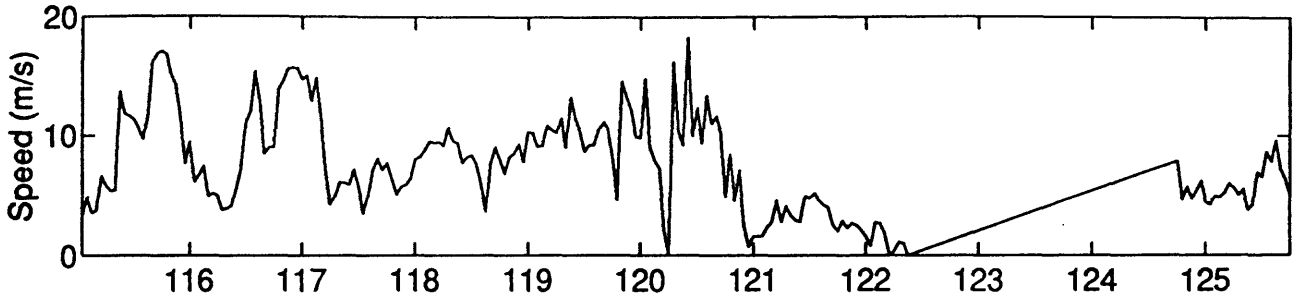
Average Period



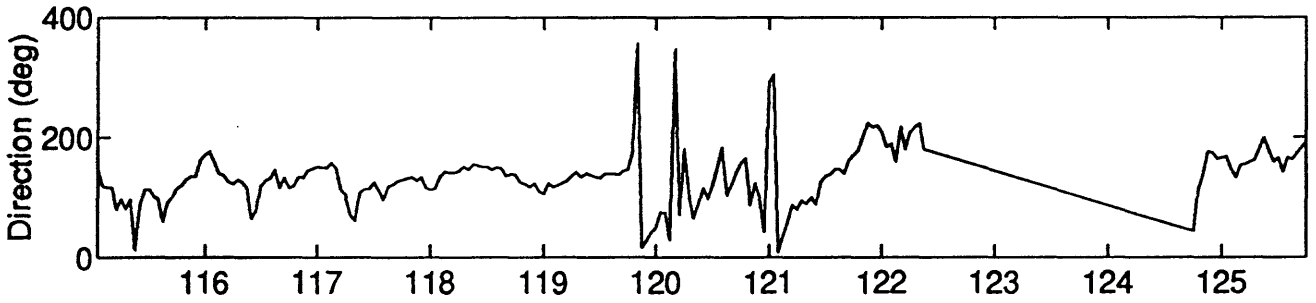
Water Depth



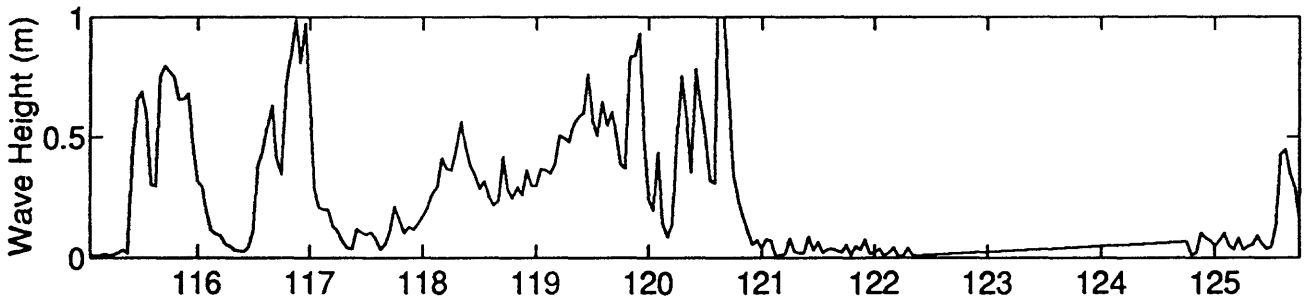
Wind Speed



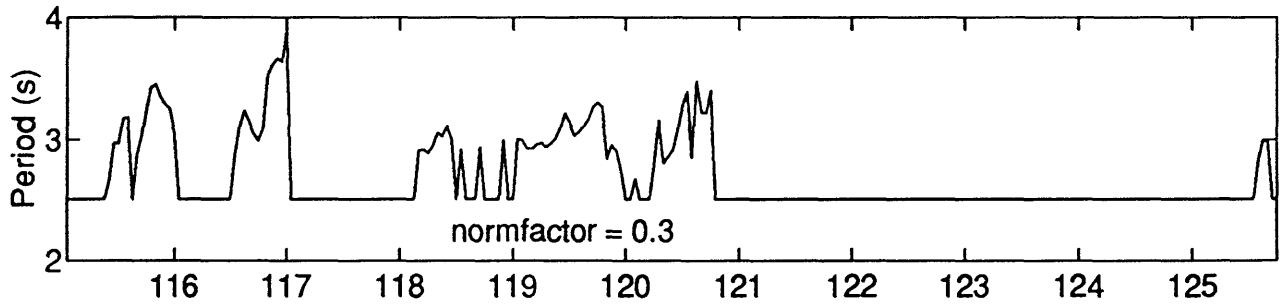
Wind Direction



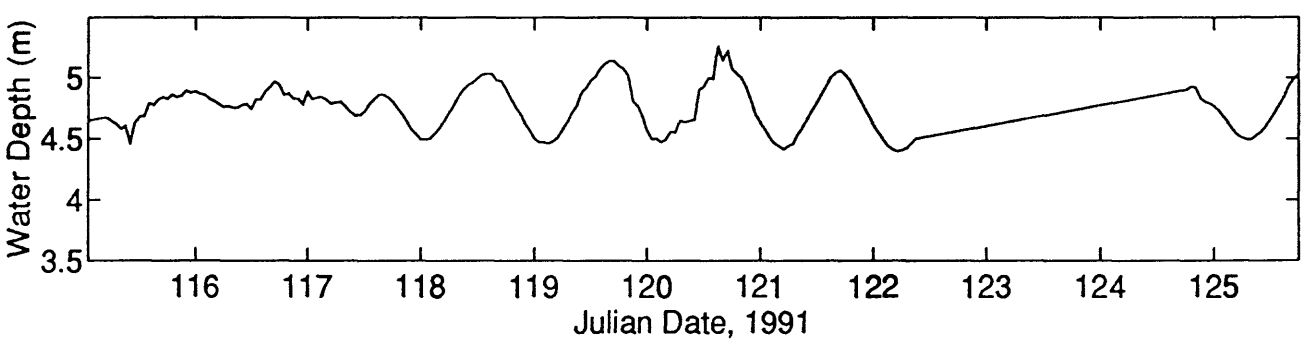
Significant Wave Height

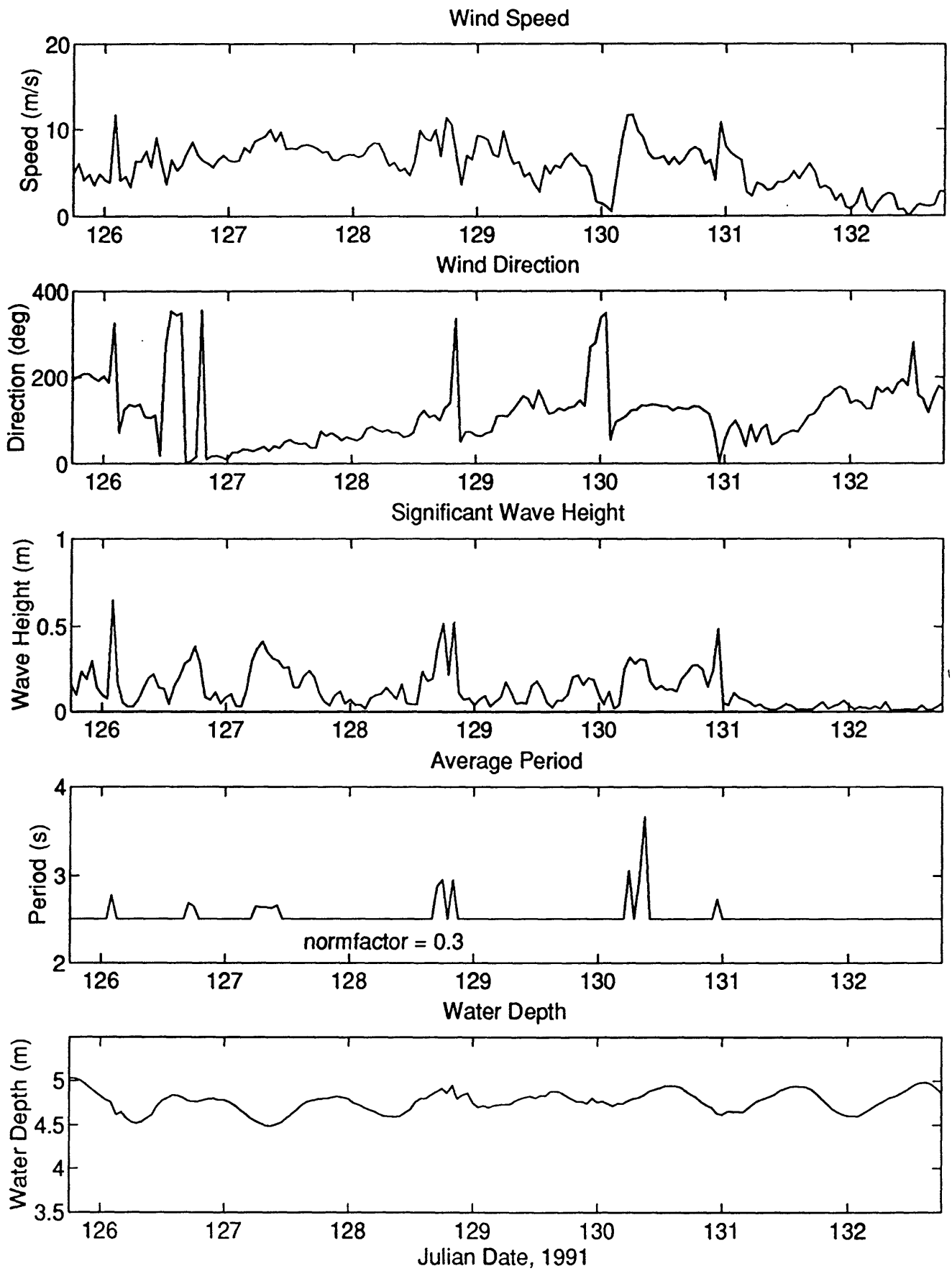


Average Period



Water Depth



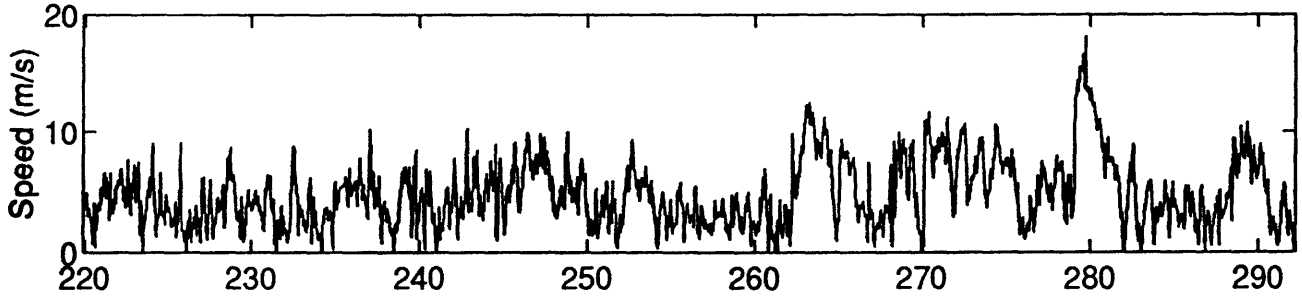


APPENDIX D

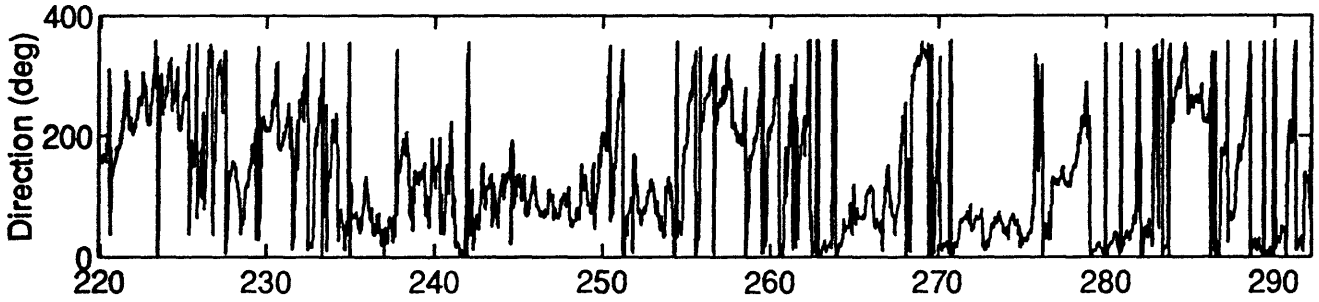
Time Series Graphs

Mooring 3871

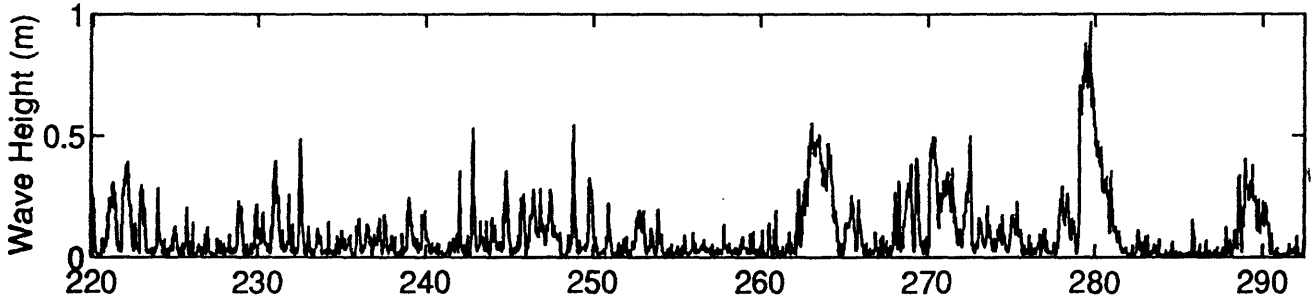
Wind Speed



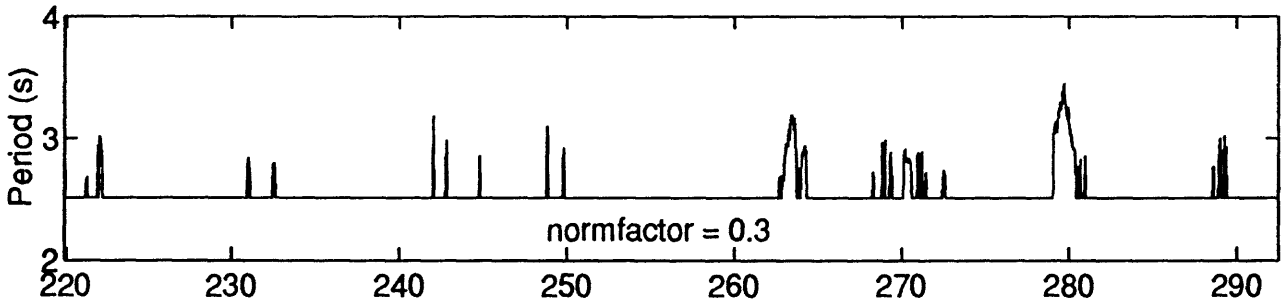
Wind Direction



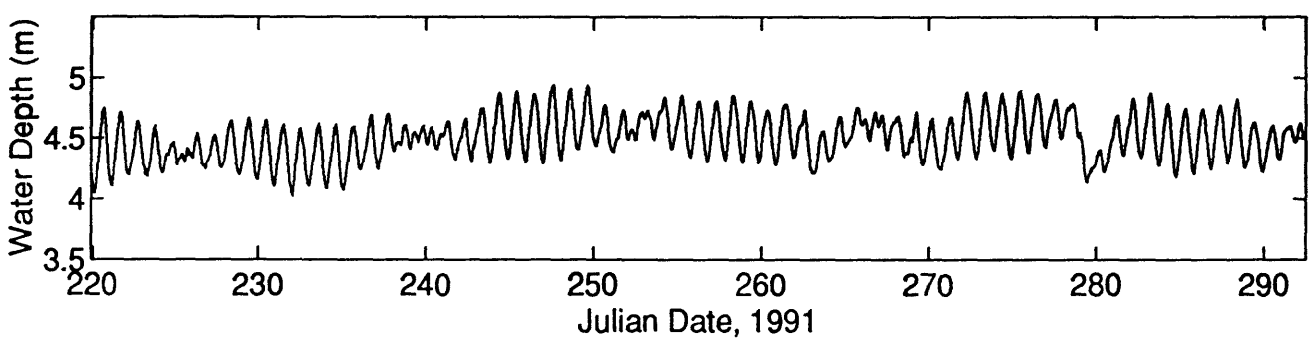
Significant Wave Height

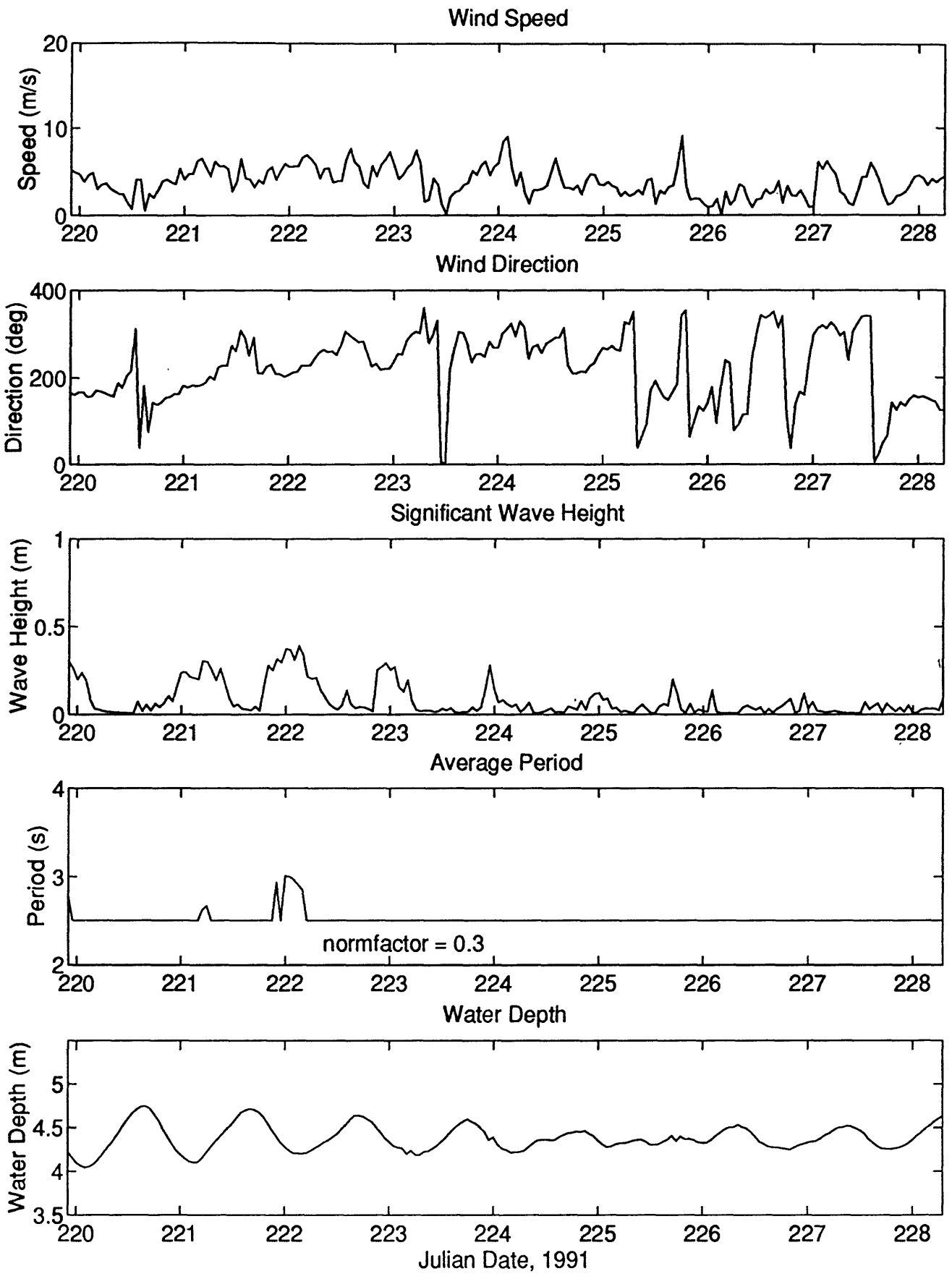


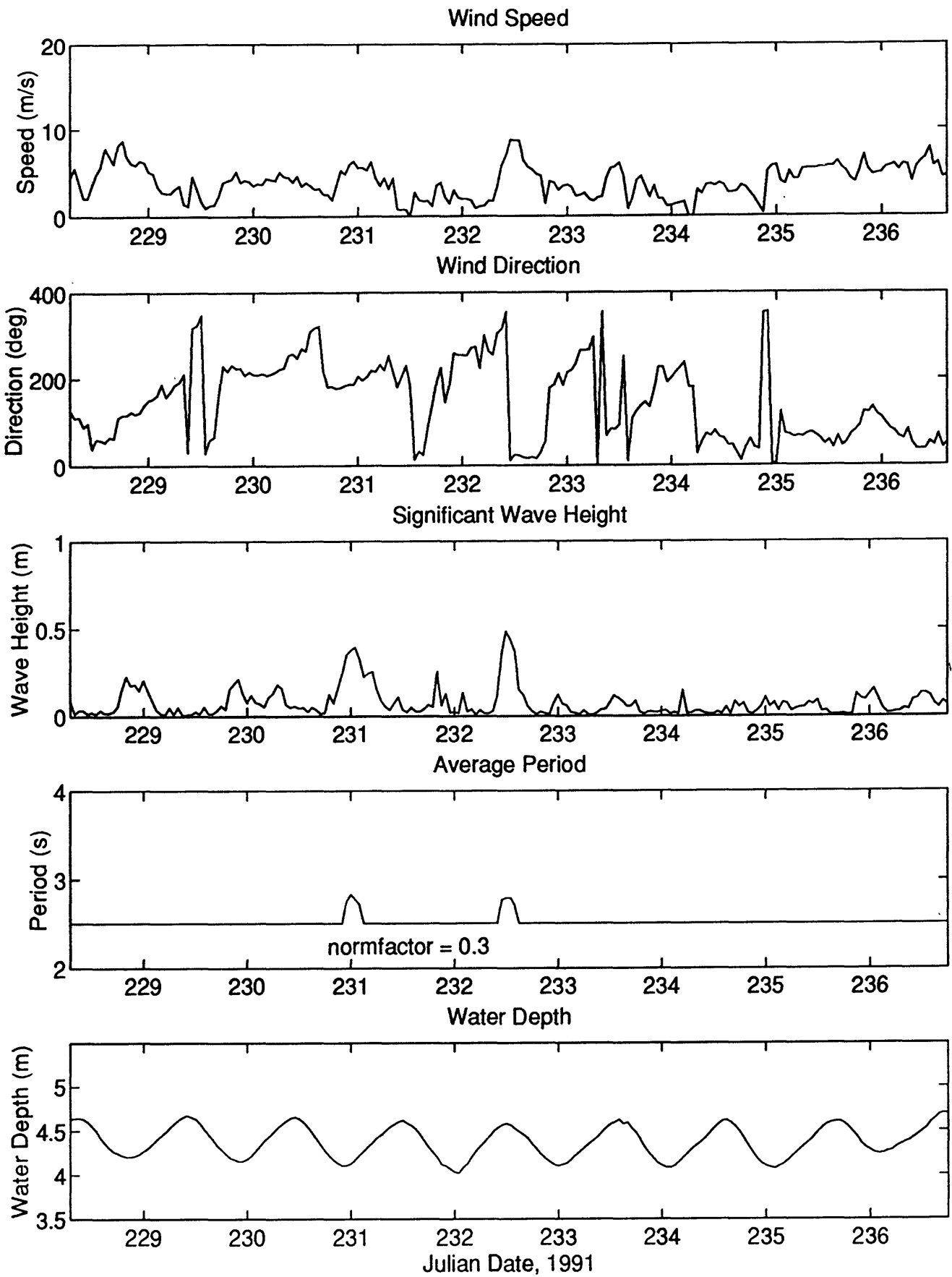
Average Period

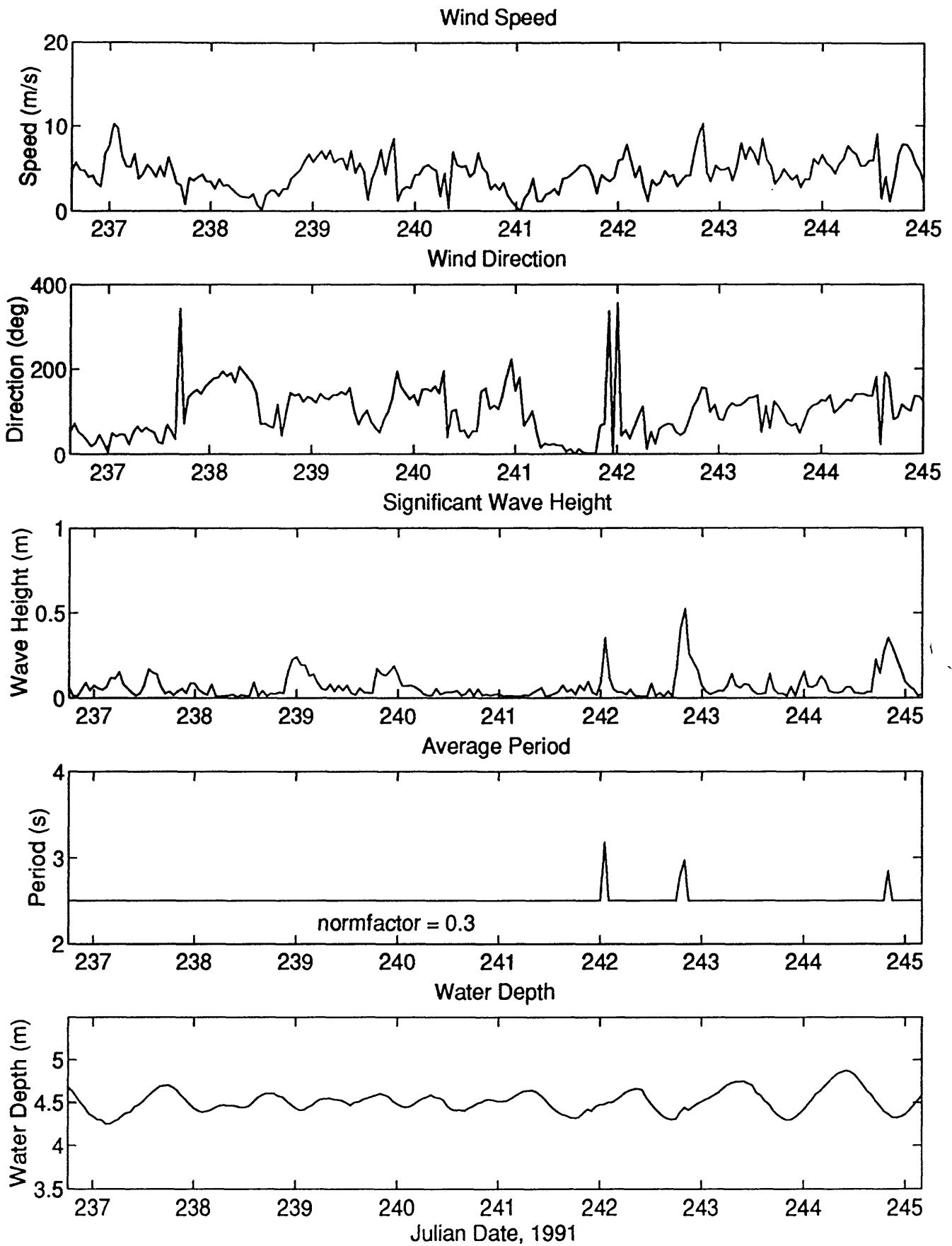


Water Depth

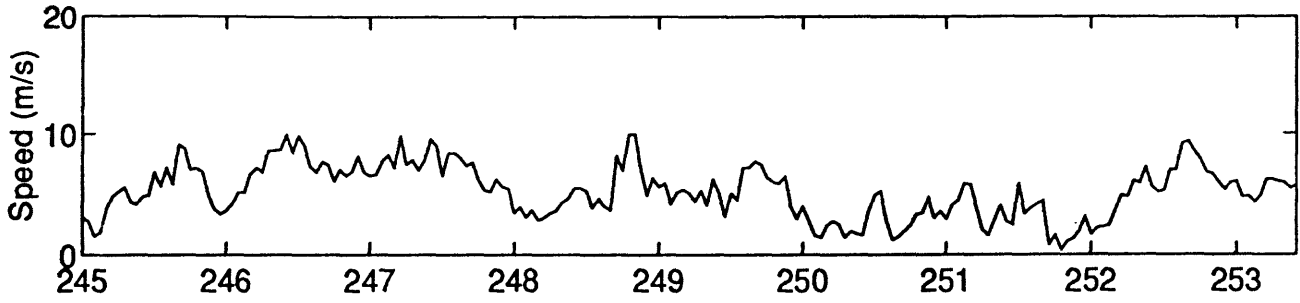




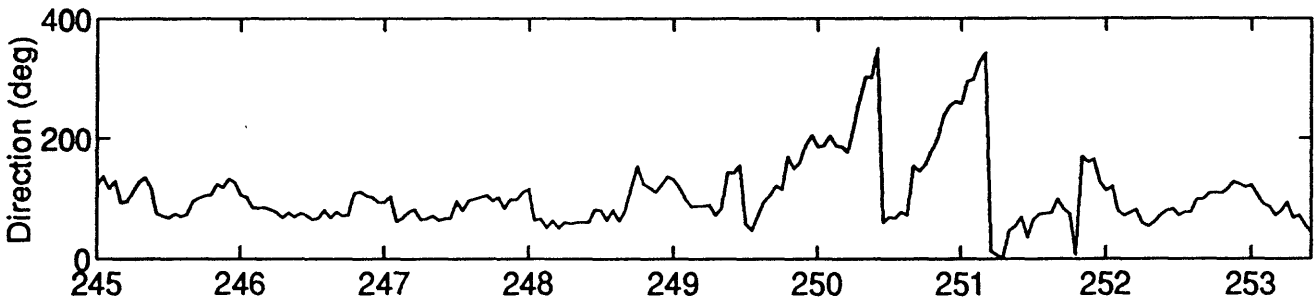




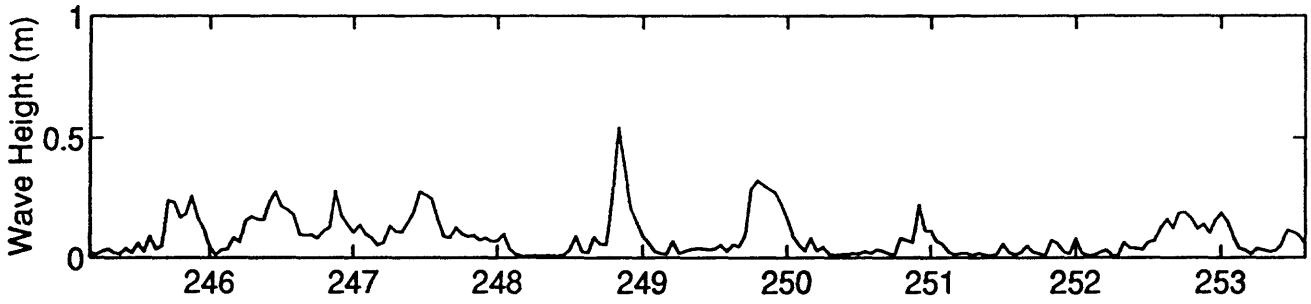
Wind Speed



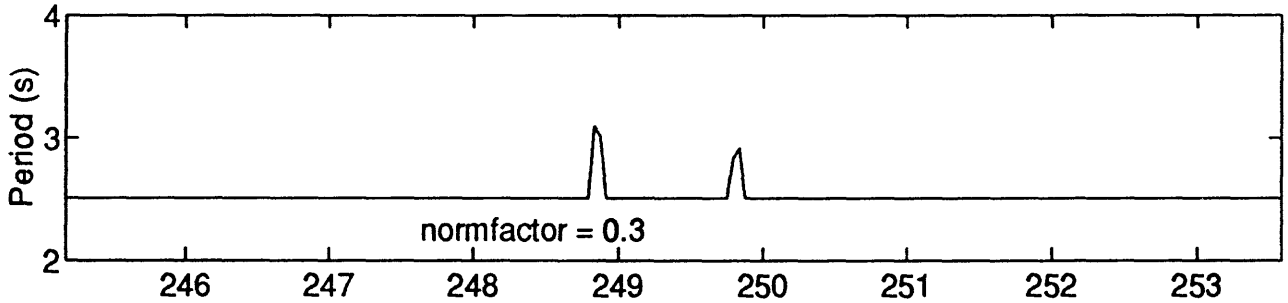
Wind Direction



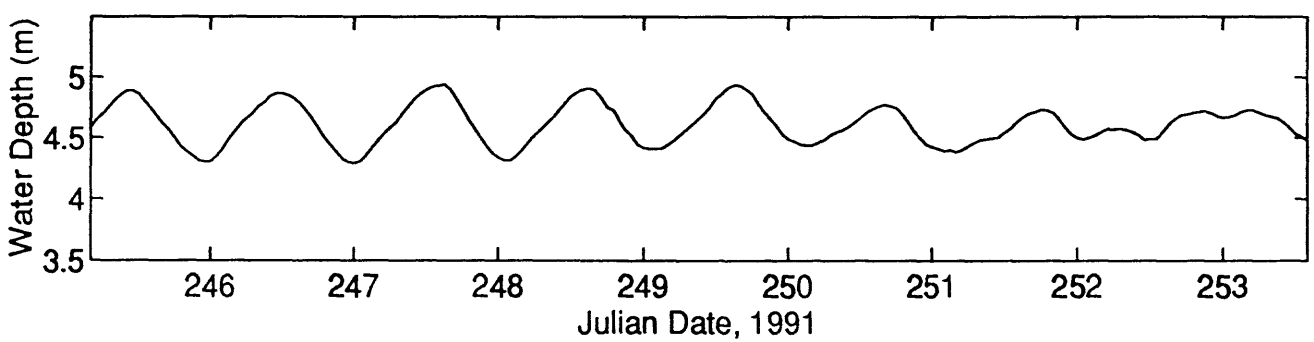
Significant Wave Height



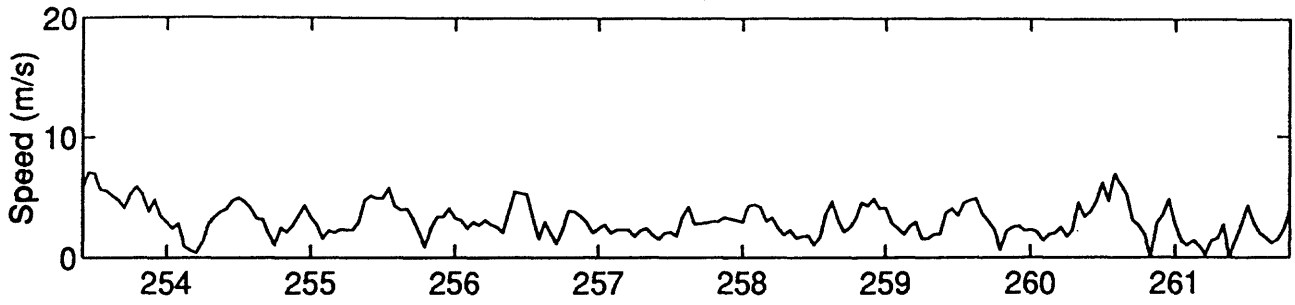
Average Period



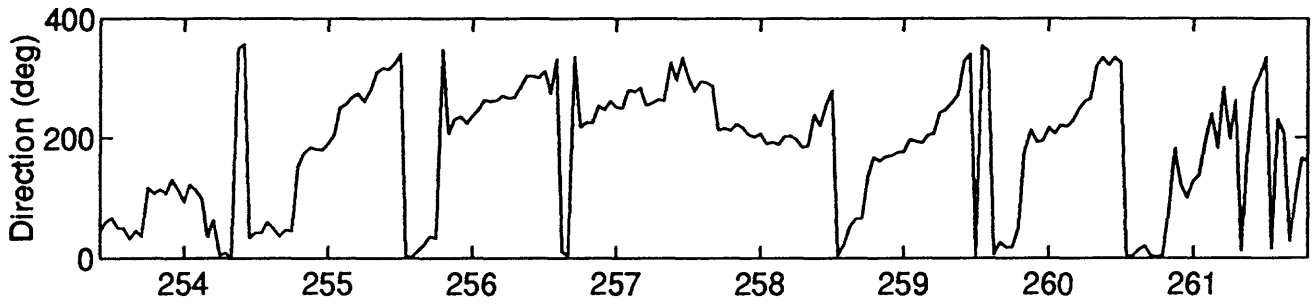
Water Depth



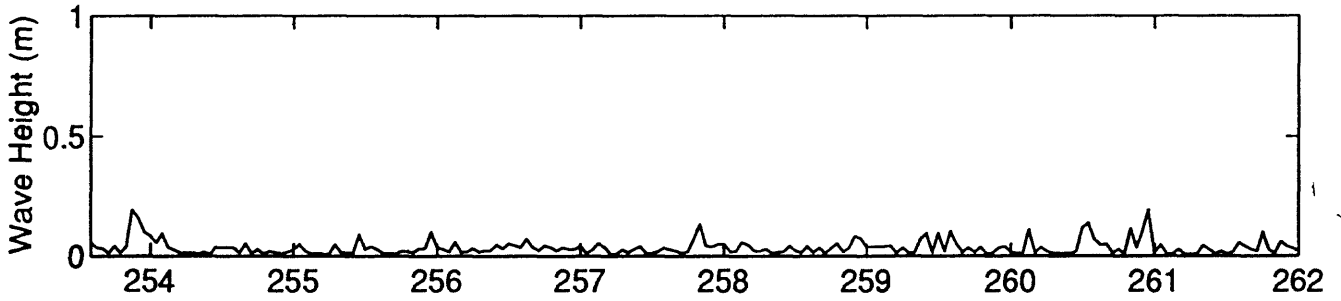
Wind Speed



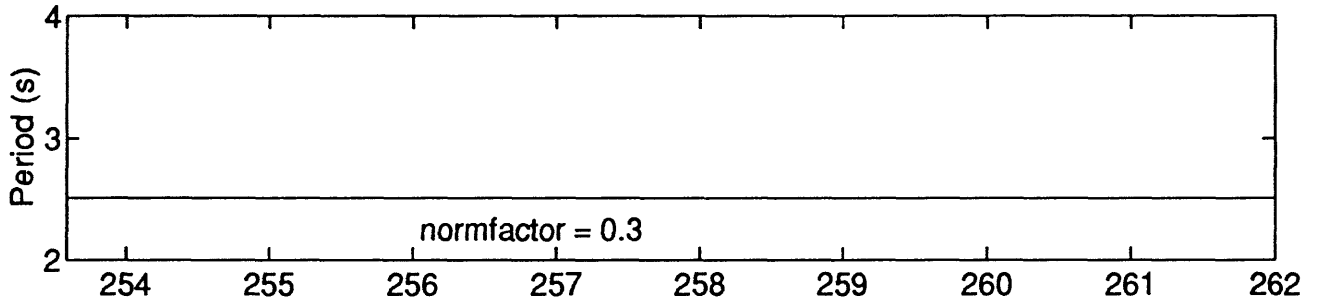
Wind Direction



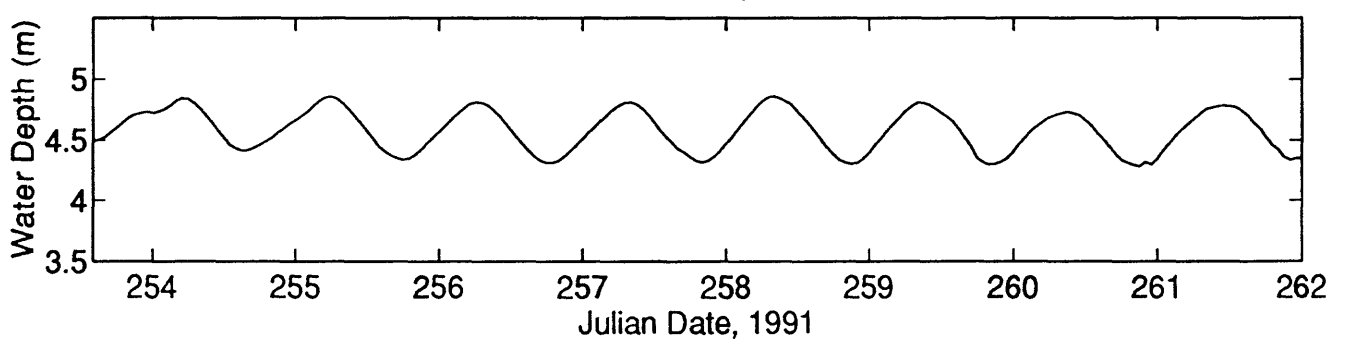
Significant Wave Height



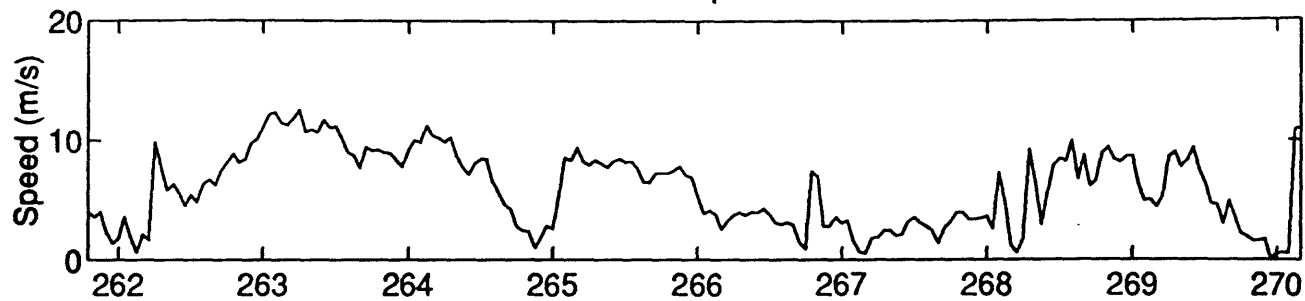
Average Period



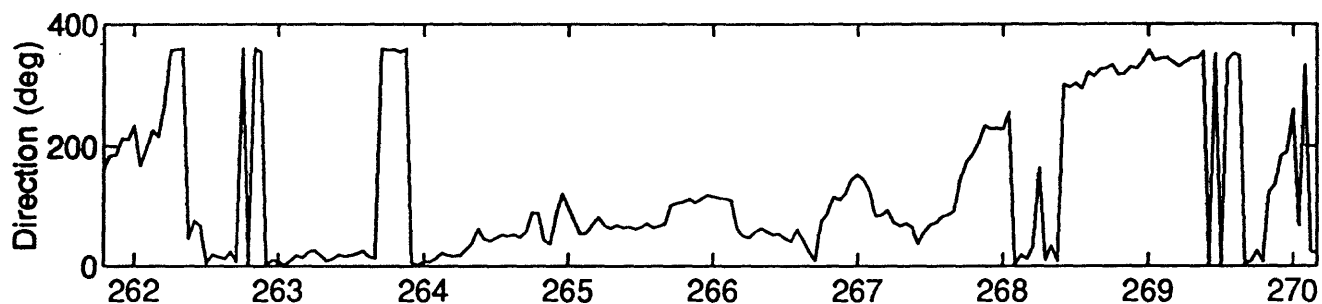
Water Depth



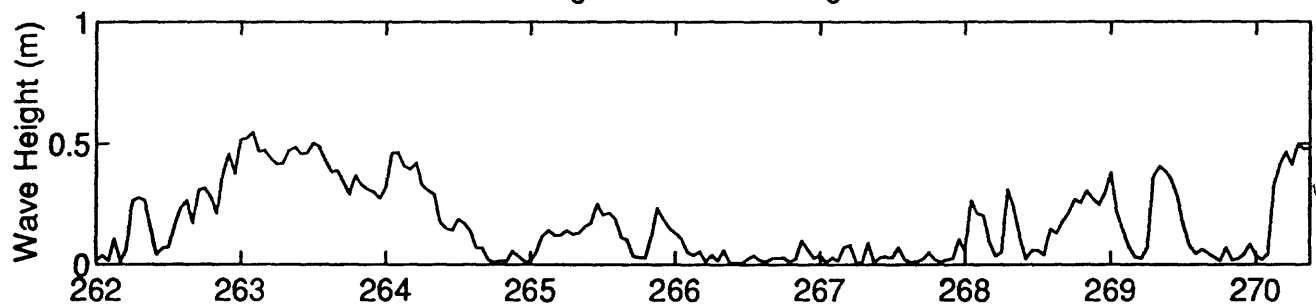
Wind Speed



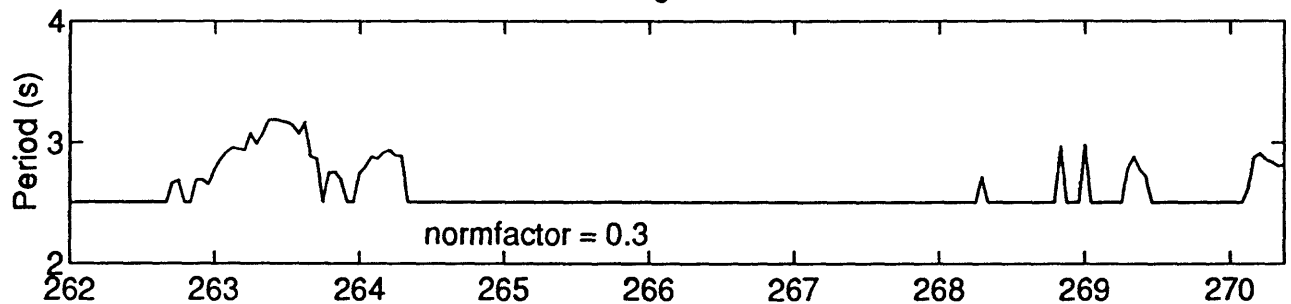
Wind Direction



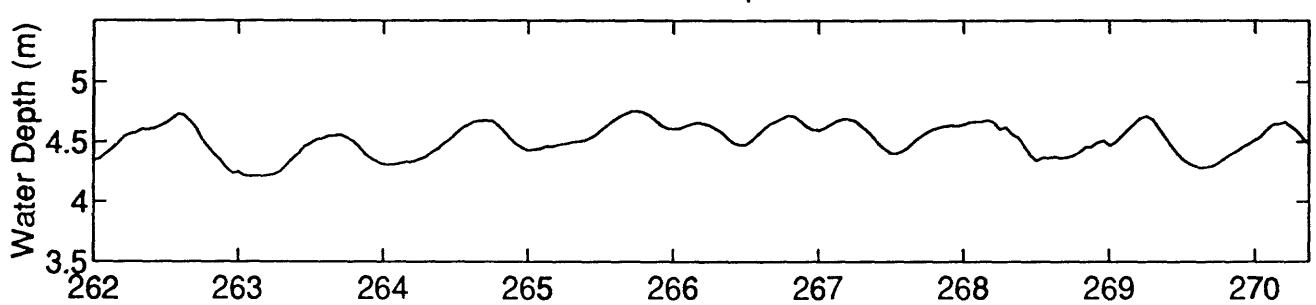
Significant Wave Height



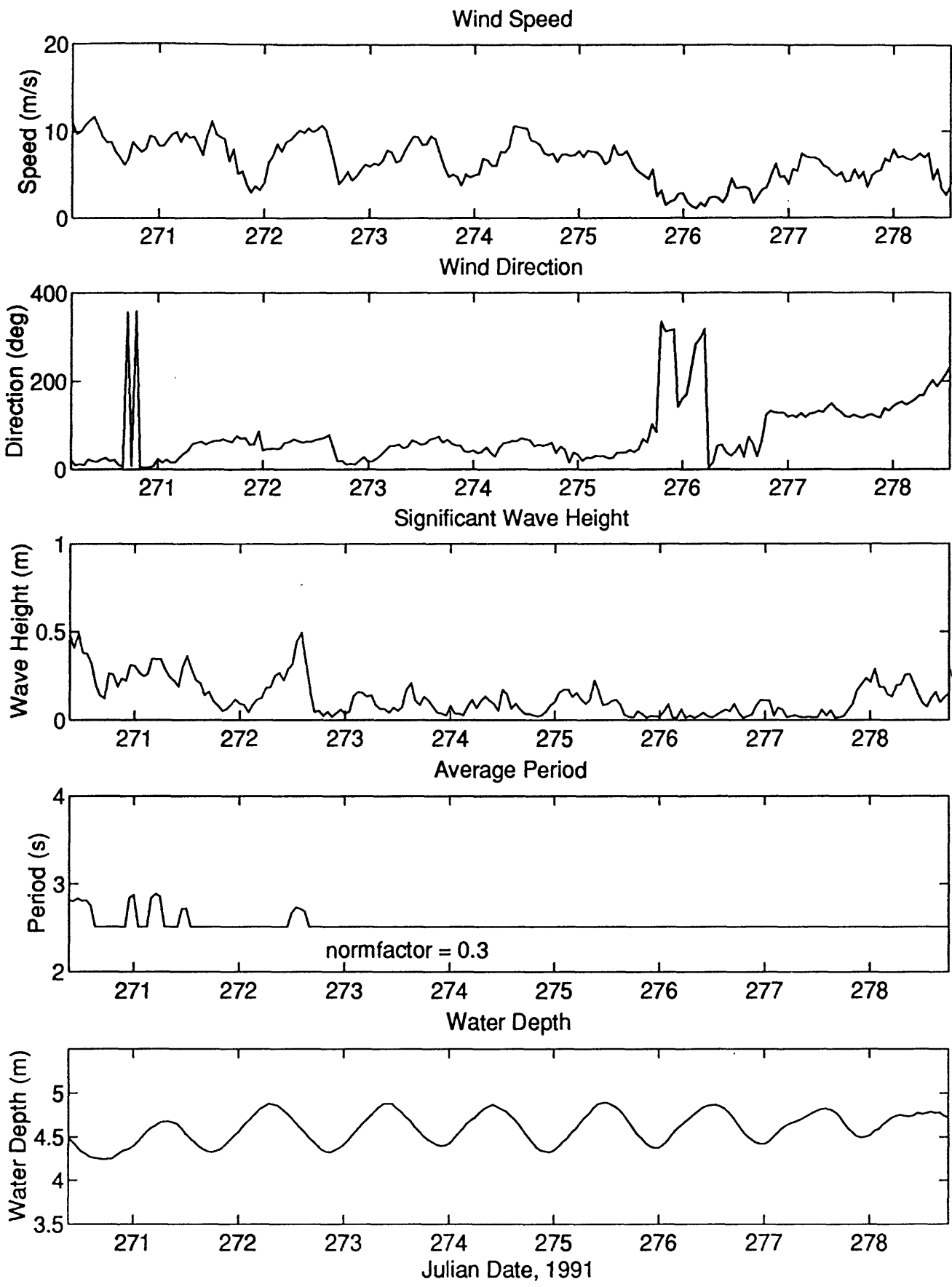
Average Period

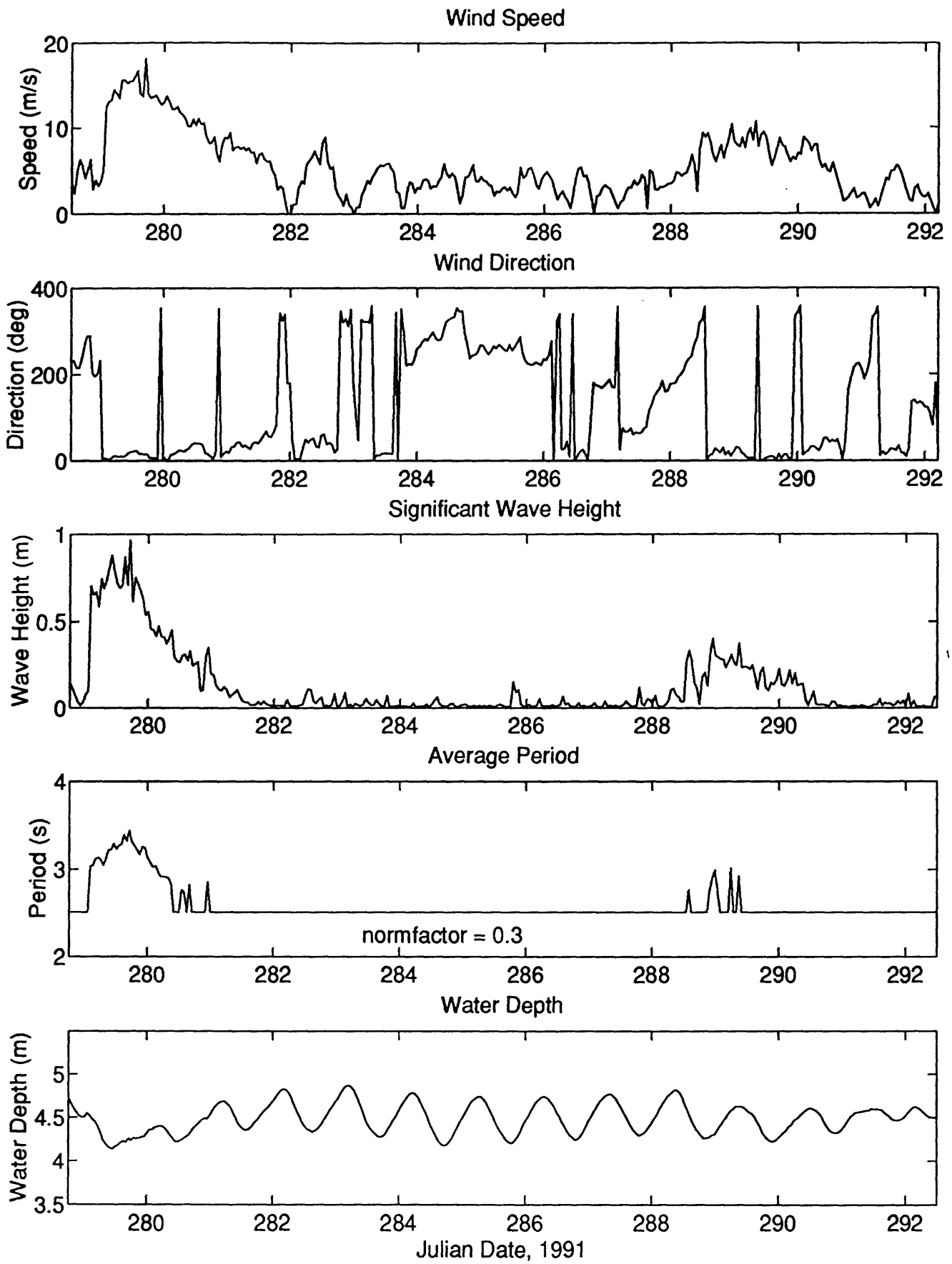


Water Depth



Julian Date, 1991



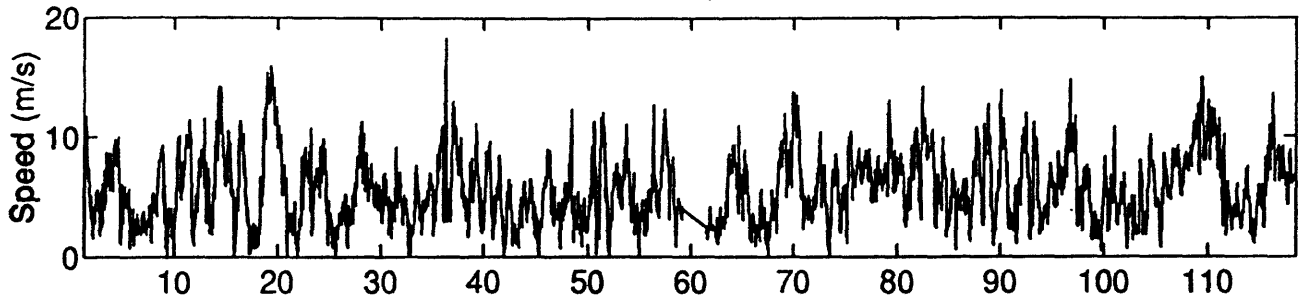


APPENDIX E

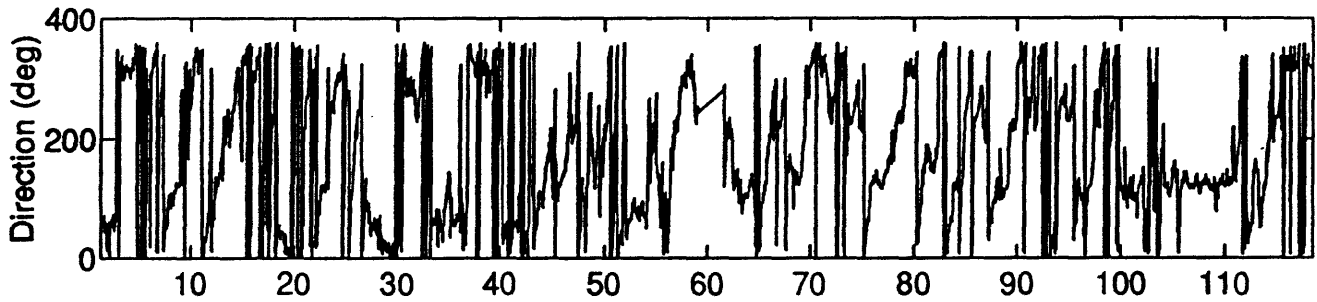
Time Series Graphs

Mooring 3951

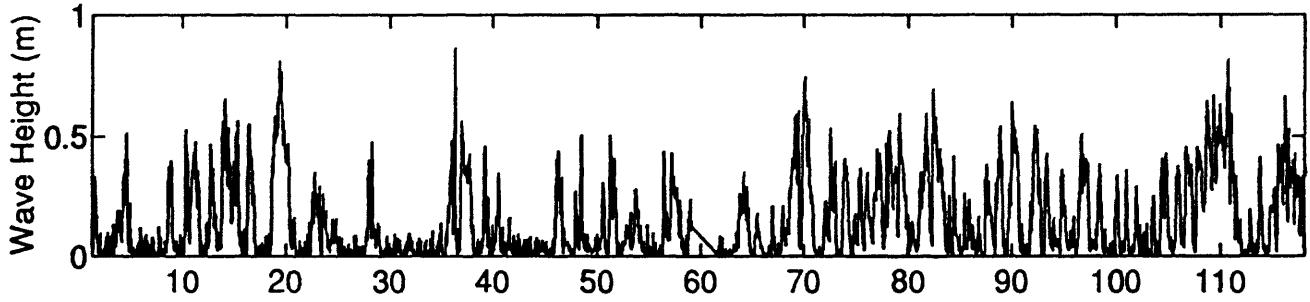
Wind Speed



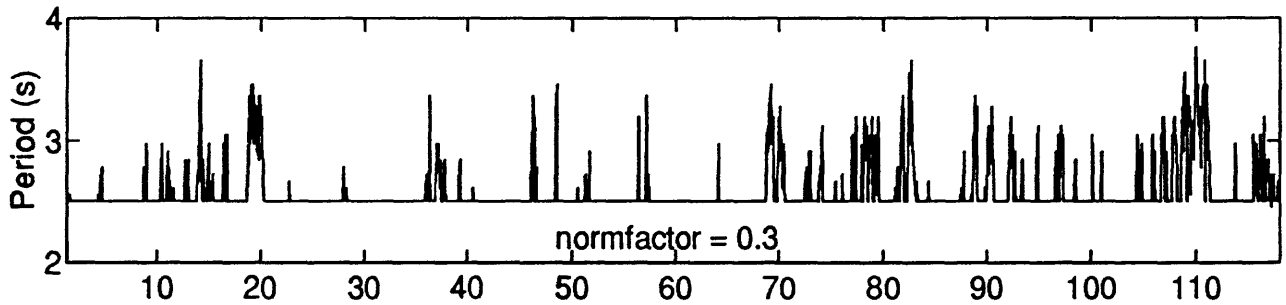
Wind Direction



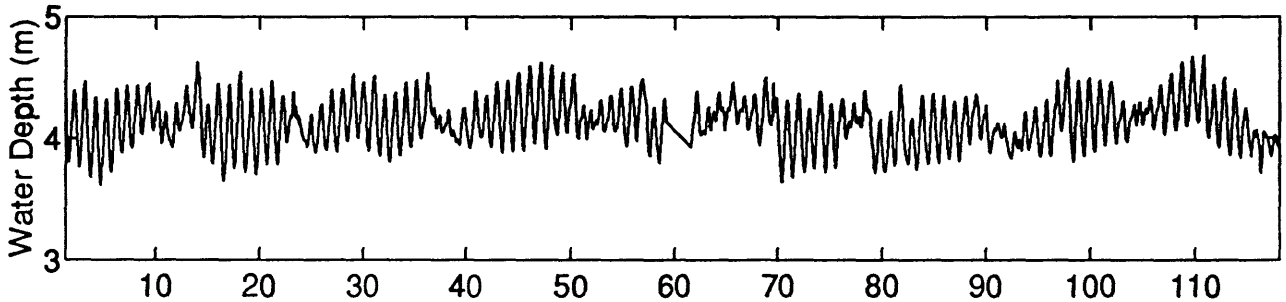
Significant Wave Height



Peak Period

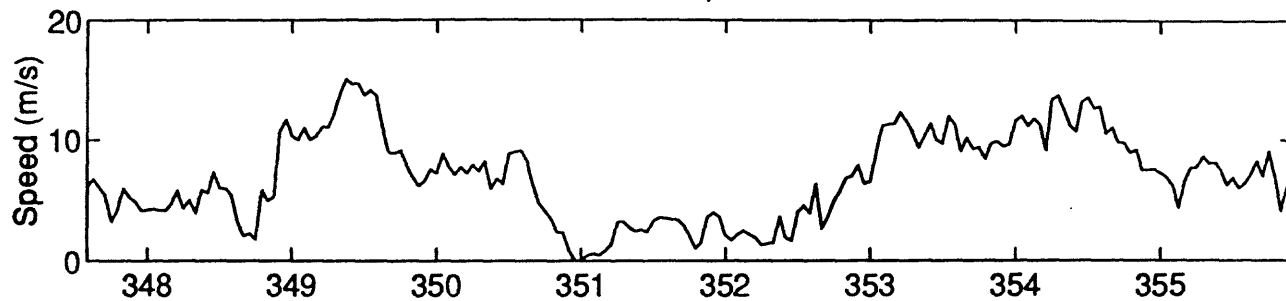


Water Depth

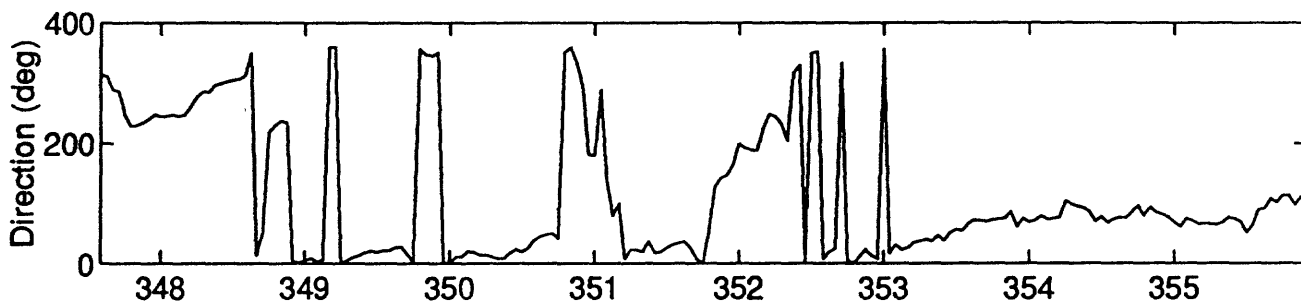


Julian Date, 1991

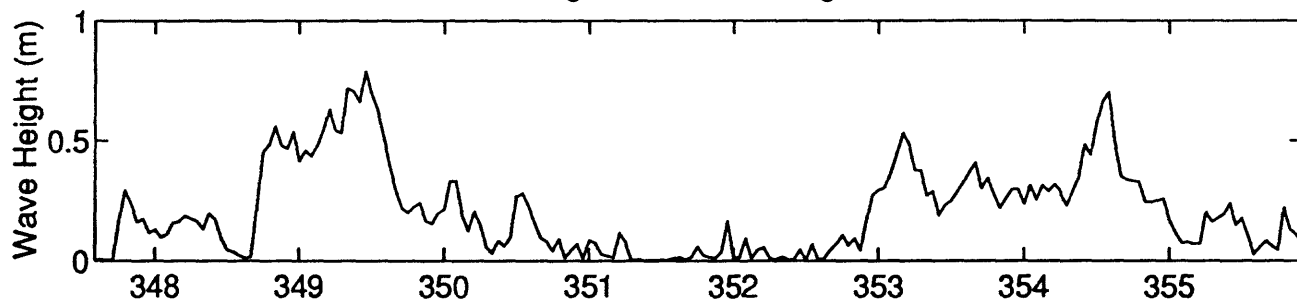
Wind Speed



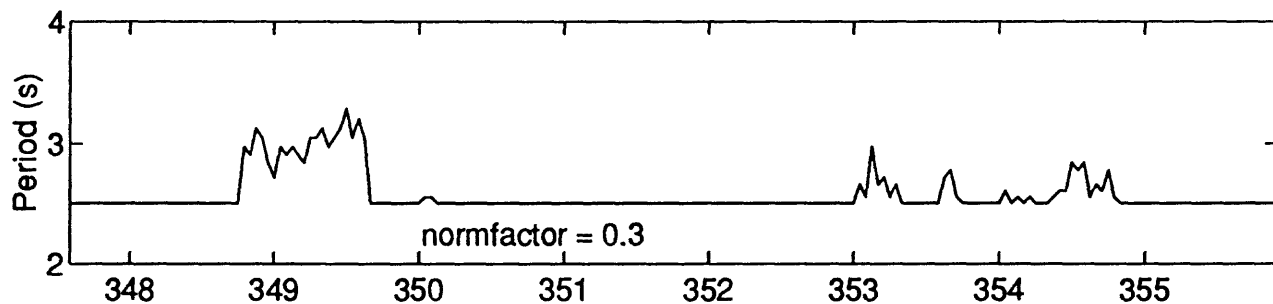
Wind Direction



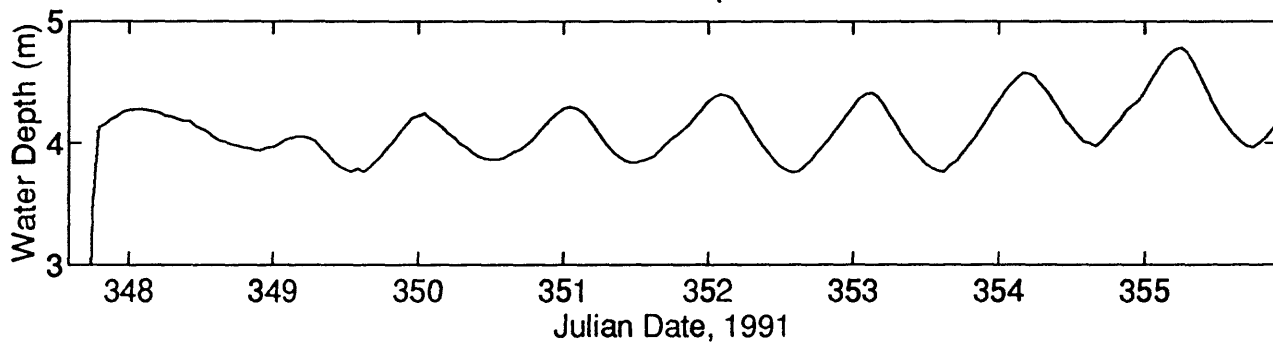
Significant Wave Height



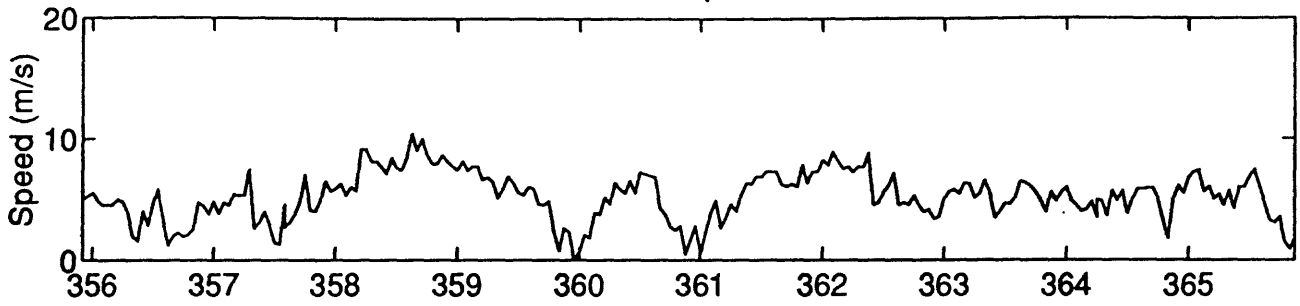
Peak Period



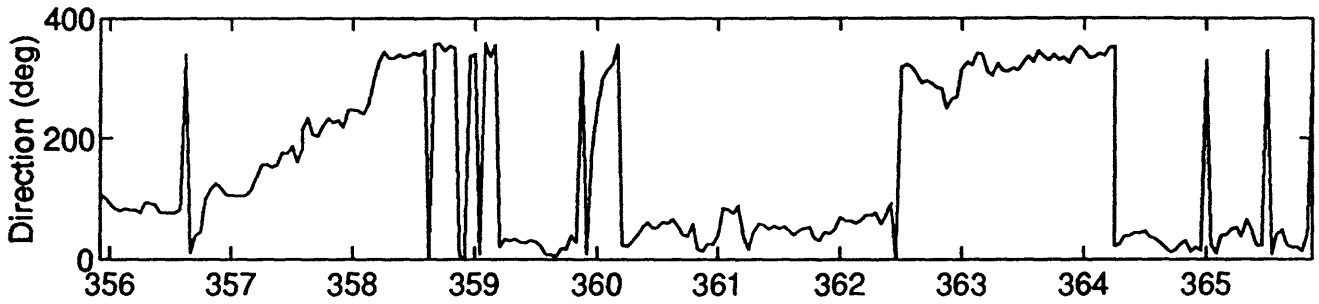
Water Depth



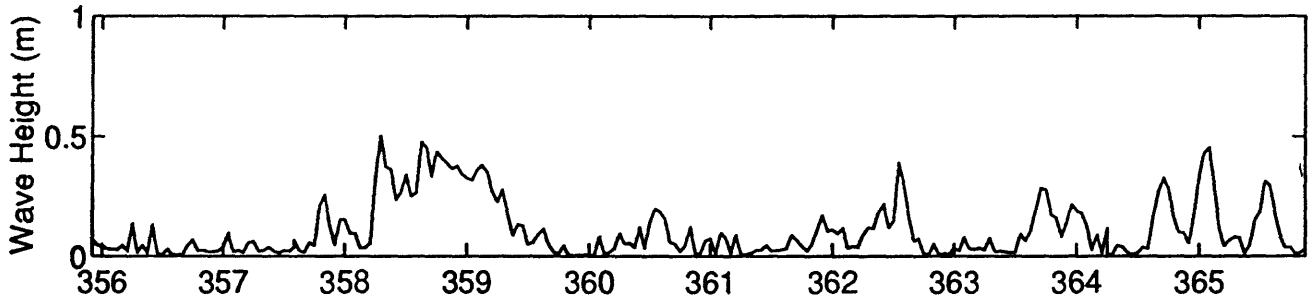
Wind Speed



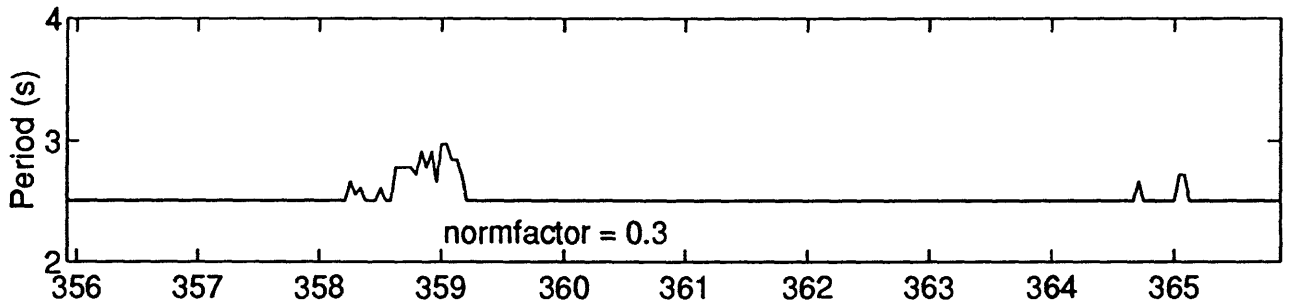
Wind Direction



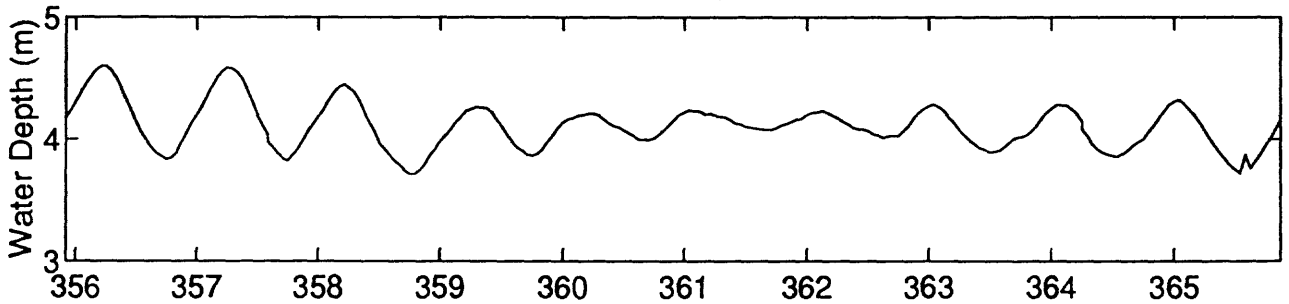
Significant Wave Height



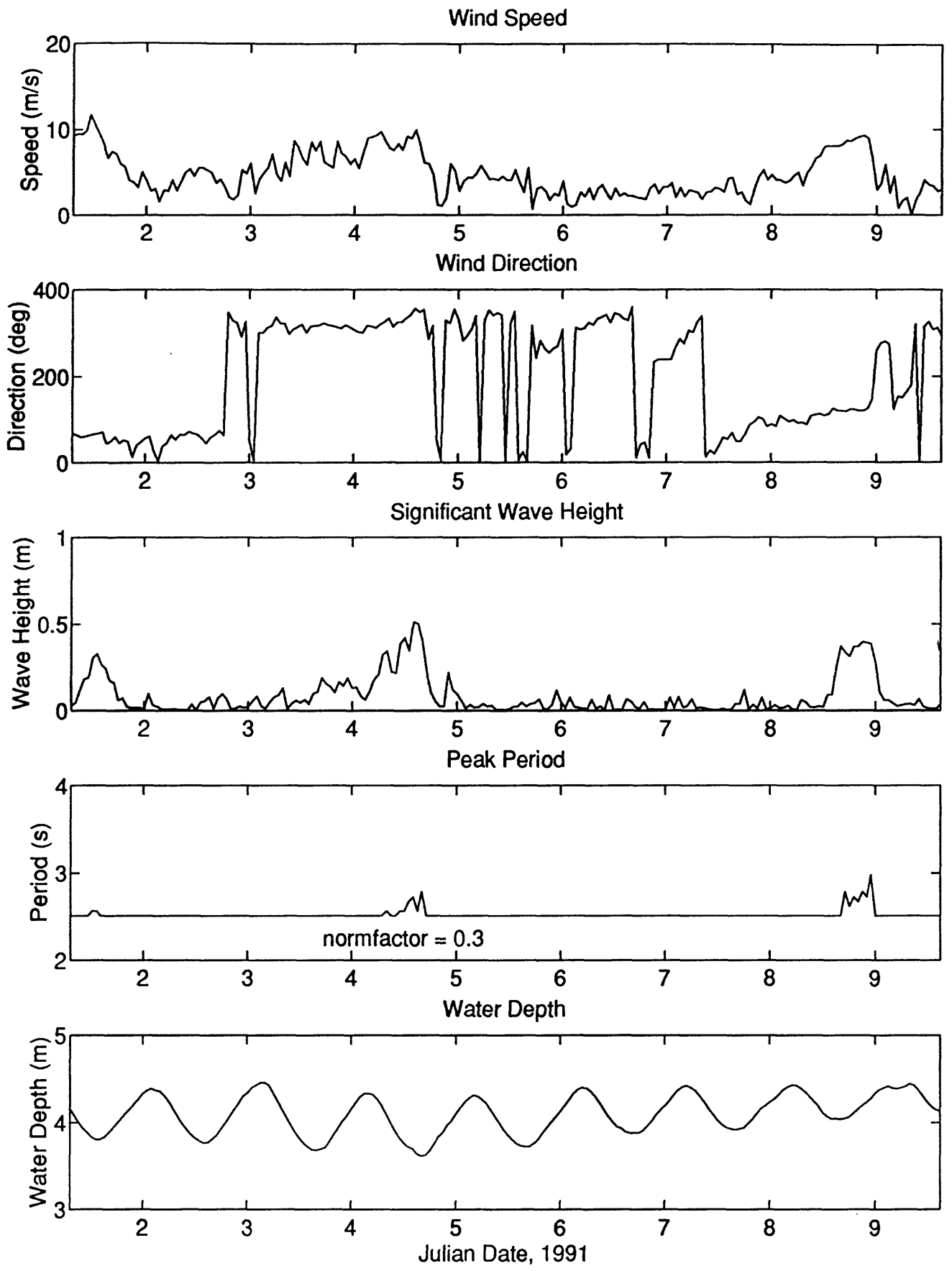
Peak Period

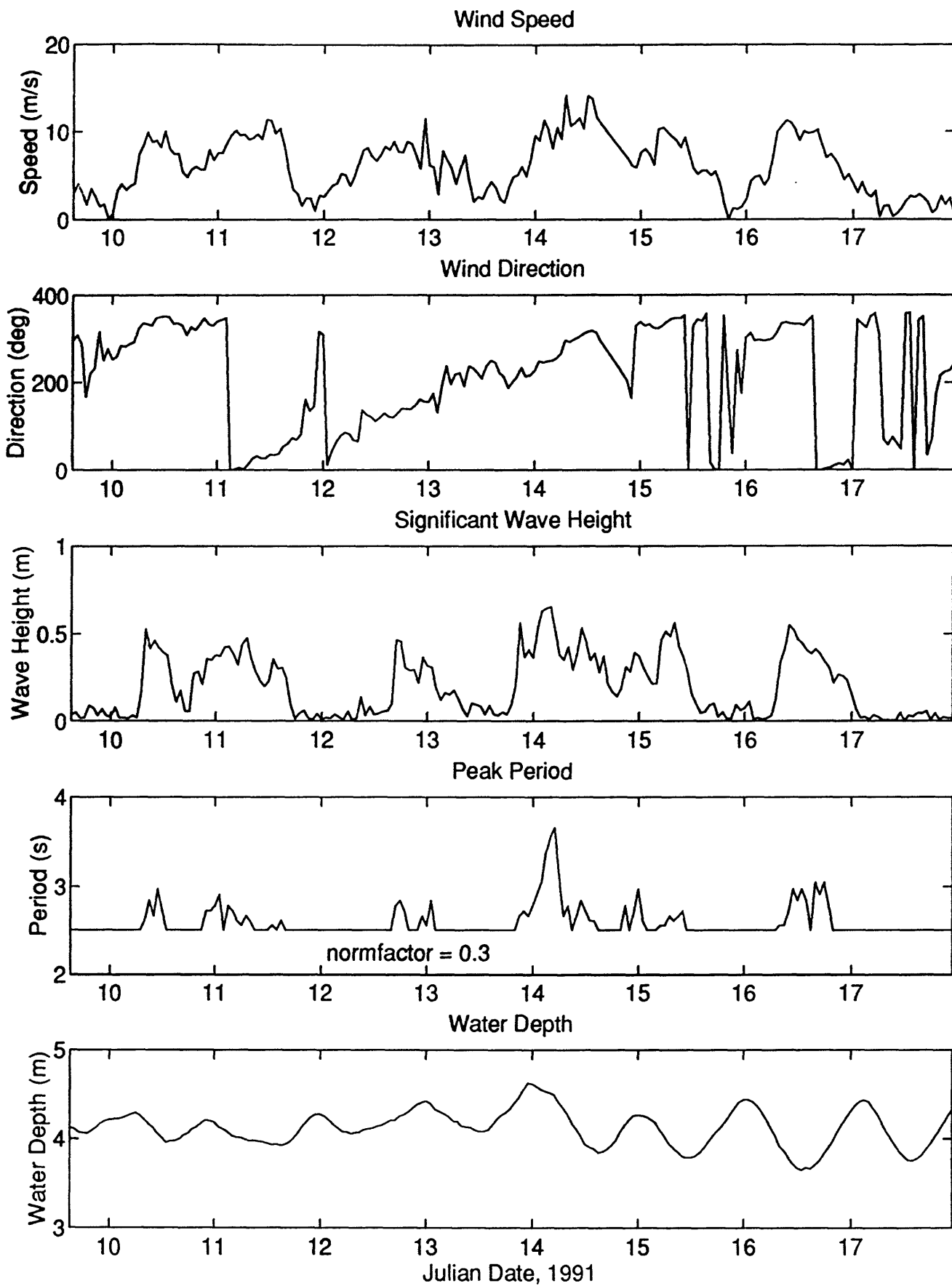


Water Depth

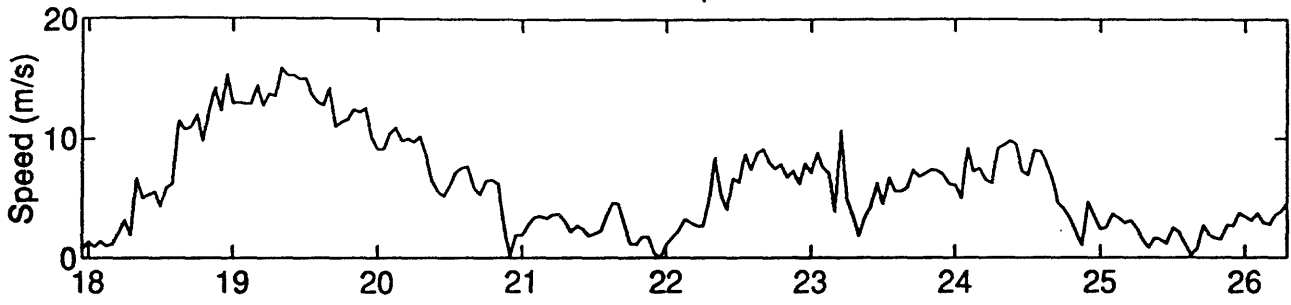


Julian Date, 1991

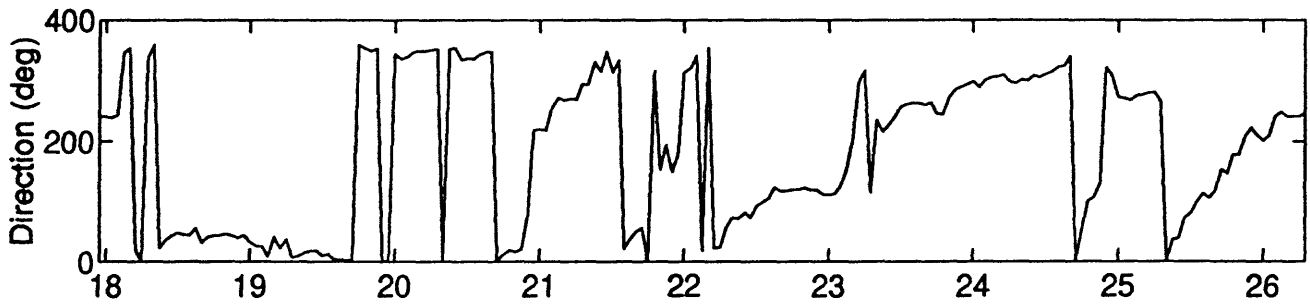




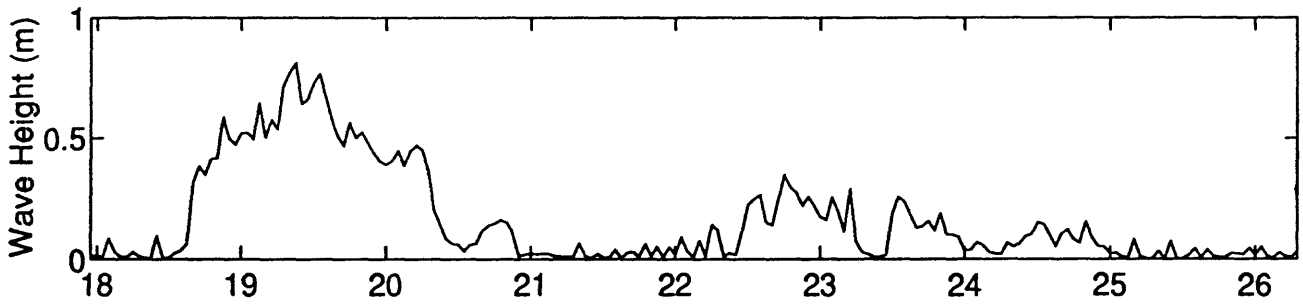
Wind Speed



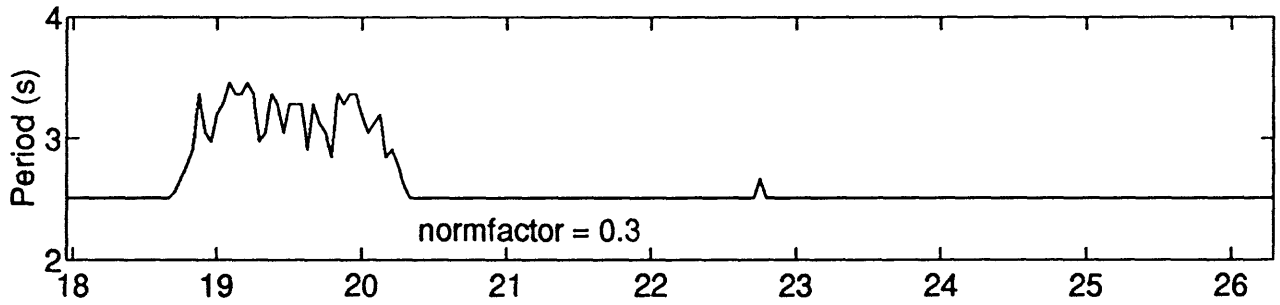
Wind Direction



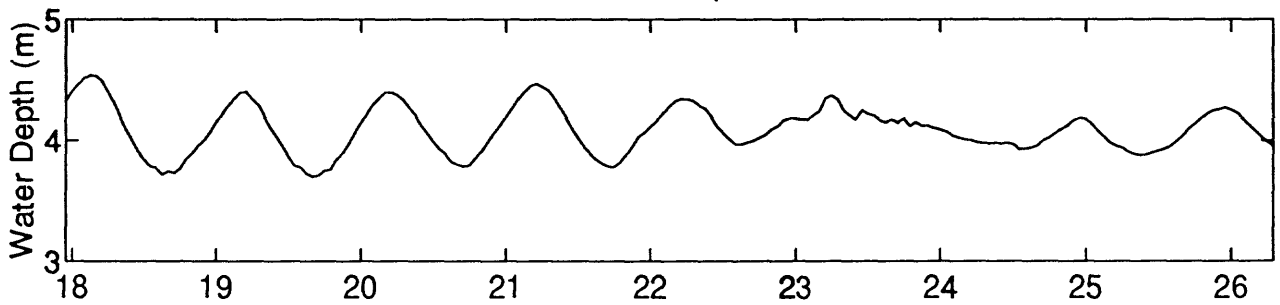
Significant Wave Height



Peak Period

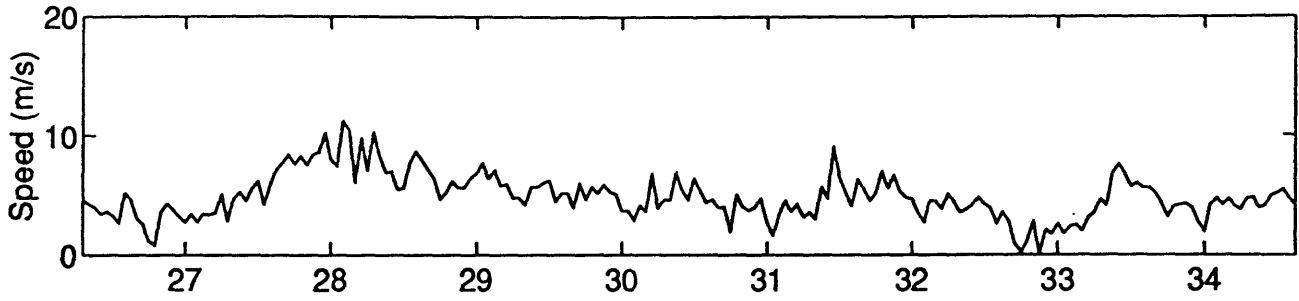


Water Depth

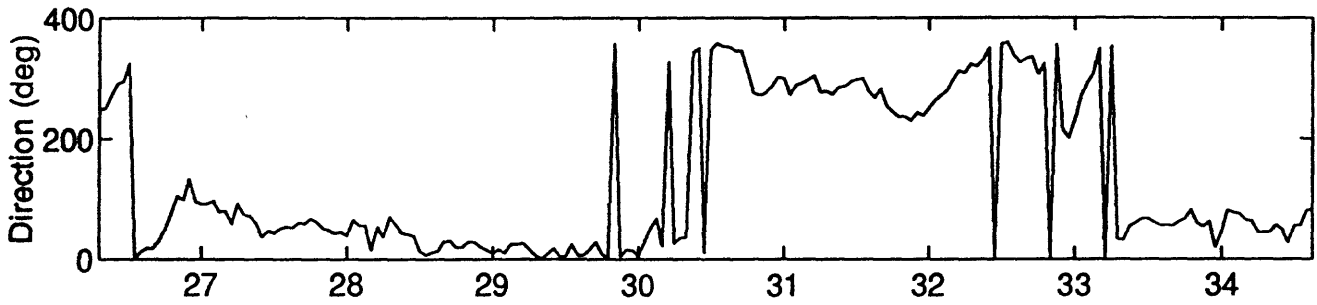


Julian Date, 1991

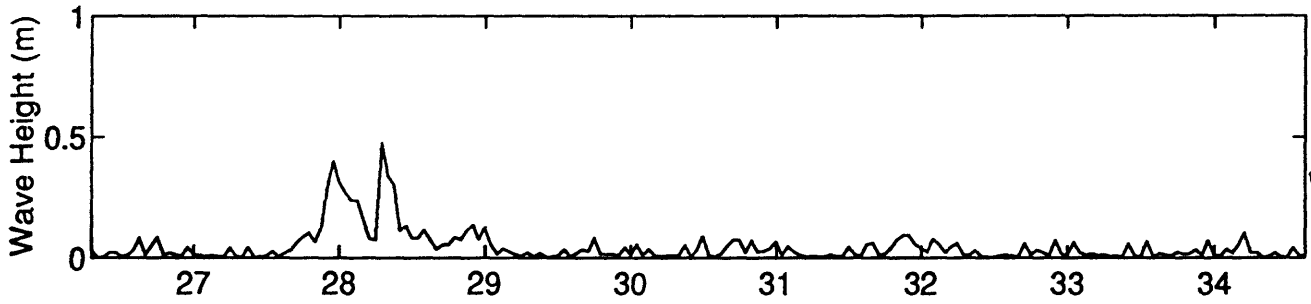
Wind Speed



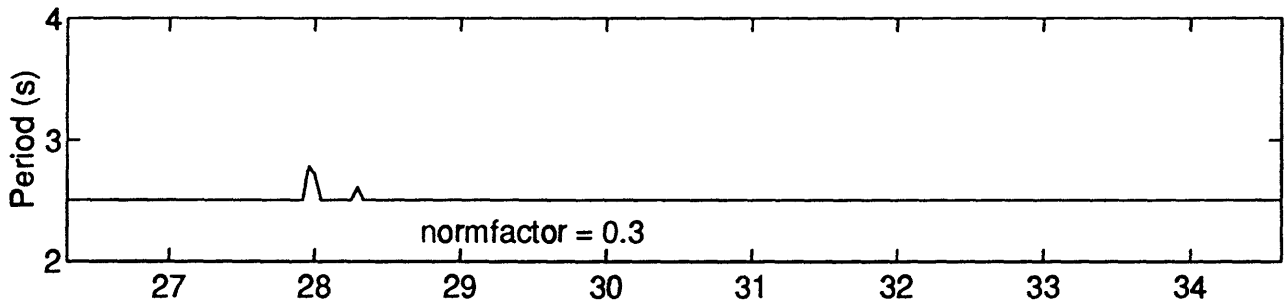
Wind Direction



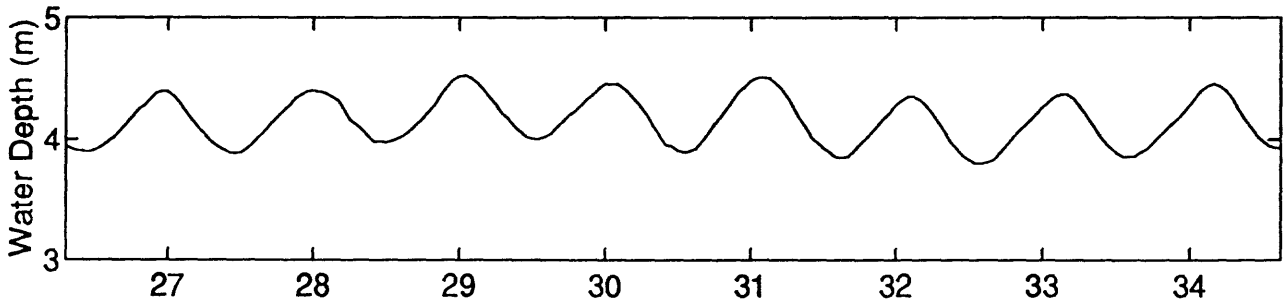
Significant Wave Height



Peak Period

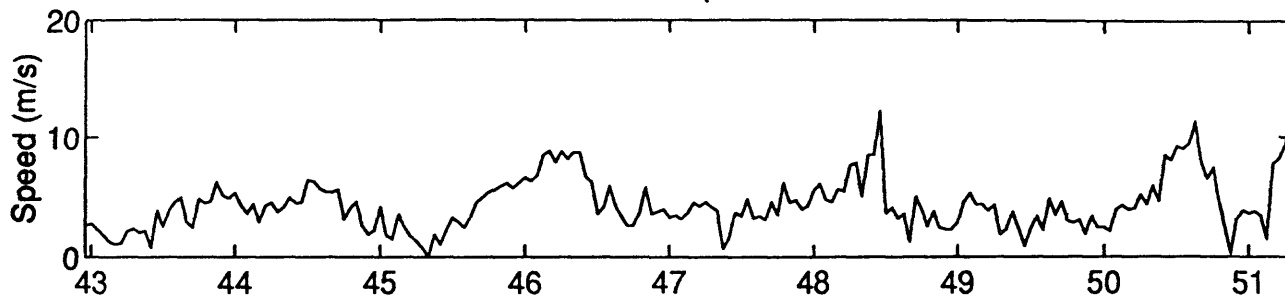


Water Depth

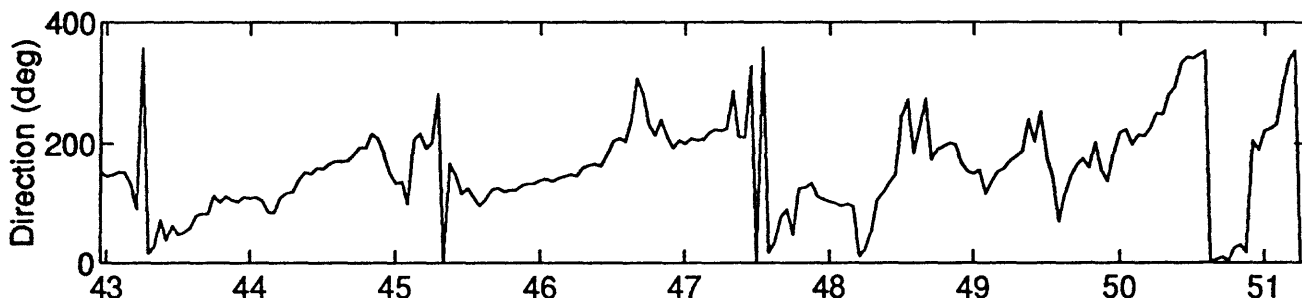


Julian Date, 1991

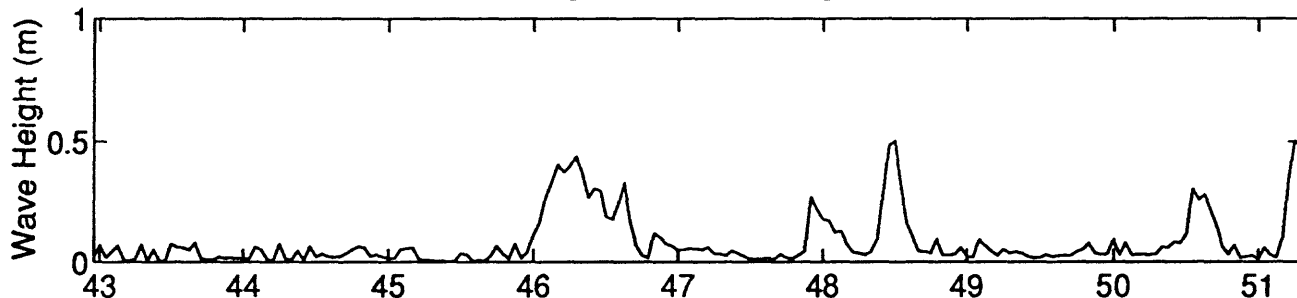
Wind Speed



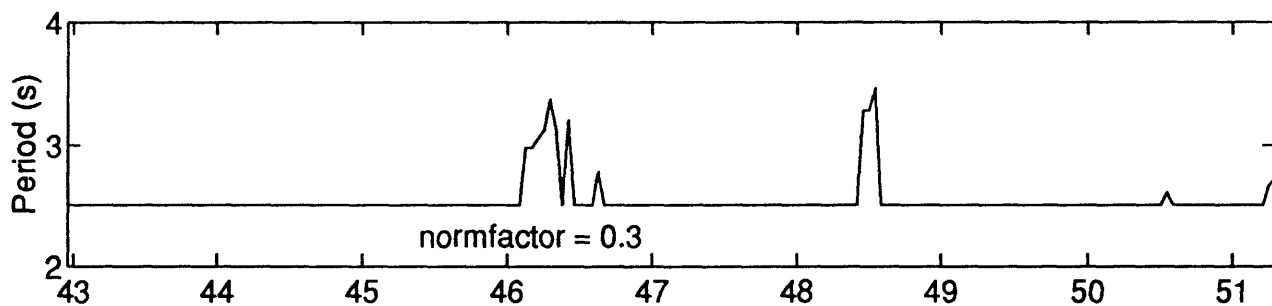
Wind Direction



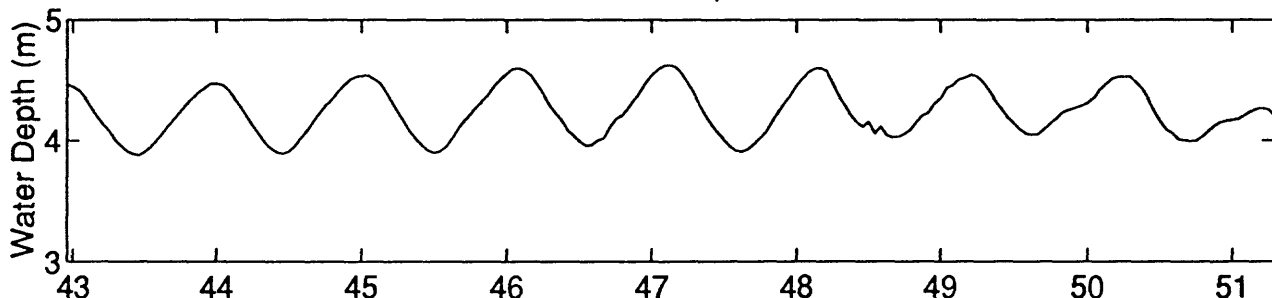
Significant Wave Height



Peak Period

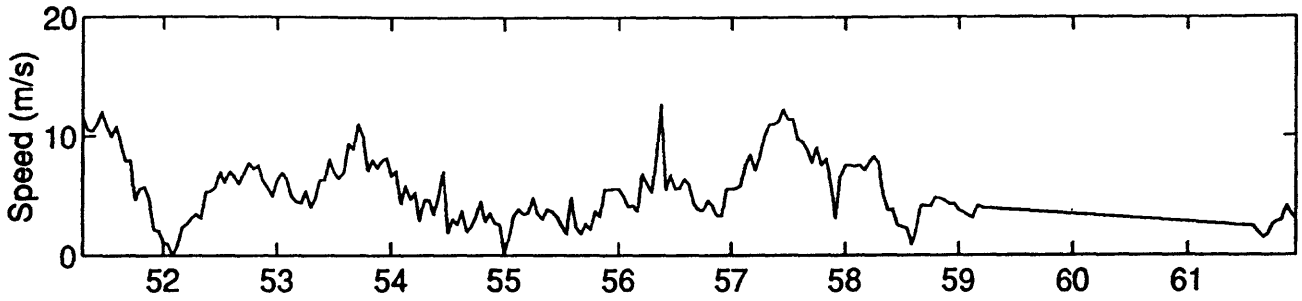


Water Depth

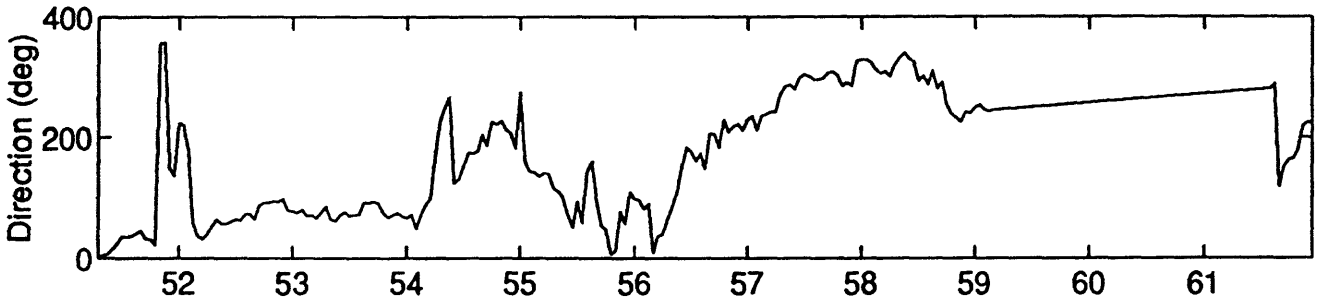


Julian Date, 1991

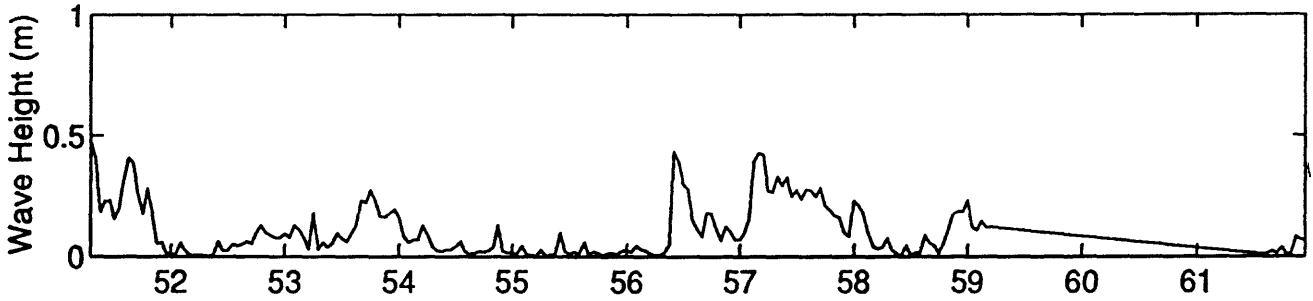
Wind Speed



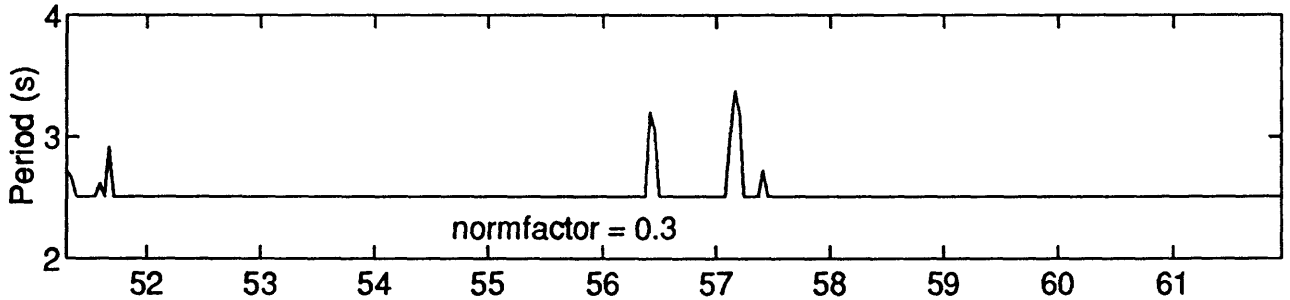
Wind Direction



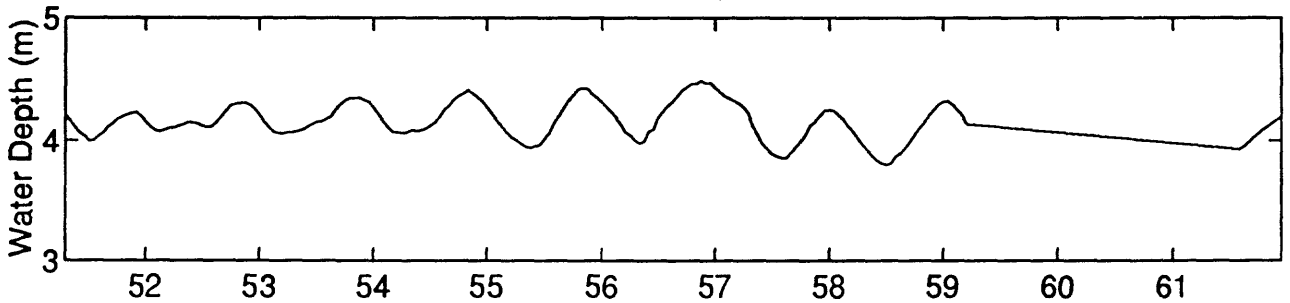
Significant Wave Height



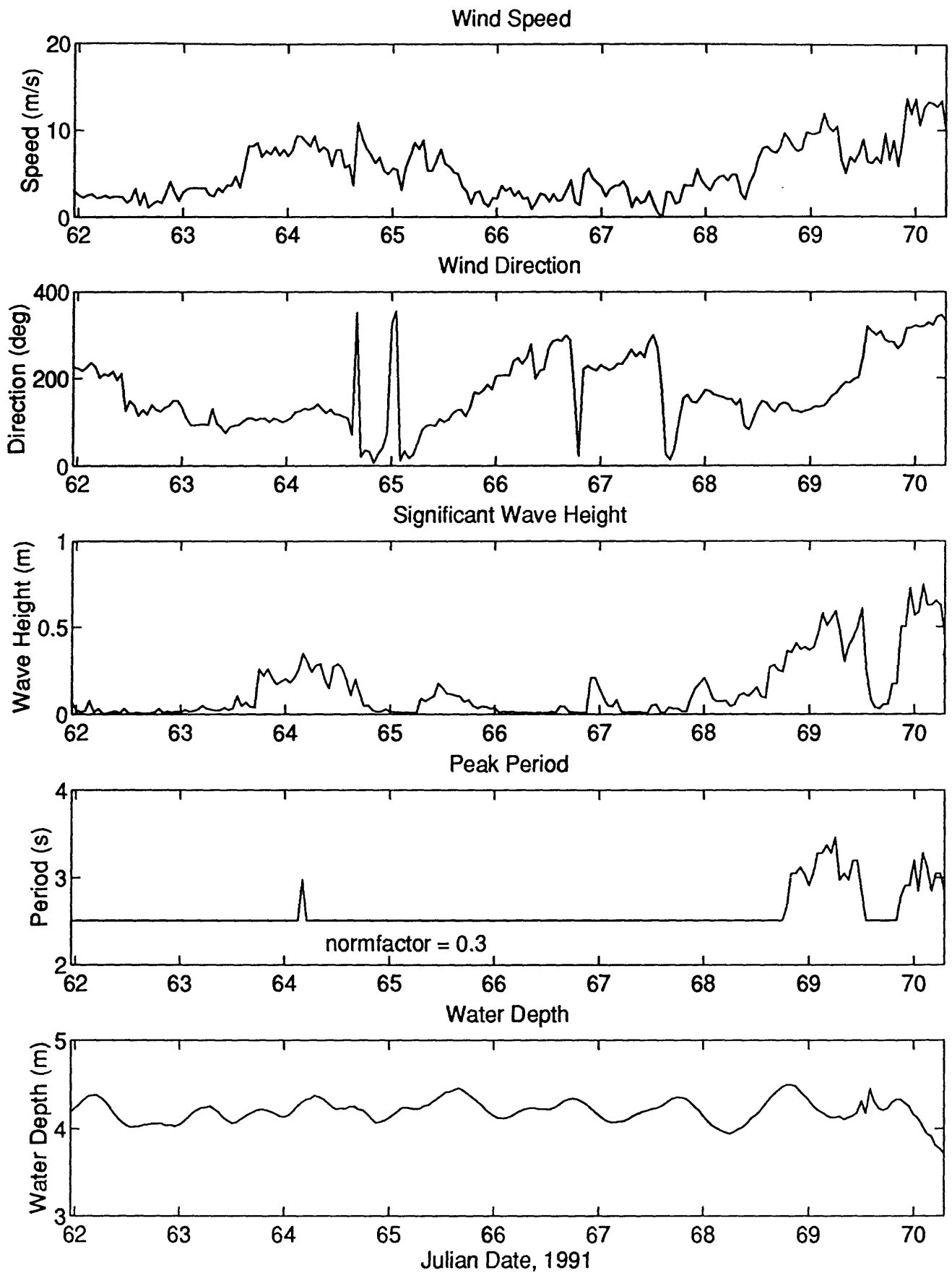
Peak Period



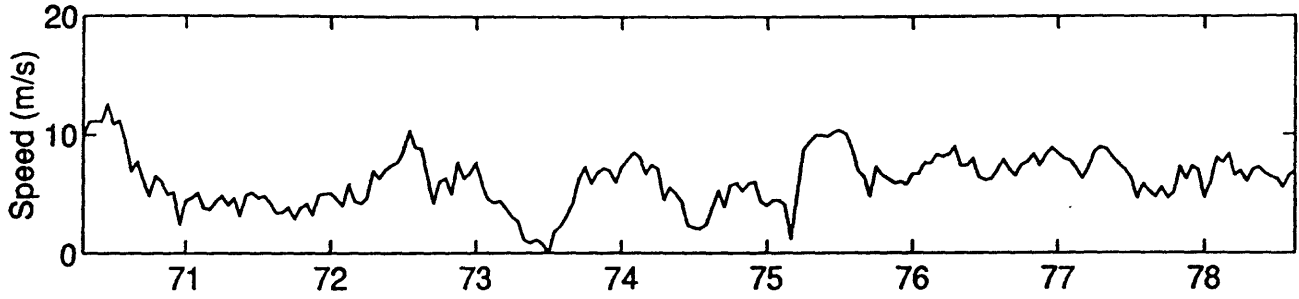
Water Depth



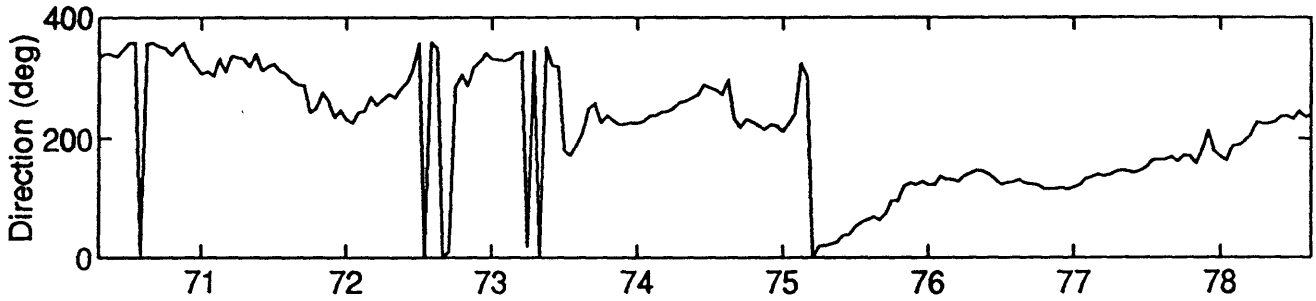
Julian Date, 1991



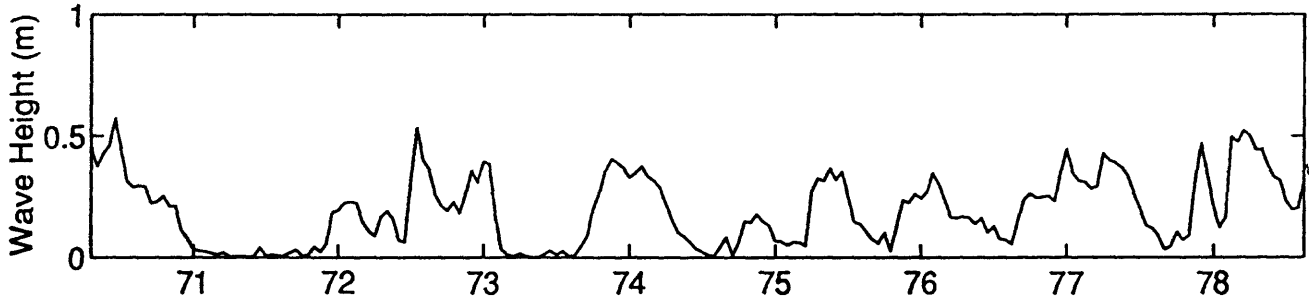
Wind Speed



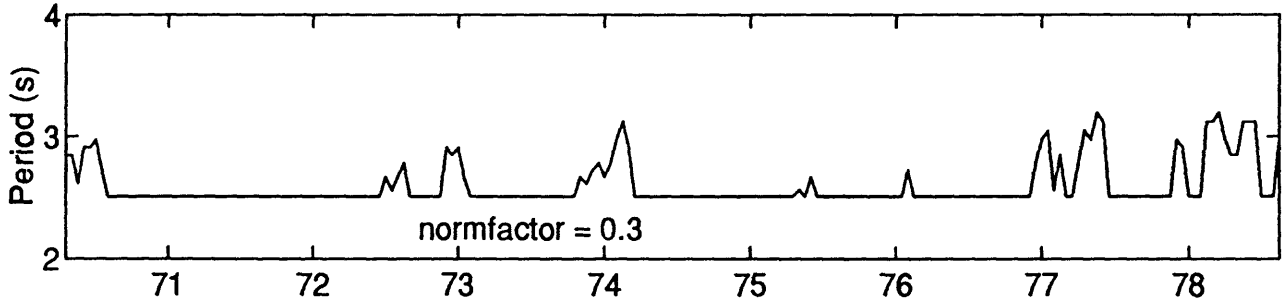
Wind Direction



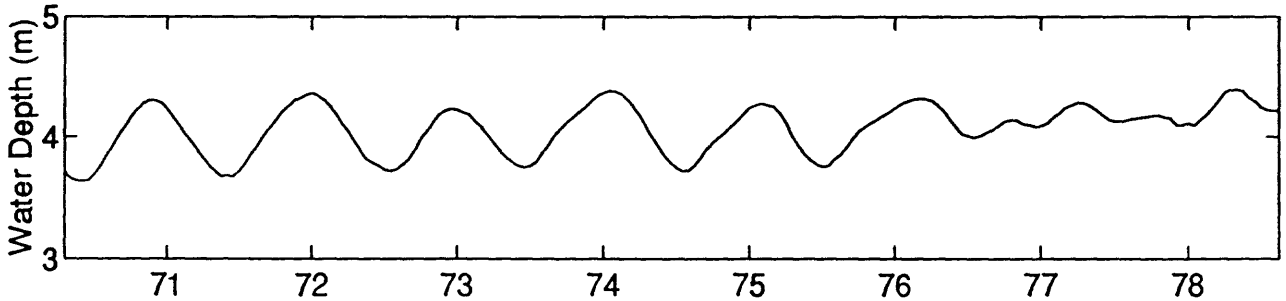
Significant Wave Height



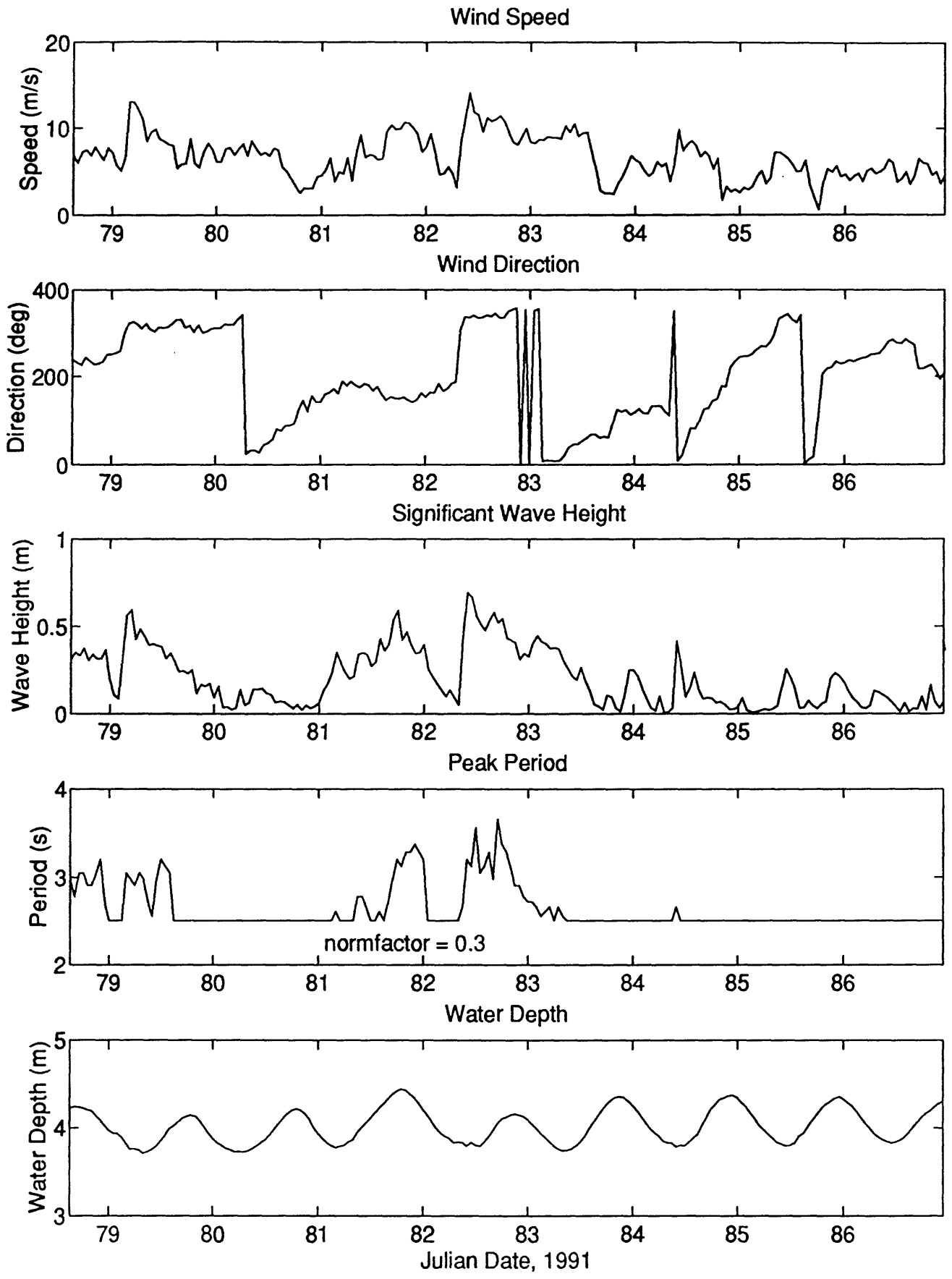
Peak Period



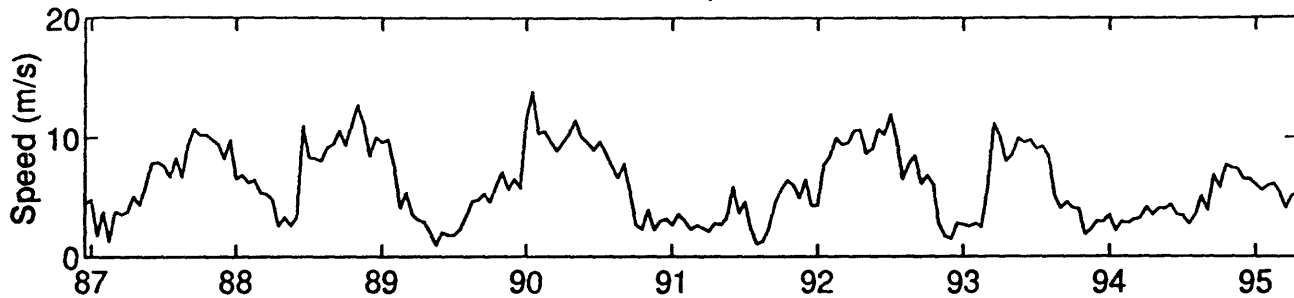
Water Depth



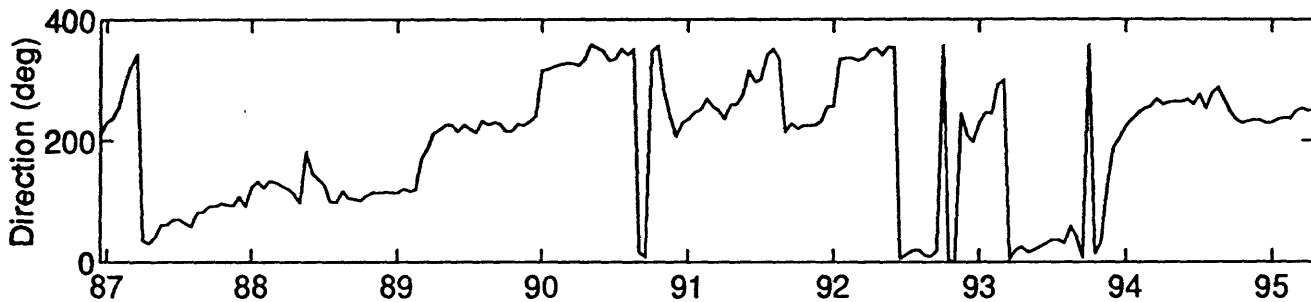
Julian Date, 1991



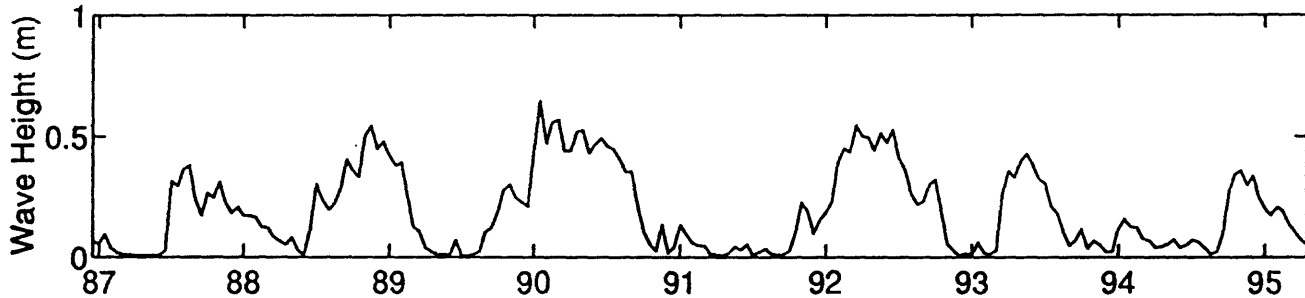
Wind Speed



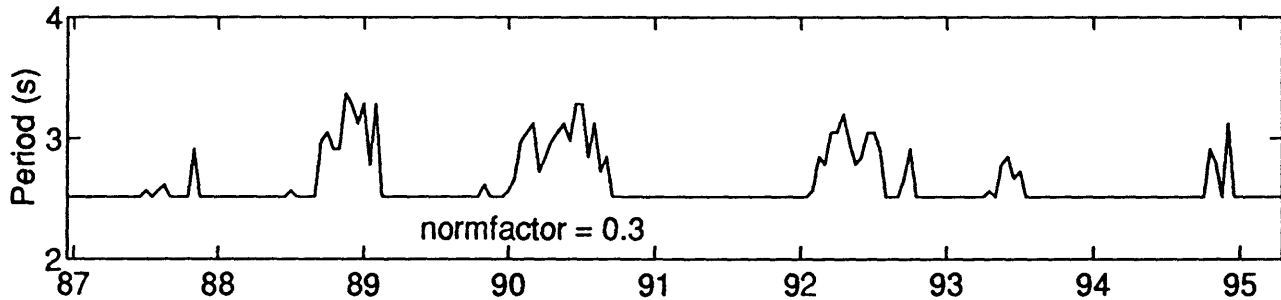
Wind Direction



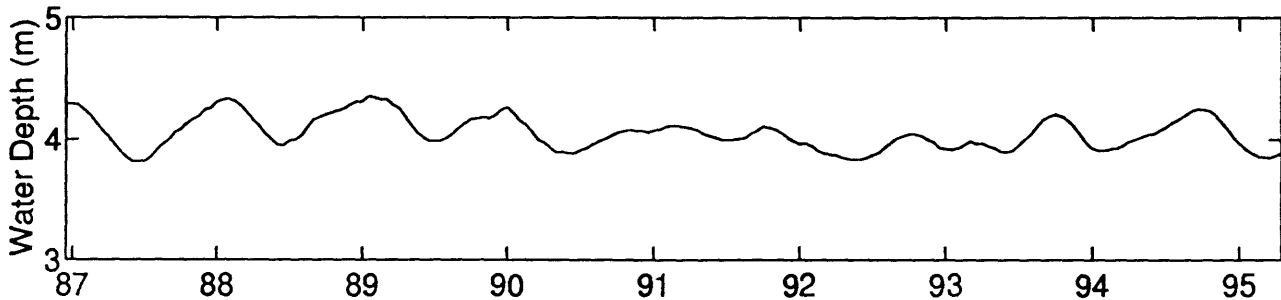
Significant Wave Height



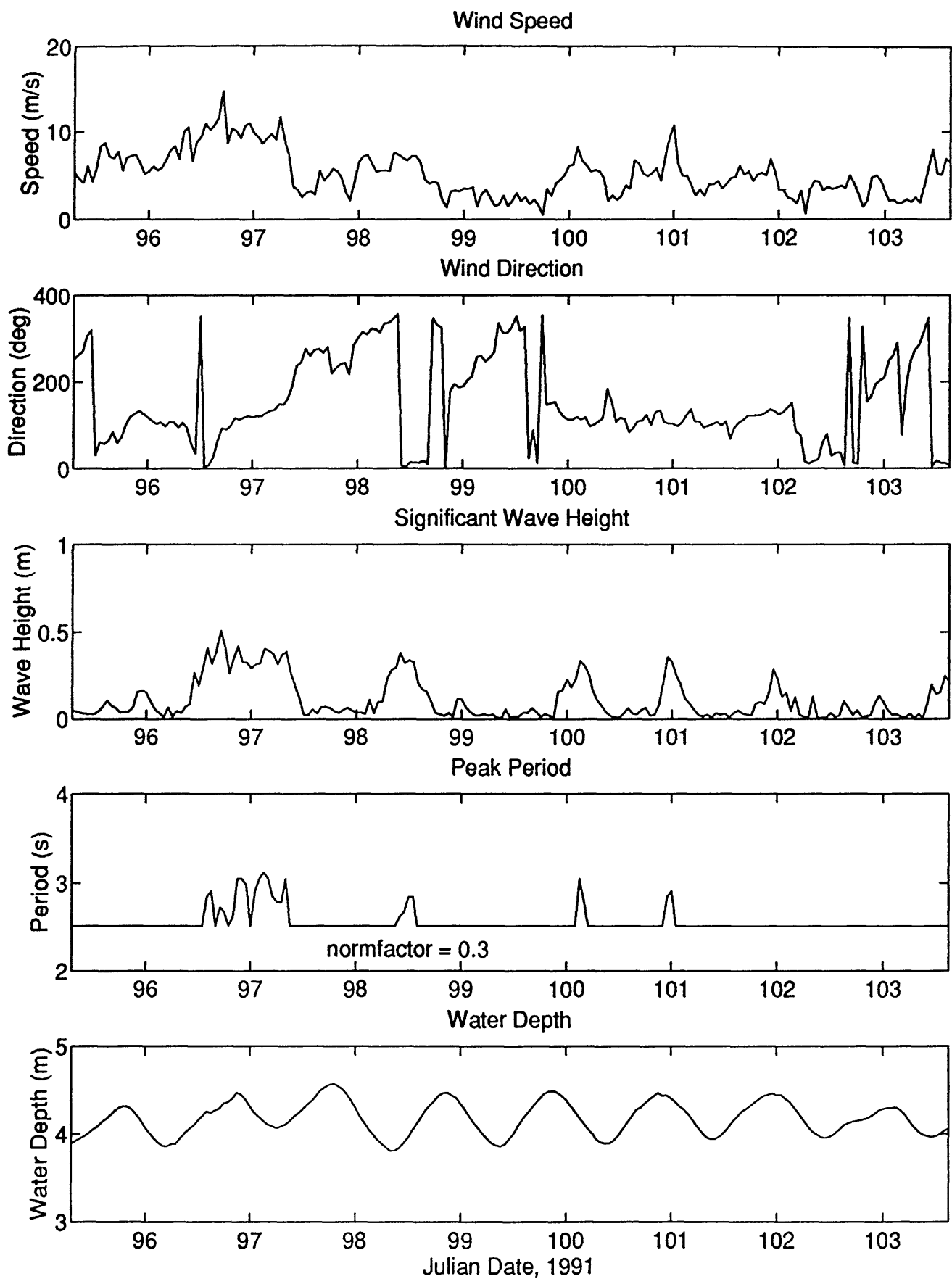
Peak Period



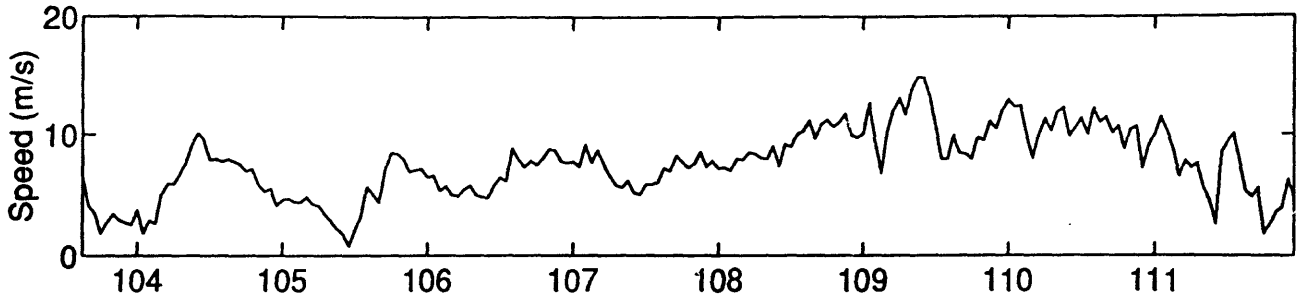
Water Depth



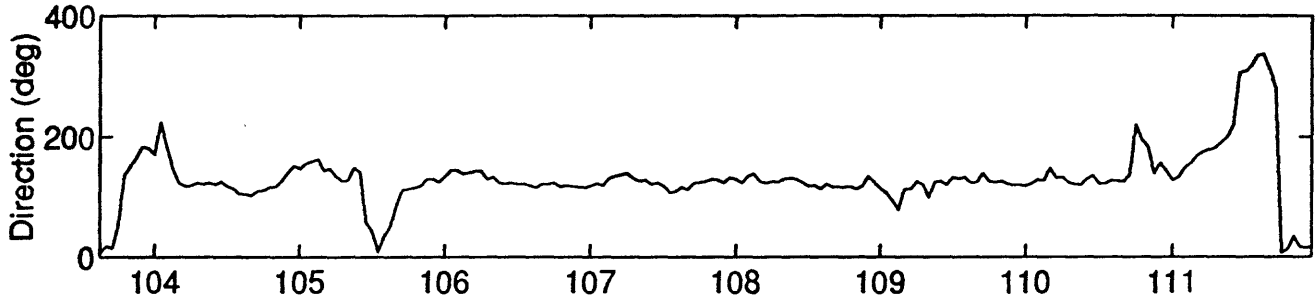
Julian Date, 1991



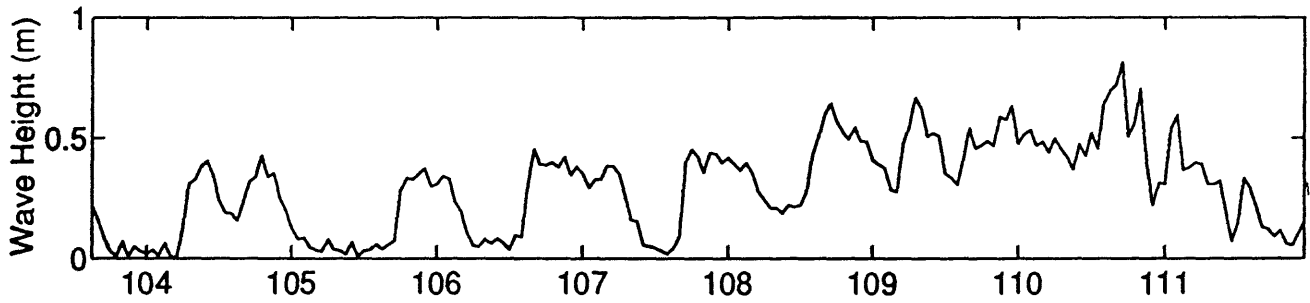
Wind Speed



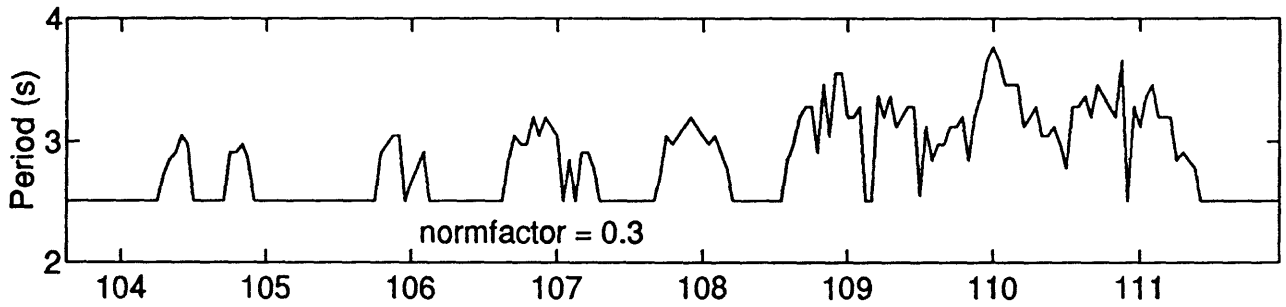
Wind Direction



Significant Wave Height



Peak Period



Water Depth

